POLARIZED NEUTRON DIFFRACTION DATA ANALYSIS

$$F_M\,(hkl) \Rightarrow M_z\,(x,y,z)$$

$$F_M\,(q) \Rightarrow \rho_s\,(x,y,z)$$

- **Fourier method** $\rho_s = \Sigma F_M(q)e^{-iqr}$
- **Refinement of multipoles** $\rho_s = \Sigma\, p_{lm} R_l Y_{lm}$
- **MEM, maximum entropy method and others…**

Model-free methods

Fourier summation

$$\rho(\vec{r}) = \frac{1}{V}\sum_{\vec{K}}^{Nobs} F_M(\vec{K})e^{-i\vec{K}\vec{r}}$$

Limitations:

- centrosymmetrical space group only
- exact only if infinite number of F_M's
- artefacts due to missing F_M for weak nuclear F_N

NUMERICAL INVERSION PROBLEM

DATA $F_M(q) \Rightarrow \rho_s(x,y,z)$ **IMAGE**

- **Complete, noise -free data**

1- to -1 mapping one set $F_M(q) \Leftrightarrow$ one ρ_s

- **Incomplete, noise data**

1- to -many mapping one $F_M(q) \Leftrightarrow$ many ρ_s

Which map to chose?

Representation of complex numbers on 2Dmap

by Kevin Cowtan, http://www.ysbl.york.ac.uk/~cowtan

amplitudes and phases or Re (F) and Im(F)
Amplitude is represented by colour **saturation** and **brightness**, while phase is given by **hue**.

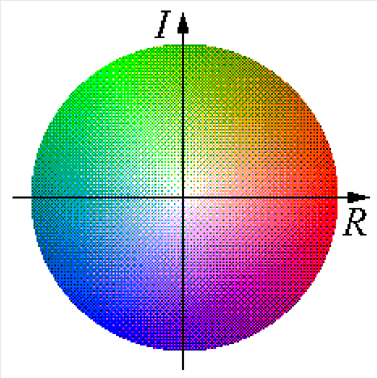

Phase **0 degrees** is ***red***, **120 degrees** is *green*, and **240 degrees** is *blue*.
positive Real's are ***red***, and **negative** Real 's are ***cyan***.
White represents **zero** magnitude.

Fourier transform (*FT*) and Diffraction pattern

by Kevin Cowtan, http://www.ysbl.york.ac.uk/~cowtan

$$\rho_s = \sum F_M(q) e^{-iqr}$$

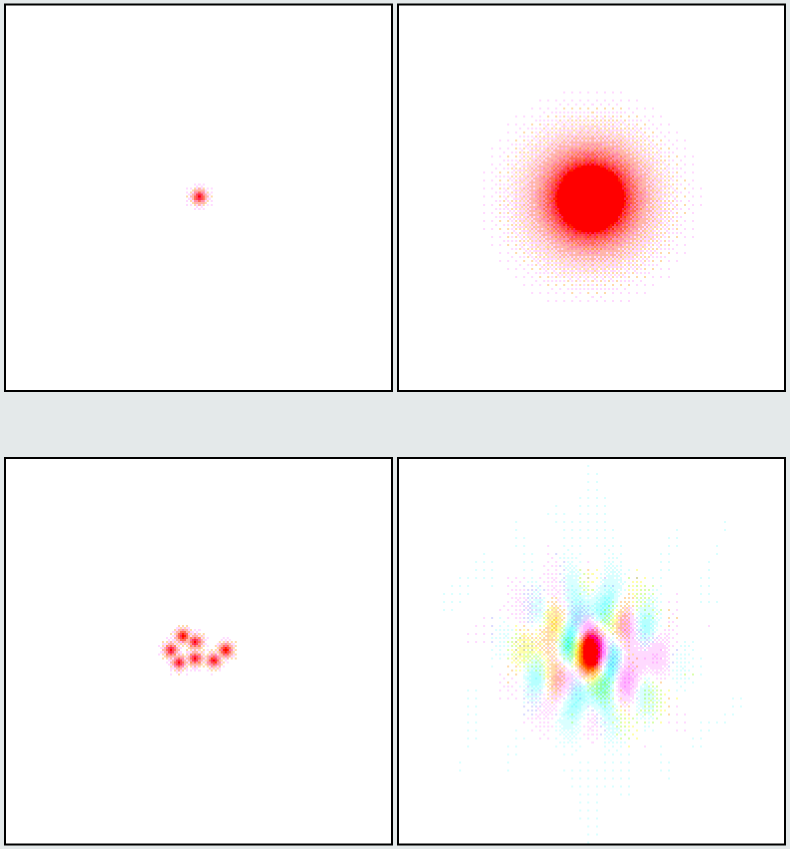

Fourier transform (*FT*) and Diffraction pattern

by Kevin Cowtan, http://www.ysbl.york.ac.uk/~cowtan

Lattice , and its FT :

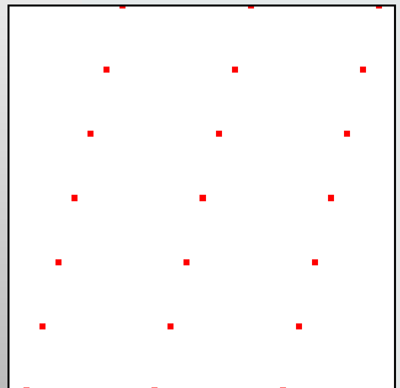

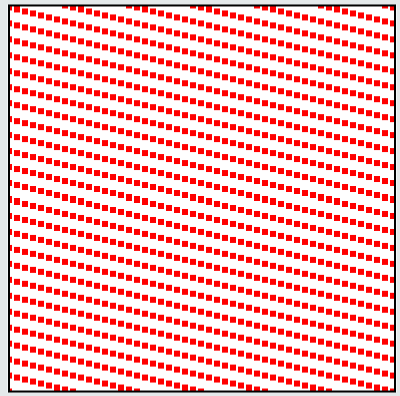

FT of the crystal =

Product of molecule FT and Rec. Latt. FT

Crystal

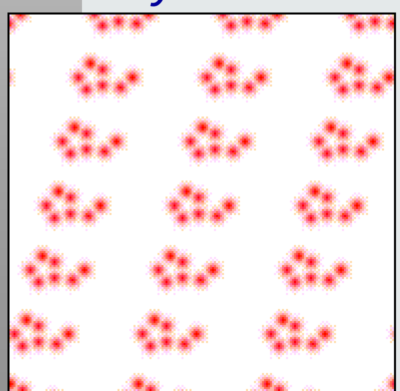

1 Molecule FT:

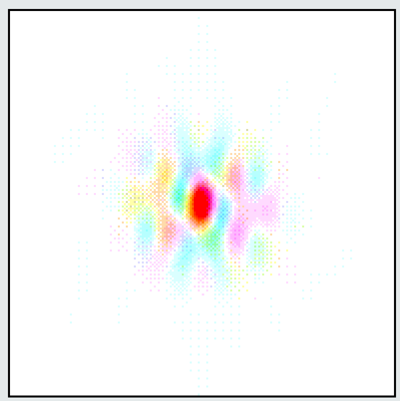

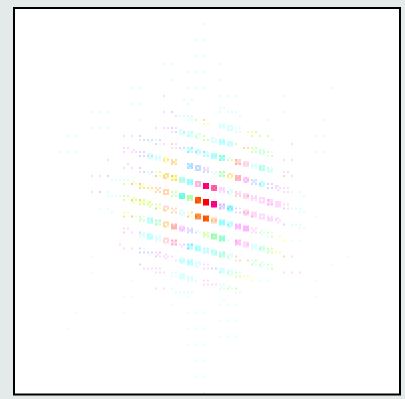

Duck Fourier Transform

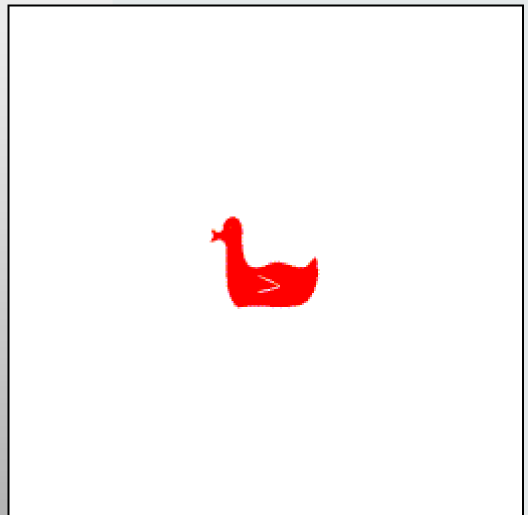

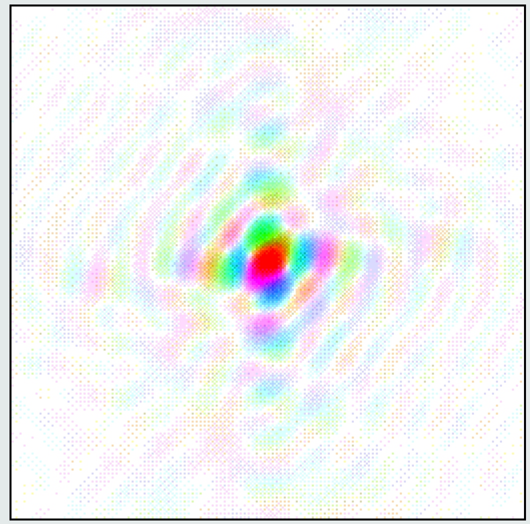

Image id real but its FT is complex (hermitian) !!

by Kevin Cowtan, http://www.ysbl.york.ac.uk/~cowtan

Low resolution Duck

High resolution Duck

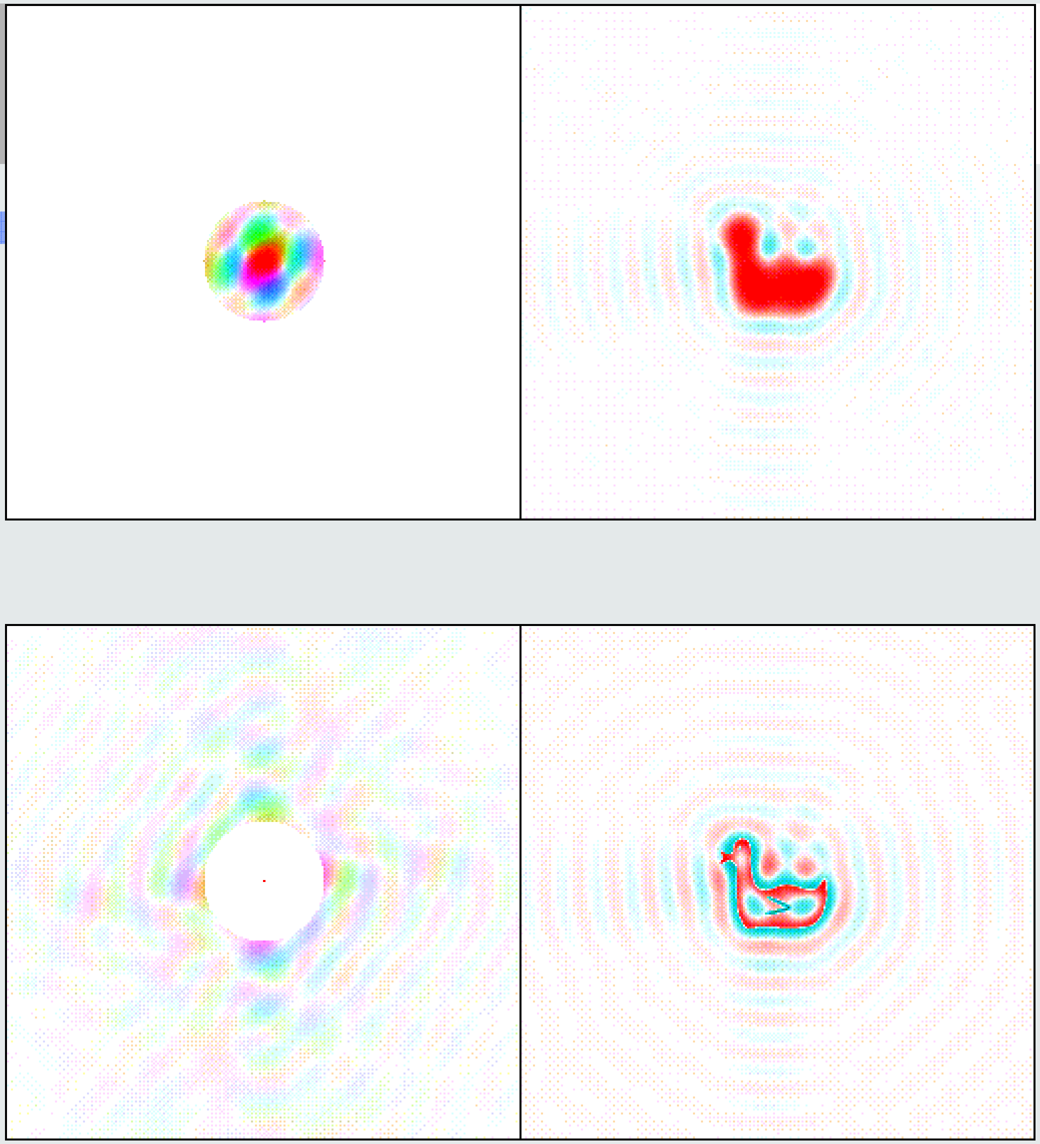

Random Missing of 10% data

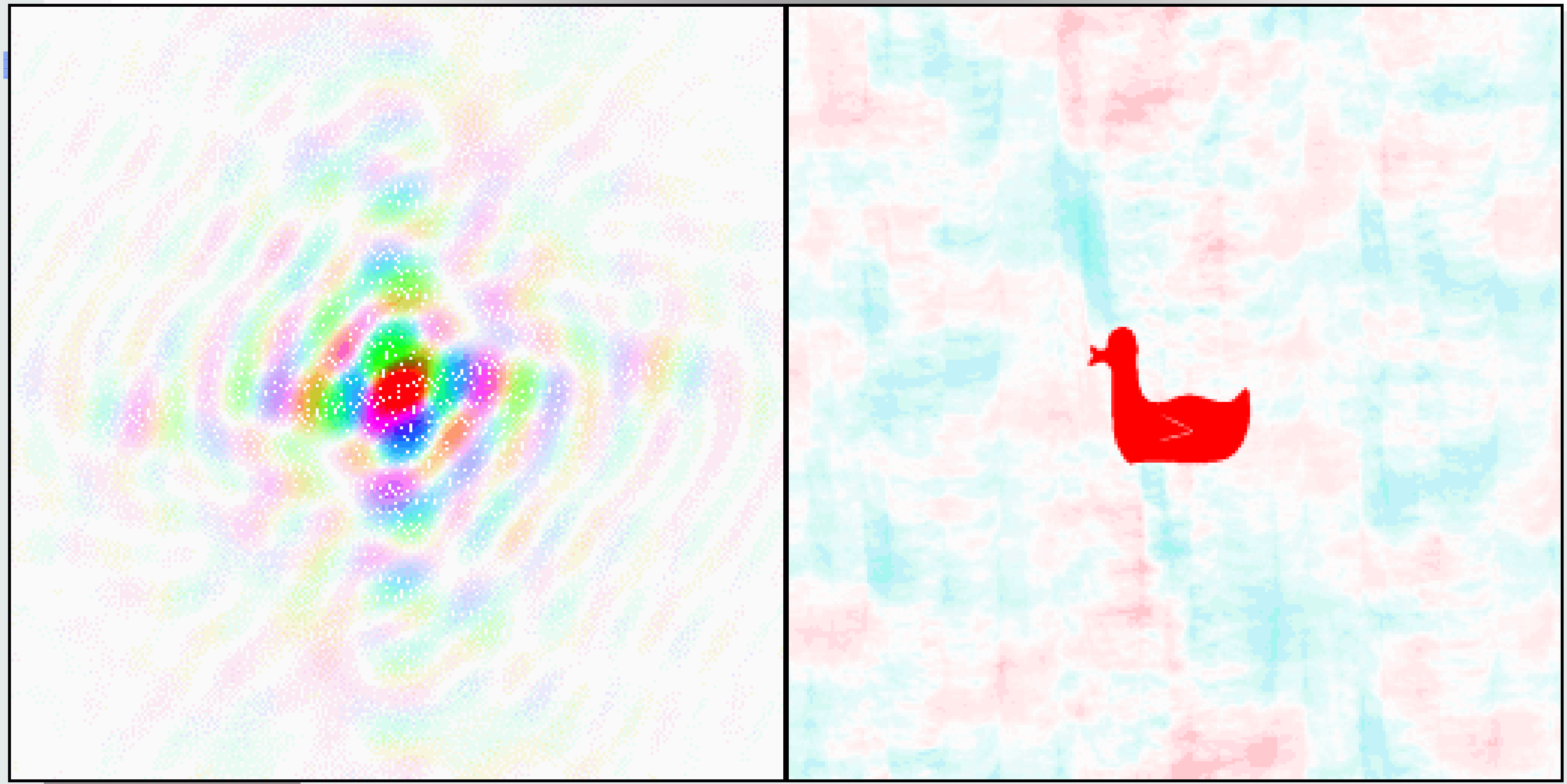

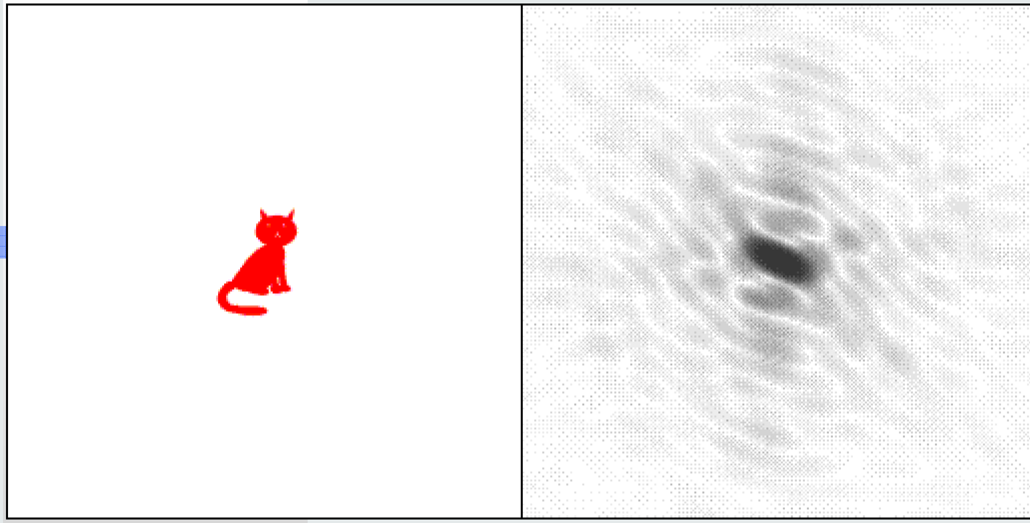

experiment

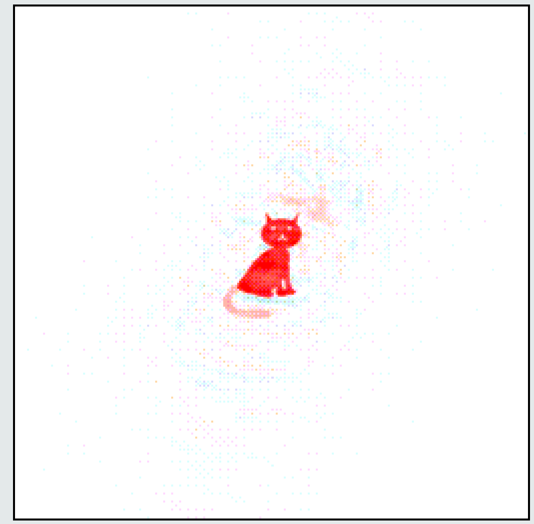

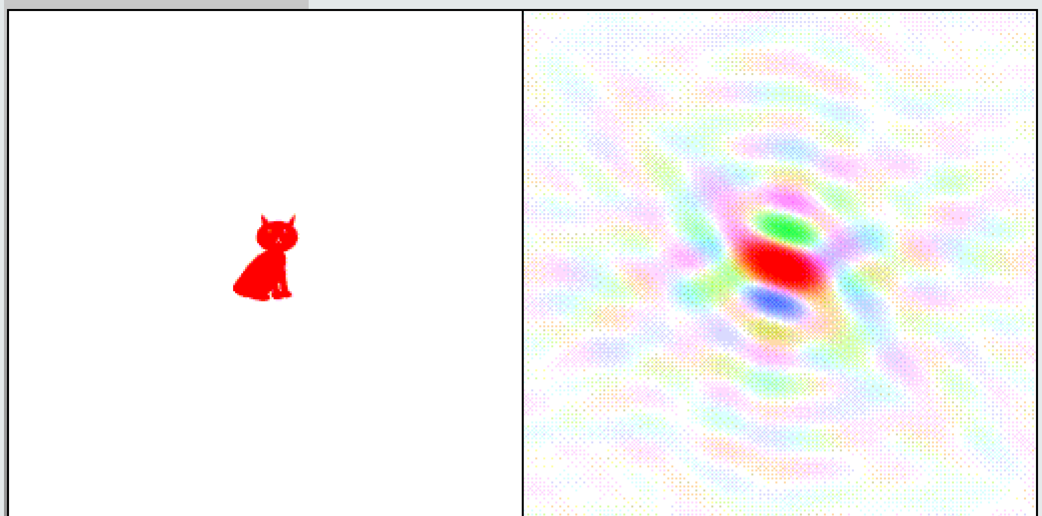

similar cat

Iteration

REFINEMENT OF A MODEL

Experiment: n_{obs}; $F_i^{obs}(q), \sigma_i(q)$

Model $\rho_s(r)$, m_{par}

$$\chi^2 = \Sigma (F_i^{obs} - F_i^{calc})^2 / \Sigma \sigma_i^2 (n_{obs}-m_{par})$$

where $F_i^{calc} = \int \rho_s(r)\, e^{-iqr}$

- **Spherical approximation** $\rho_s = \Sigma p_j \rho_j(r)$
- **Multipoles approximation** $\rho_s = \Sigma p_{lm} R_l Y_{lm}$
- **Wave function approximation** $\rho_s = \Sigma p_{lm} \psi_{lm}$

GLOBAL OPTIMISATION ALGORITHM

Possible Moment Distributions in the unit cell containing $4\ (\pm\ 1)\ \mu_B$

?

Consider everything. Keep good.

Avoid evil whenever you recognize it. (St. Paul)

GLOBAL OPTIMISATION

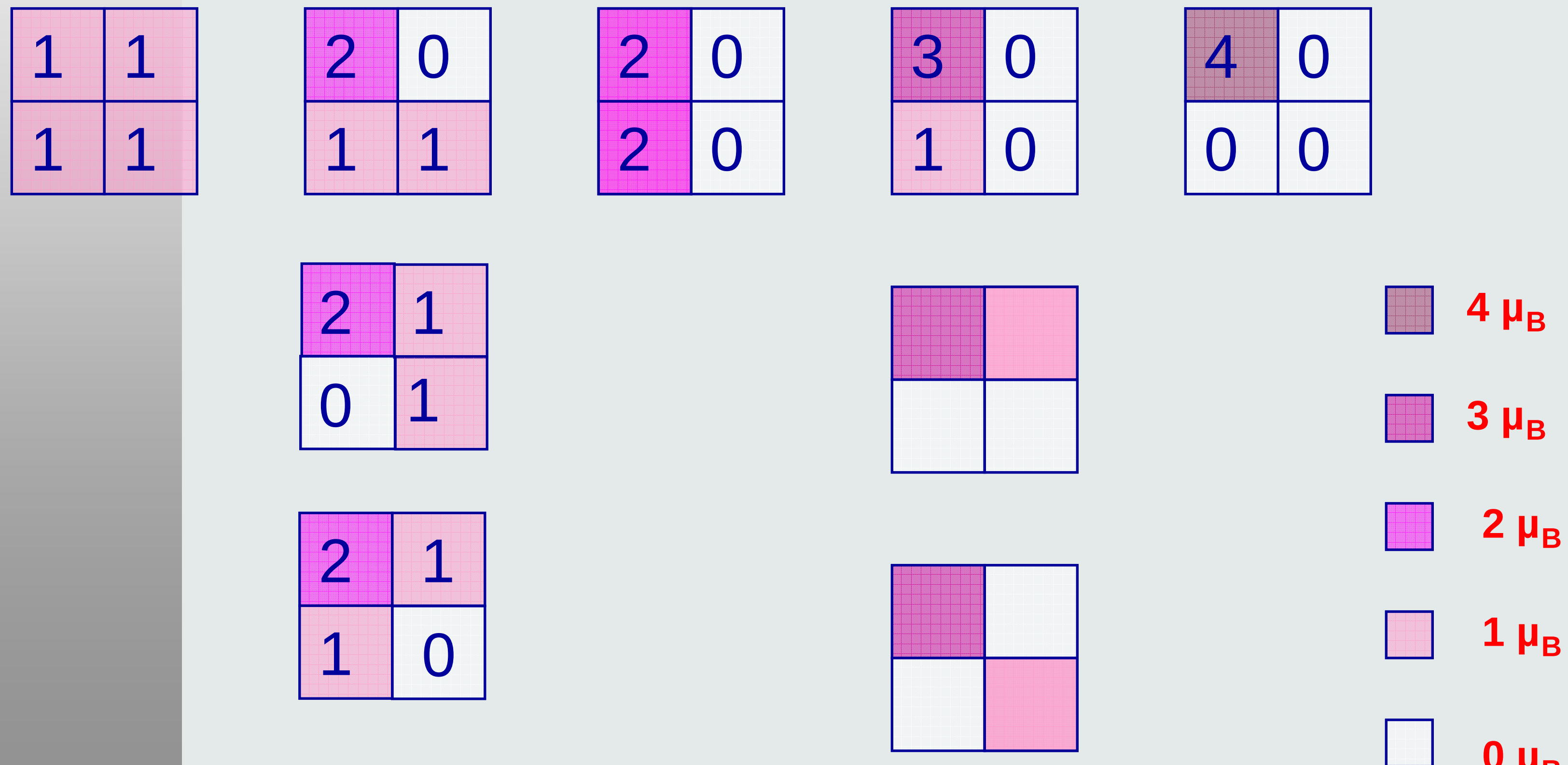

GLOBAL OPTIMISATION

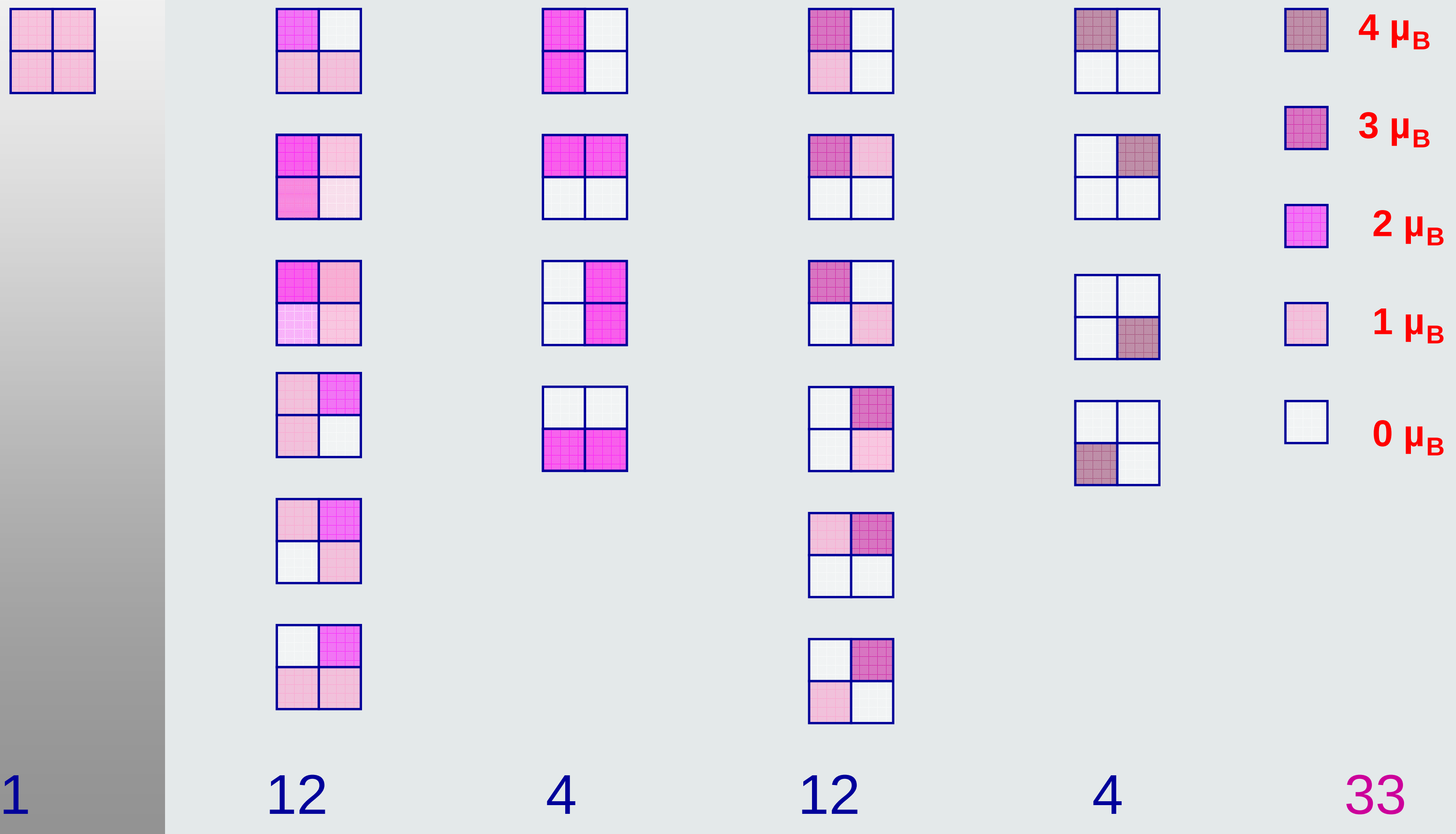

4	0
0	0

SPIN DISTRIBUTION $M_{tot}=4$

EXPERIMENT GIVES =>

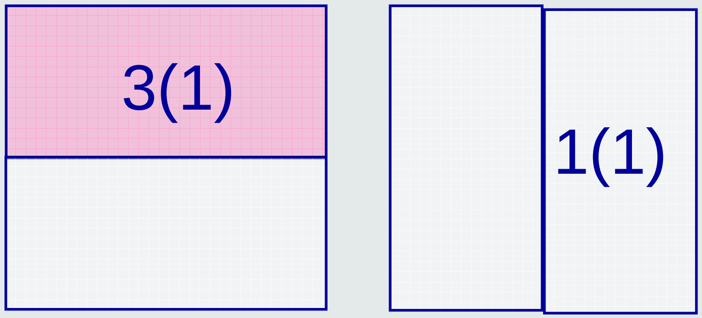

EXPERIMENT GIVES =>

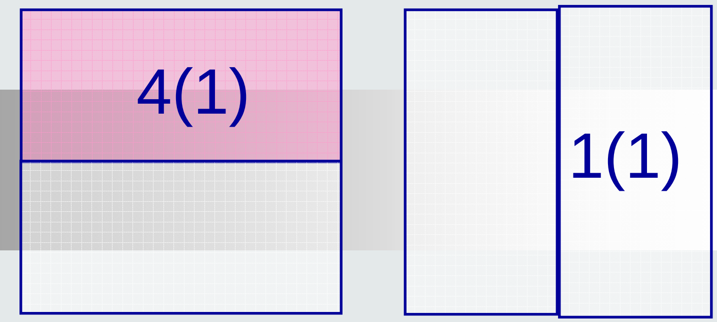

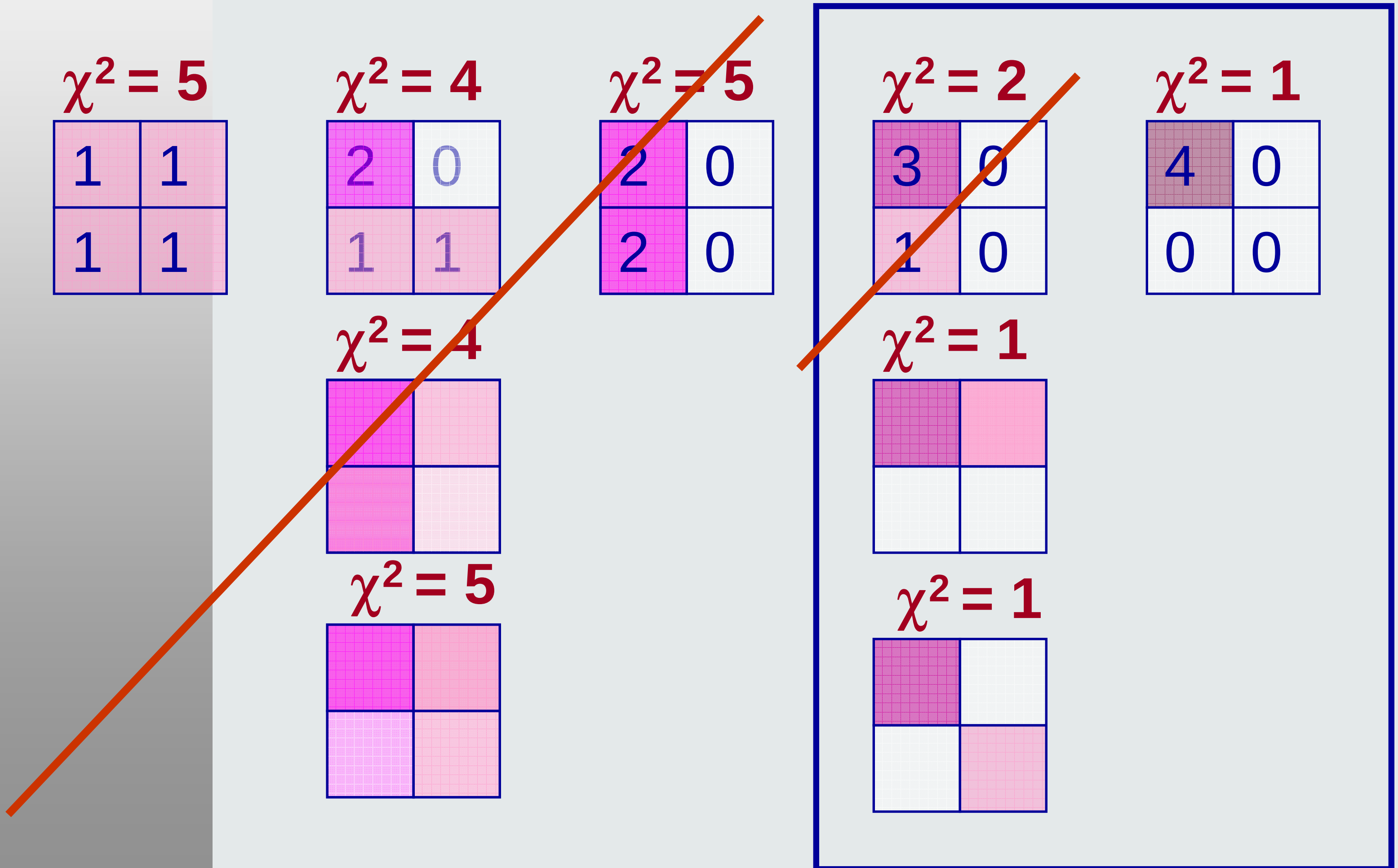

χ^2 VERSUS GO and MEM

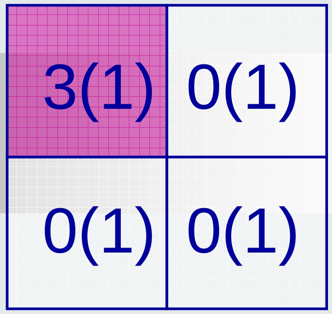

- χ^2 (ref.) **no solution**
- **Gl. Opt.** **3 maps**
- **MEM** **1 map**

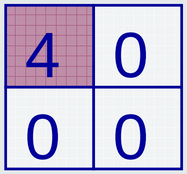

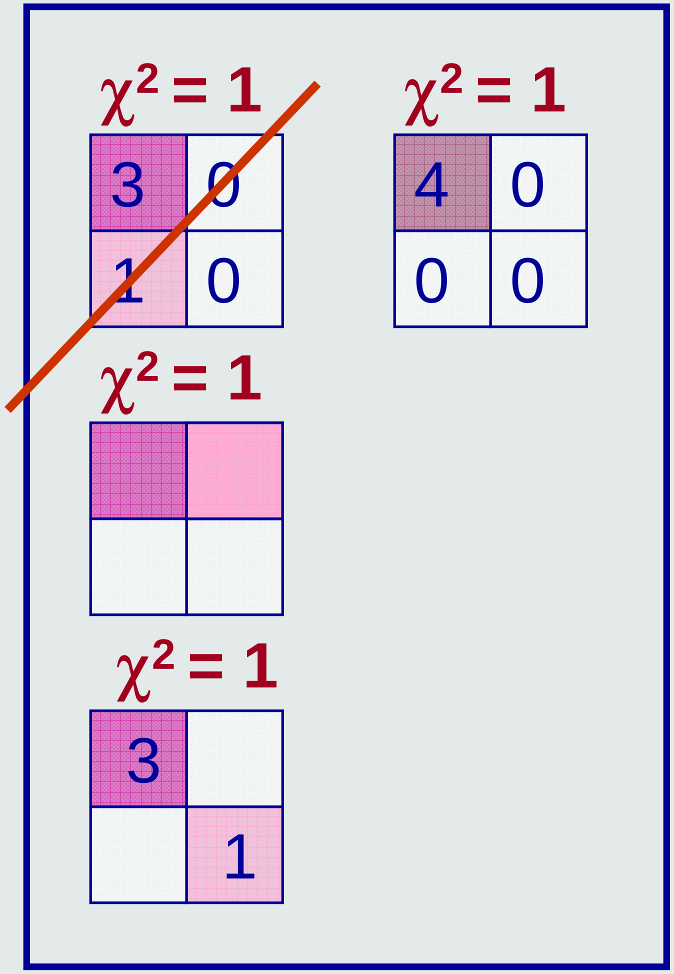

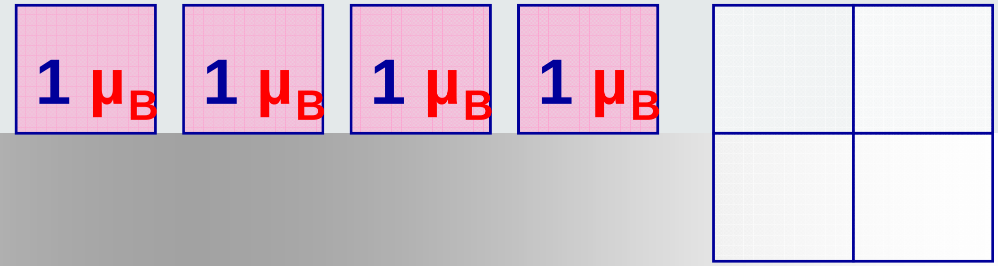

MEM

- 4 moments of 1 μ_B in 4 celles
- N moments of 1 μ_B in M celles

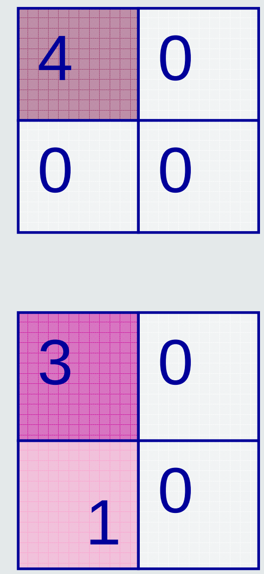

- Number of way to get a map

$$g = \frac{N!}{\prod_{1}^{M} n_j!}$$

- Entropy of the map

$$S = \ln g \approx -N \sum_{1}^{M} f_j \ln f_j$$

- Refinement on

$$\chi^2 - \ln g$$

GLOBAL OPTIMISATION ALGORITHM

Possible Moment Distributions in the unit cell containing 3.95 (± 0.5) μ_B

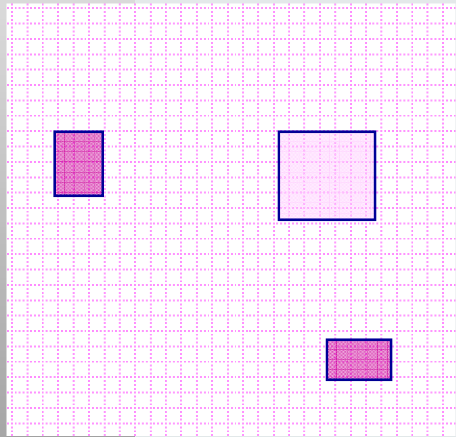

20x20=400 cells
of 0.01 μ_B ▫

> N! maps > 400!

MEM SOLUTION

For given $F_M(q)$ => MEM chose an IMAGE ρ_s that is minimally changed form a default image (prior distribution) as to achieve desired χ^2

For given $F_M(q)$ => MEM chose a most featureless map that allows to achieve desired χ^2

MEM SOLUTION

MEM has acquired a certain “cult” popularity; one sometimes hears that it gives an intrinsically “better” estimate than other methods. Don’ t believe it. MEM has the very cute property of being able to fit sharp features, but there is nothing else magical about it. (*Num. Recipes*)

NOUVELLES APPROCHES DANS LA DIFFRACTION DE NEUTRONS POLARISES

A. GUKASOV

Laboratoire Léon Brillouin, CEA-CNRS, Saclay, France

RESUME

Dans l'état paramagnétique les moments d'atomes équivalents sont égaux, mais sous champ magnétique certains sont plus égaux que d'autres

POLARIZED NEUTRON APPLICATIONS

- Localization of magnetic density (position and magnitude)
- Space distribution of magnetic moment (formfactor, L / S ratio)
- Magnetic structure refinement
- Site magnetization and susceptibility

COLLINEAR DENSITIES IN PND

- Covalency in antiferromagnetic garnet $Ca_3Fe_2Ge_3O_{12}$
- Hybridization in ruthenates $Sr(Ca)_2RuO_4$
- Photo-induced spin density of the $[Fe(ptz)_6](BF_4)_2$ (ptz=1-propyltetrazole)
- Field-induced ferro-metallic state in $La(Pr)_{1.2}Sr_{1.8}Mn_2O_7$

NONCOLLINEAR MAGNETIZATION IN PND

- Non-collinear spin distribution in ferr(o)imagnets
- Site susceptibility tensors and Anisotropic Susceptibility Parameters (ASPs)

NEUTRON AND X-RAYS DIFFRACTION

$I(q) \propto |F(q)|^2 \qquad F_n(q) = b_N + b_M + b_{SO} + \ \ldots$

- Nuclear interaction
- X-rays

$F_N \propto b_N$

$(-3.7\ Fm < b_N < 12.6\ Fm)$

$Fm = 10^{-13} cm$

$b_X \propto r_0 Z f(q)$

$r_0 = 2.8\ Fm$

Hydrogen, $Z=1$ $b_X = 2.8\ Fm$

X- RAYS AND MAGNETIC NEUTRON DIFFRACTION

- X-rays

$$b_X \propto r_0 Z\, f(q)$$

$$r_0 = 2.8\ Fm$$

- Magnetic interaction

$$F_M \propto (\gamma r_0 / 2)\,(S_{\perp}{}^{*}\,\sigma) f(q)$$

$$b_M = \pm 2.7\ Fm \text{ for } S=1/2$$

FORMFACTOR AND ORBITAL/SPIN RATIO

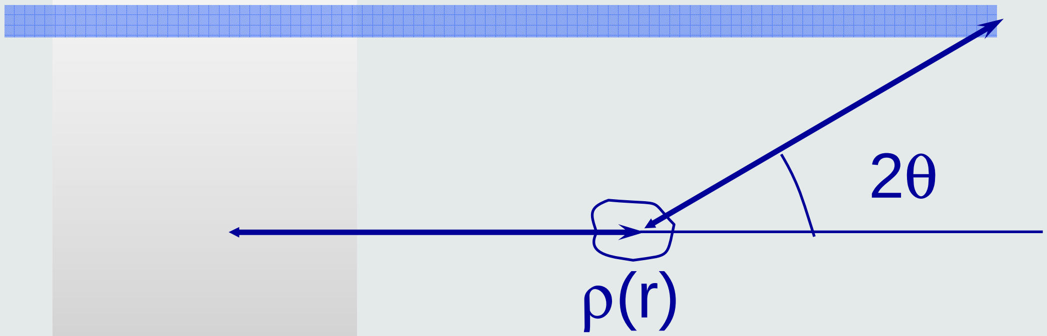

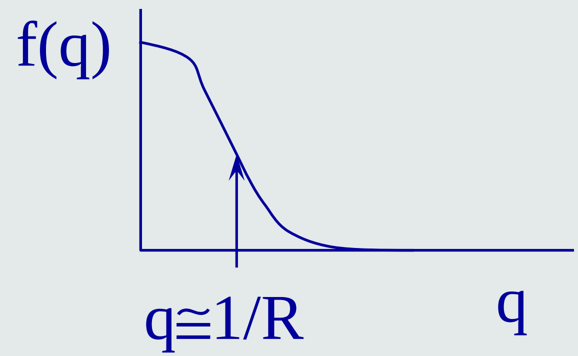

$f_X(q) = \int \rho(r)\, \exp(i\mathbf{qr})\, dr^3/Z$

$f_m(q) = \int m(r)\, \exp(i\mathbf{qr})\, dr^3/\, m$

$f_m(q) = \langle J_0 \rangle + (L/L+S)\, \langle J_2 \rangle + \ldots$

$\langle J_0 \rangle$ are radial integrals

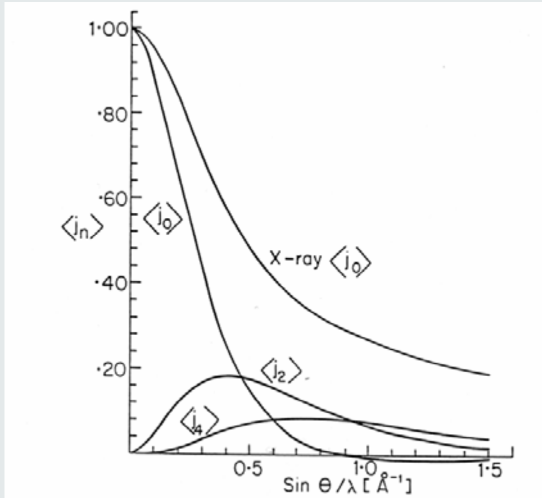

Fig. 2 — The radial integrals $\langle j_0 \rangle$, $\langle j_2 \rangle$ and $\langle j_4 \rangle$ for the 3d electrons of an Fe^{2+} free ion. Also shown is the X-ray form factor to which all electrons contribute.

MAGNETIC FORMFACTOR AND ORBITAL/SPIN RATIO

- **Polarized neutron diffraction study of spin and orbital moments in UAsSe**

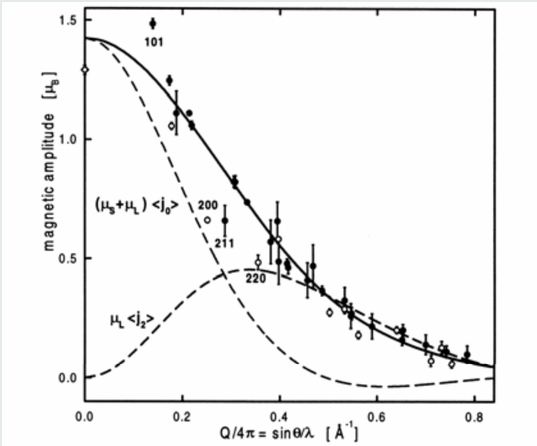

Figure 2. The magnetic amplitudes of uranium ions in UAsSe. Empty and full circles represent in-plane and off-plane reflections, respectively. The solid line is the magnetic amplitude calculated with the U^{4+} 5f form factor taken in the dipole approximation. Dashed lines show moment components proportional to $(\mu_S + \mu_L)$ and to μ_L. A diamond represents a value of the moment from the magnetization measurement.

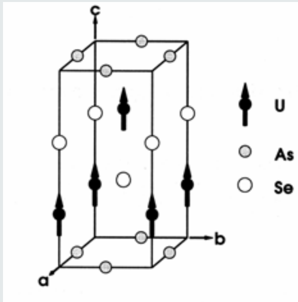

Figure 1. Crystal and magnetic structure of UAsSe.

P. Wisniewski, A. G. Gukasov and Z. Henkie J. of Phys.: Condens. Matt. 11, 6311, 1999

UNPOLARIZED NEUTRON DIFFRACTION

$$I \propto |F_N|^2 + |F_M|^2$$

- Coherent scattering

$$I(q) \propto |\Sigma F_i|^2$$

- Incoherent scattering

$$I(q) \propto \Sigma |F_i|^2$$

- Nuclear interaction

$$F_N \propto b_N$$

- Magnetic interaction

$$F_M \propto (\gamma r_0 / 2)\, S_\perp * \sigma_n f(q)$$

NEUTRON AND X-RAYS DIFFRACTION

X-rays → $r_0 Zf(\theta=0)$

Neutrons $b_{nuclear}$

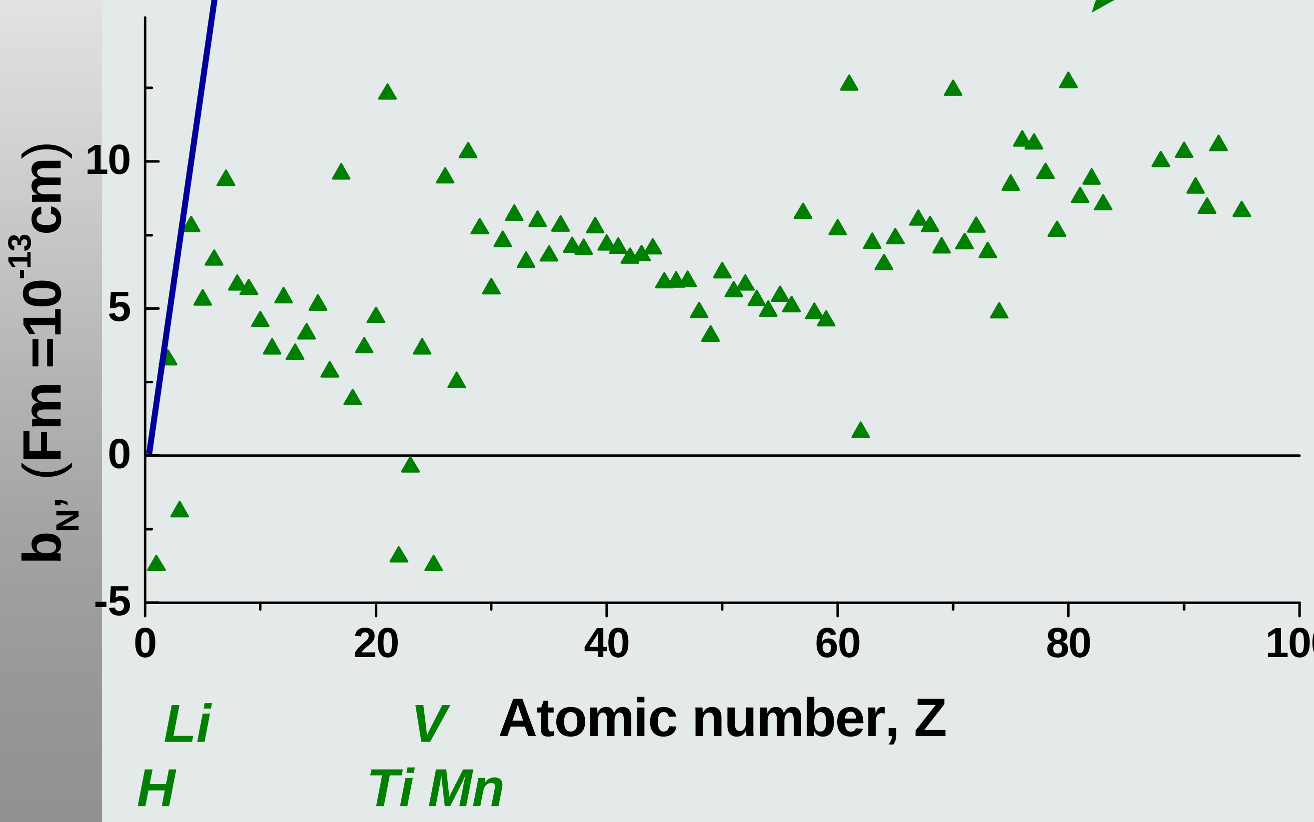

NUCLEAR AND MAGNETIC SCATTERING AMPLITUDES

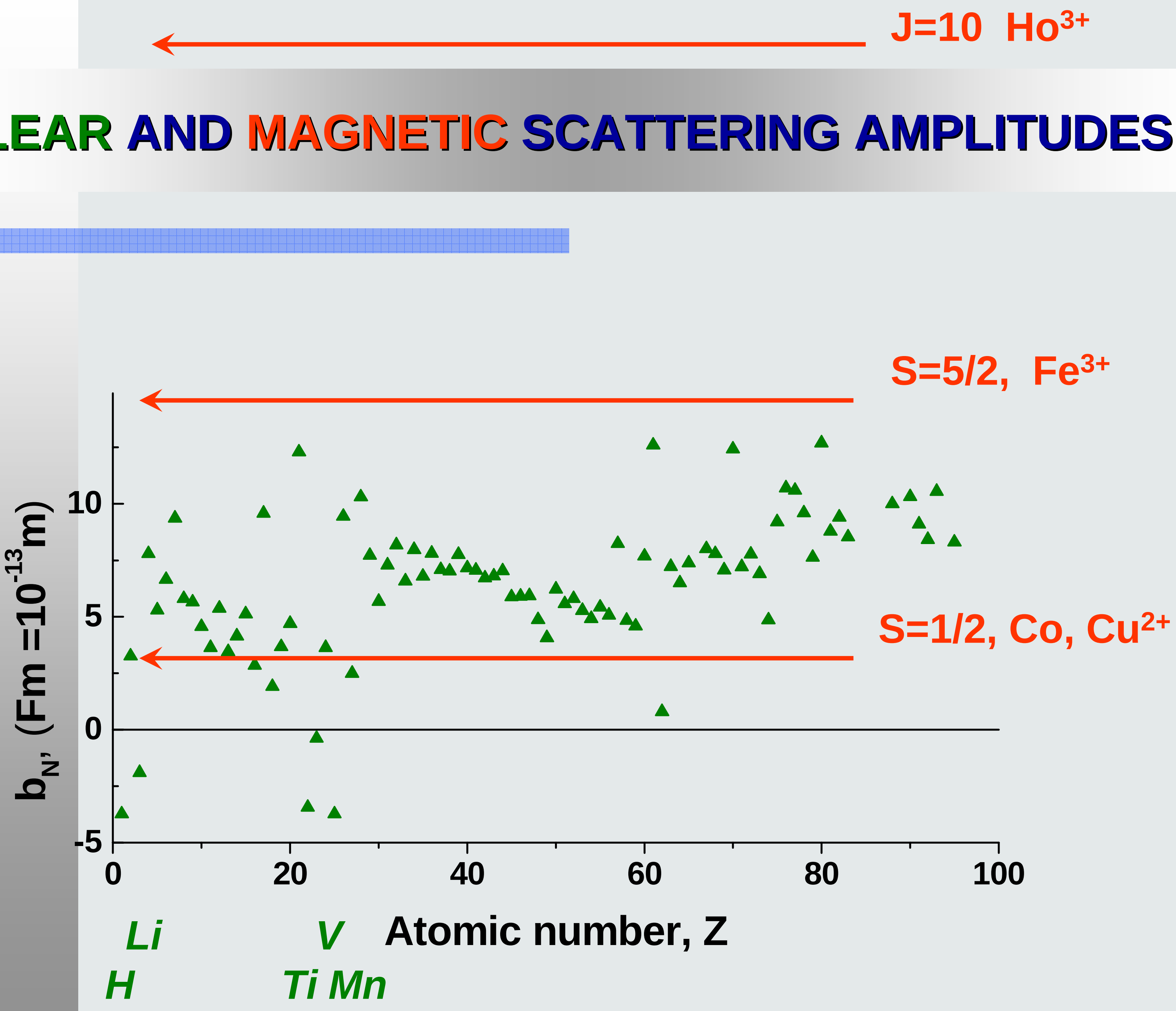

POLARIZED NEUTRON DIFFRACTION

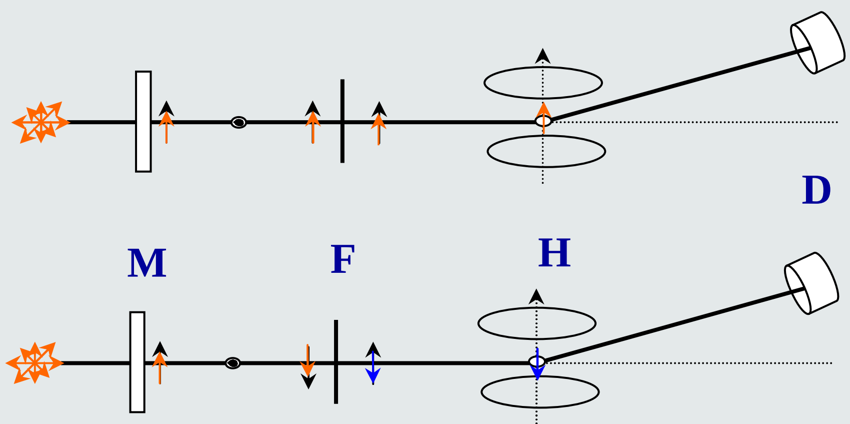

I^{+} P_0 parallel to H

I^{-} P_0 antiparallel to H

$$I^{\pm} \propto =(F_N \pm F_M)^2$$

$$I^{\pm} \propto F^2_N \pm 2F_N(P_0 * F_M) + F_M^2 \qquad (P_0=1)$$

If $F_N = F_M$ $\quad I^{+} = 4F_N^2 \quad I^{-} = 0$

if $P_0=0$ $\quad I \propto F_N^2 + F_M^2 = 2F_N^2$

FLIPPING RATIO MEASUREMENTS

$I^{+} \propto (F_N + F_M)^2$ $\quad\quad$ $I^{-} \propto (F_N - F_M)^2$

$$R = I^{+} / I^{-} = (F_N + F_M)^2 / (F_N - F_M)^2$$

$R = (1+\gamma)^2 / (1-\gamma)^2$, $\quad$ **where** $\gamma = F_M / F_N$

for small γ $\quad$ $R \cong 1+4\gamma$ $\quad$ $\gamma = (1-R)/4$

$$F_M(q) = \gamma * F_N(q)$$

ADVANTAGES OF FLIPPING RATIO MEASUREMENTS

Polarized neutrons:

$$I^{+} = F_N^{\,2}\,(1+\gamma)^2 = (1+2\gamma + \gamma^2)$$

$$I^{-} = F_N^{\,2}\,(1-\gamma)^2 = (1-2\gamma + \gamma^2)$$

for $\gamma = 0.1$ $\quad I^{+} = \mathbf{1.21} * F_N^{\,2}$ $\quad I^{-} = \mathbf{0.81} * F_N^{\,2}$

Unpolarized neutrons:

for $\gamma = 0.1$ $\quad I = F_N^{\,2}\,(1+\gamma^2)$ $\quad I = \mathbf{1.01} * F_N^{\,2}$

POLARIZED NEUTRONS AND MAGNETIC SUSCEPTIBILITY

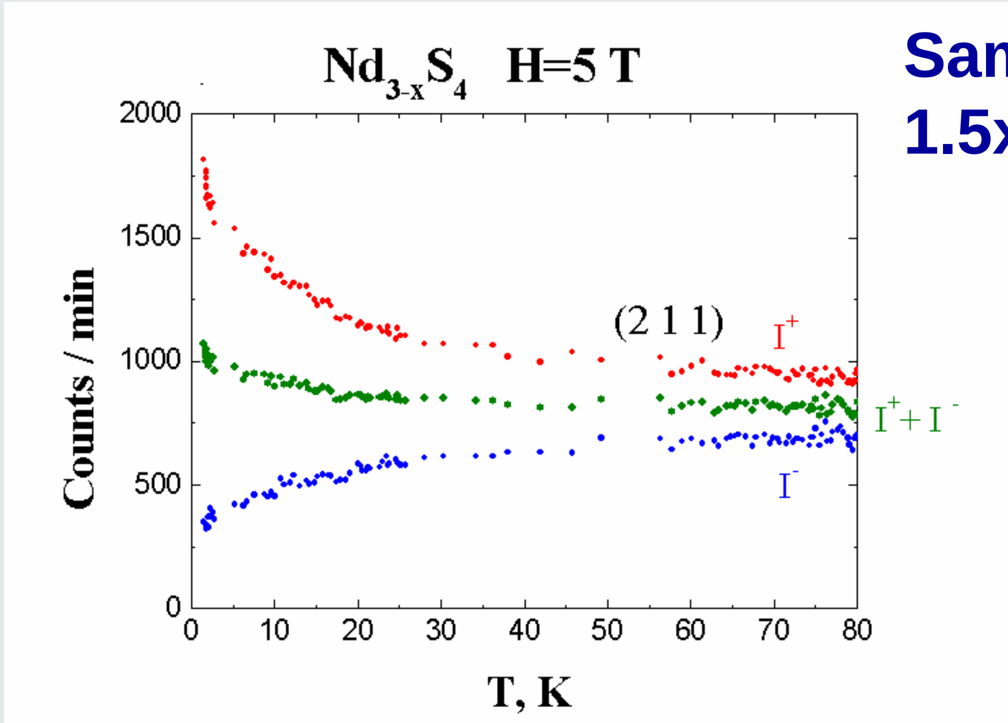

Sample size: 1.5x1.5x1.5 mm^3

$$I^{\pm} \propto F_N^{\ 2} + |F_M|^2 \pm 2\, F_N\, |F_M|$$

POLARIZED NEUTRONS AND MAGNETIC SUSCEPTIBILITY

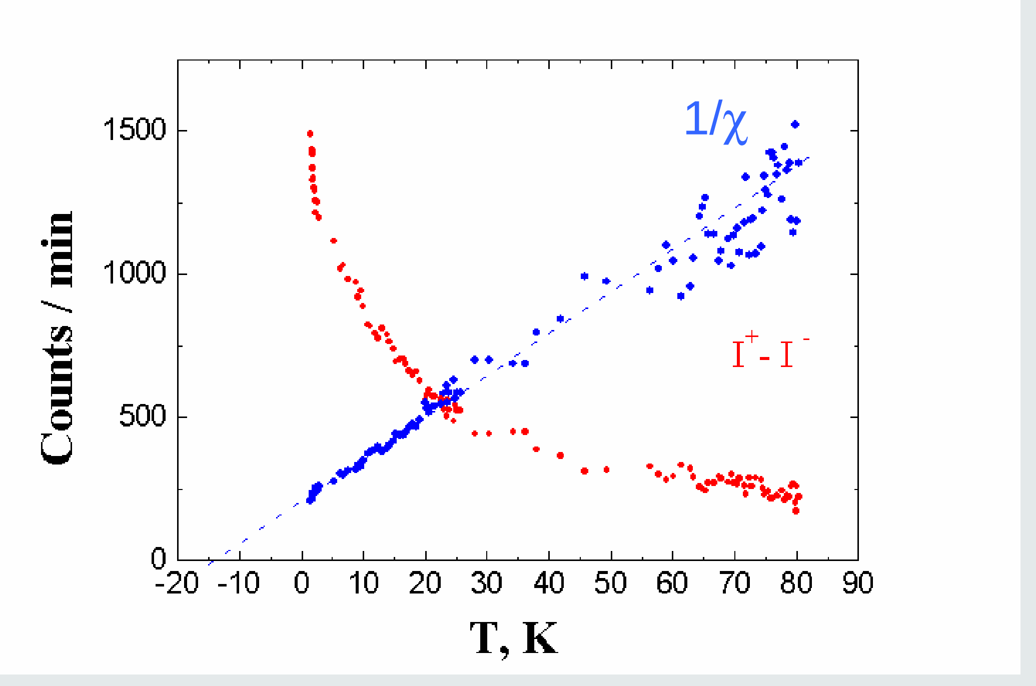

$$I(q)^{+} - I(q)^{-} = 4N(P_0 \cdot M_{\perp z}) \sim P^{\alpha} \cdot \chi^{\alpha\beta}(q) \cdot H^{\beta}$$

SPIN DENSITY ON LIGANDS O^{2-} AND COVALENCY OF Fe^{3+} IN $Ca_3Fe_2Ge_3O_{12}$ GARNET.

V. P. Plakhty, A. G. Gukasov, R. J. Papoular and O. P. Smirnov, Europhys. Lett., 48, 233,1999

SG 230

Ia3D

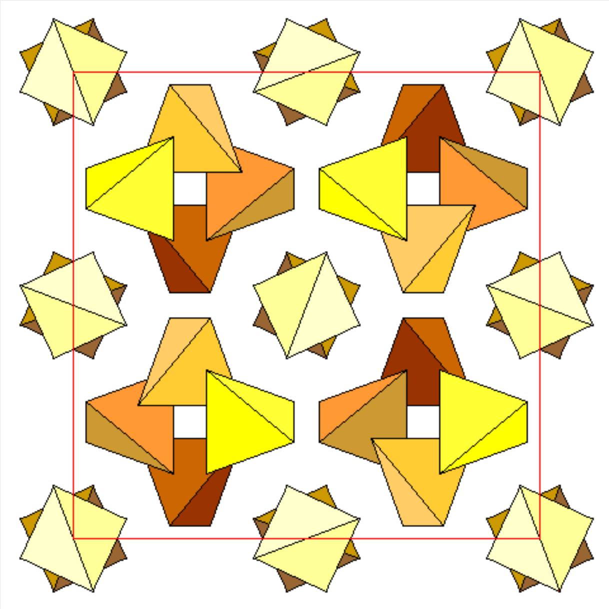

24 (d)	tetra	(3/8 0 1/4)	Si, Ge
96 (h)	general	(x y z)	O

SPIN DENSITY ON LIGANDS O^{2-} AND COVALENCY OF Fe^{3+} IN $Ca_3Fe_2Ge_3O_{12}$ GARNET.

SG 230, *Ia3D*

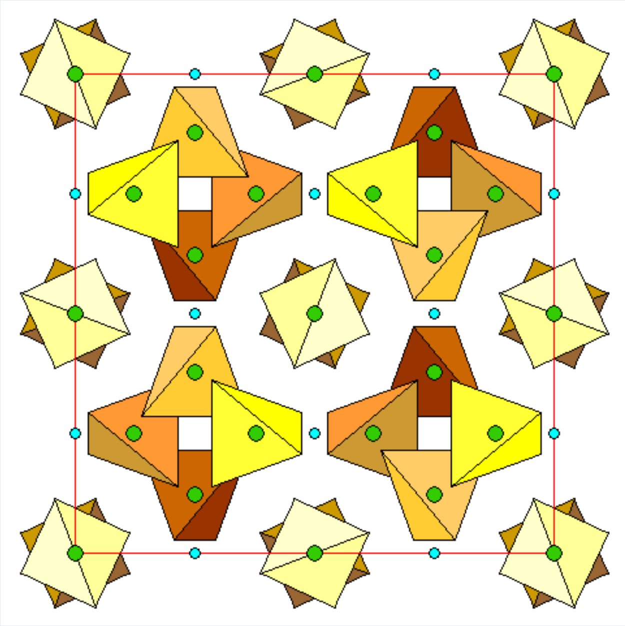

16 (a)	octa	(0 0 0)	M^{I}
24 (c)	dode	(1/8 0 1/4)	M^{II}

GARNET STRUCTURE

	3d	$1.25 < R_{ion} < 1.46$ Å	
	4f	$1.75 < R_{ion} < 1.88$ Å	
O	$R_{ion} = 1.4$ Å,	O^{2-}	$R_{ion} = 0.66$ Å
16 (a)	octa	(0 0 0)	*3d*, *4f*
24 (c)	dode	(1/8 0 1/4)	*4f*, Fe^{3+}, Mn^{2+}
24 (d)	tetra	(3/8 0 1/4)	Fe^{3+}

ALLOWED REFLECTIONS FOR GARNET

I a3d $h+k+l=2n$ (general condition for BCC)

16 (a)	octa	$h,k=2n$; $h+k+l=4n$ — (0 0 4)
24 (d)	tetra	$h,k=2n+1$; $l=4n+2$
24 (c)	dode	$h,k=2n+1$; $l=4n+2$ — (1 1 2)
96 (h)	Oxygen	$h+k+l=2n$ — (1 3 4)

POLARIZED NEUTRON DIFFRACTION DATA ANALYSIS

$$F_M\,(hkl) \Rightarrow M_z\,(x,y,z)$$

$$F_M\,(q) \Rightarrow \rho_s\,(x,y,z)$$

- **Fourier method** $\rho_s = \Sigma F_M(q) e^{-iqr}$
- **Refinement of multipoles** $\rho_s = \Sigma p_{lm} R_l Y_{lm}$
- **MEM, maximum entropy method and others…**

MEM SOLUTION

For given $F_M(q)$ => MEM chose an IMAGE ρ_s that is minimally changed form a default image (prior distribution) as to achieve desired χ^2

SPIN DENSITY ON LIGANDS O^{2-} AND COVALENCY OF Fe^{3+} IN $Ca_3Fe_2Ge_3O_{12}$ GARNET.

- *V. P. Plakhty, A. G. Gukasov, R. J. Papoular and O. P. Smirnov, Europhys. Lett., 48, 233,1999*

All reflections

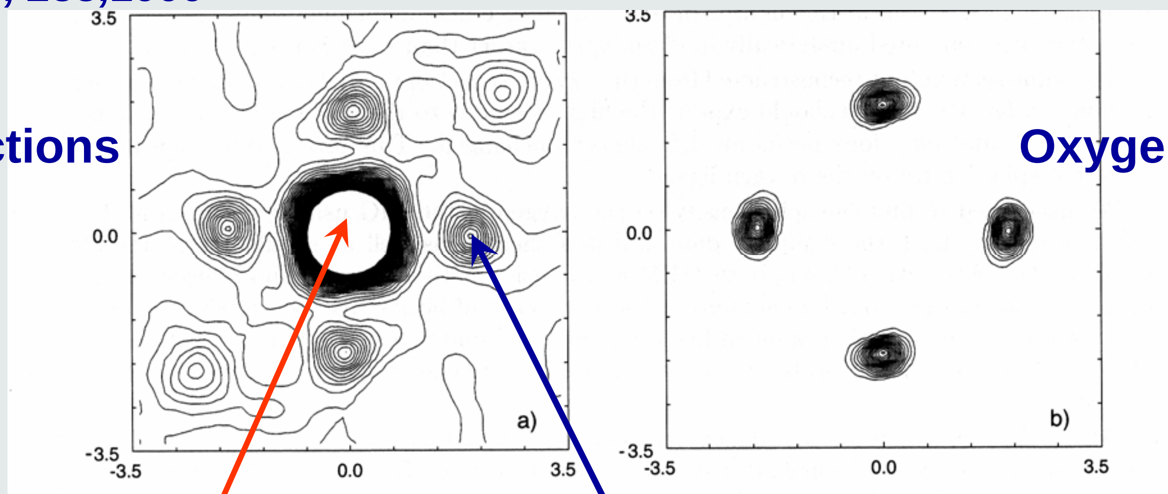

Oxygen reflections

Fe^{3+} 0.59(1)μ_B　　**O^{2-} 0.015(2)μ_B ≈ 2.5% of Fe**

$\delta M/M$ ≈ 13.% for Fe

SPIN DENSITY ON LIGANDS O^{2-} AND FORMFACTOR OF Ru in Sr2RuO4

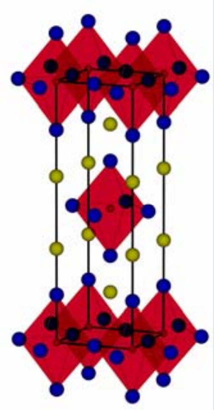

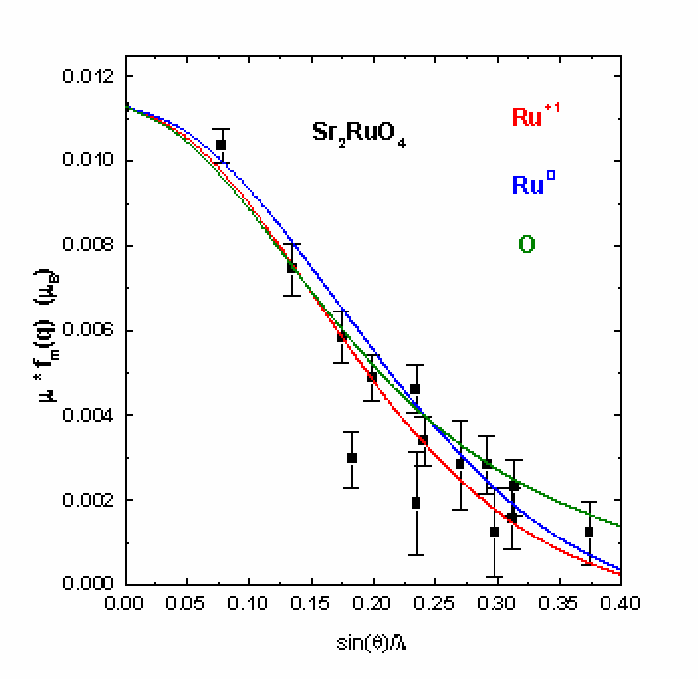

SPIN DENSITY ON LIGANDS O^{2-} IN $Ca_{1.5}Sr_{0.5}RuO4$

O. Friedt, M Braden, G.André, P. Adelemann, S Nakatsuji and Y Maeno. Phys. Rev., B63, 174432, 2001

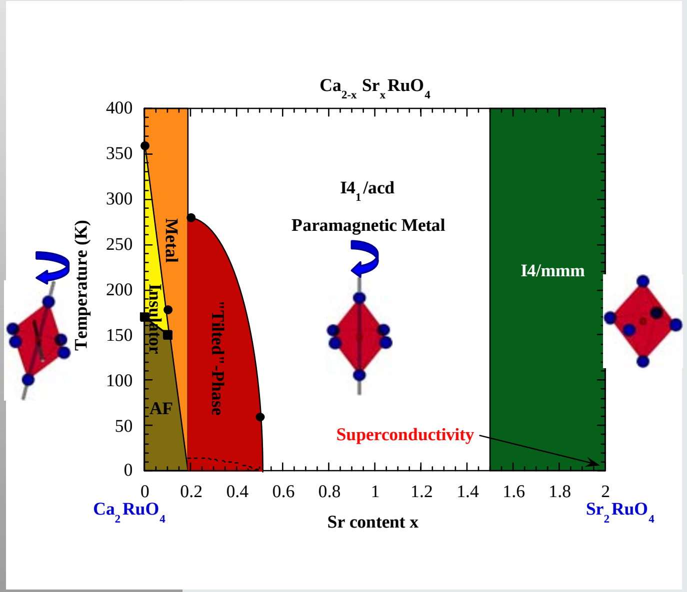

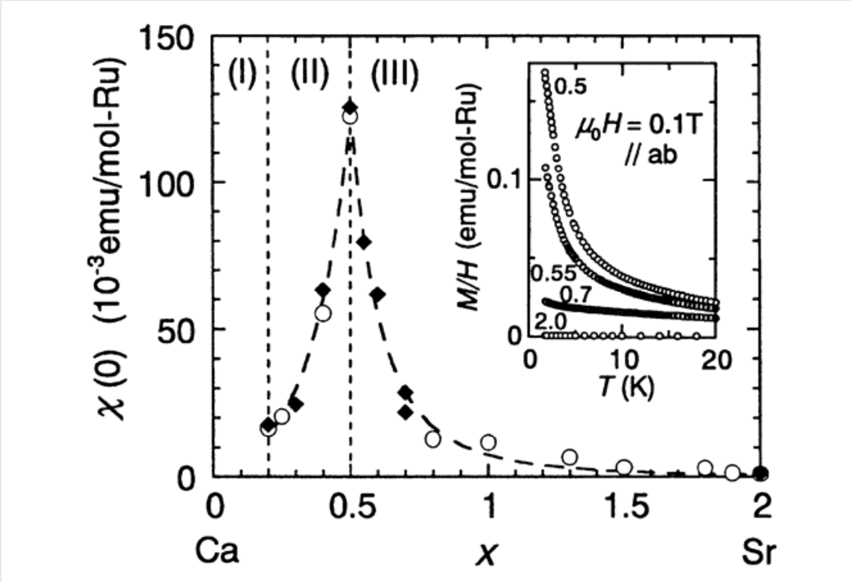

MAGNETIC SUSCEPTIBILITY OF $Ca_{1.5}Sr_{0.5}RuO4$; POLARIZED NEUTRON MEASUREMENTS

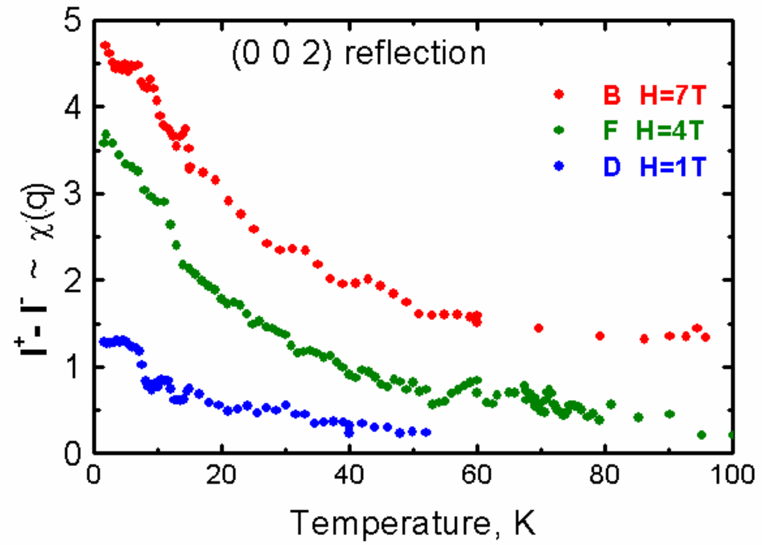

$$I^{\pm} \propto F_N^{\,2} + |F_M|^2 \pm 2\, F_N\, |F_M|$$

$$I(q)^+ - I(q)^- = 4\, N\, M_{\perp z} \sim \chi^{\alpha\beta}(q) \cdot H^{\beta}$$

ANOMALOUS SPIN DENSITY ON OXYGEN IN $Ca(Sr)_2RuO_4$

A Gukasov, M Braden, R J Papoular, S Nakatsuji and Y Maeno PRL, 89, 087202-1, 2002

Ru^{4+} 0.36(1)μ_B

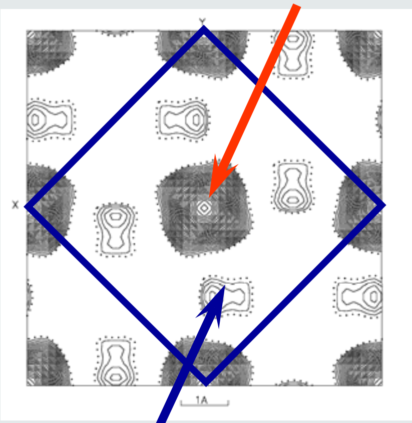

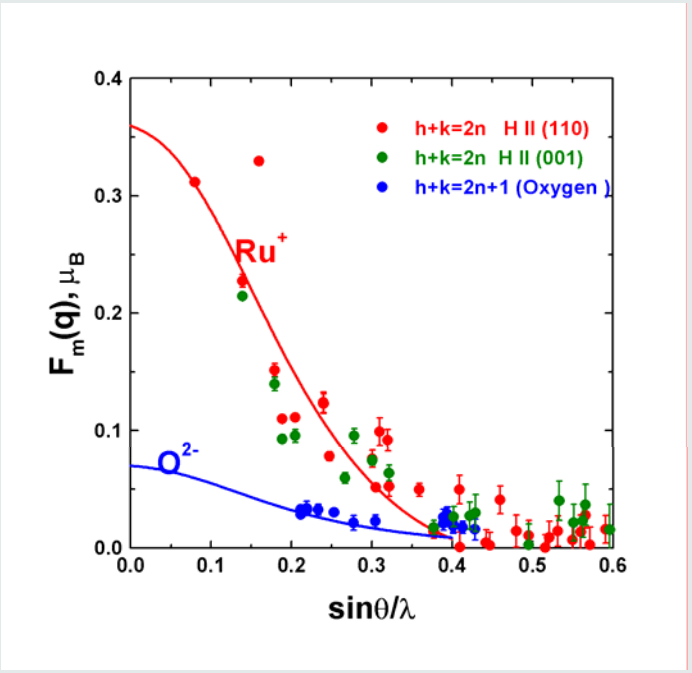

O^{2-} 0.070(2)μ_B ≈ 19% of Ru

ANOMALOUS SPIN DENSITY ON OXYGEN IN $Ca(Sr)_2RuO_4$

A Gukasov, M Braden, R J Papoular, S Nakatsuji and Y Maeno
PRL, 89, 087202-1, 2002

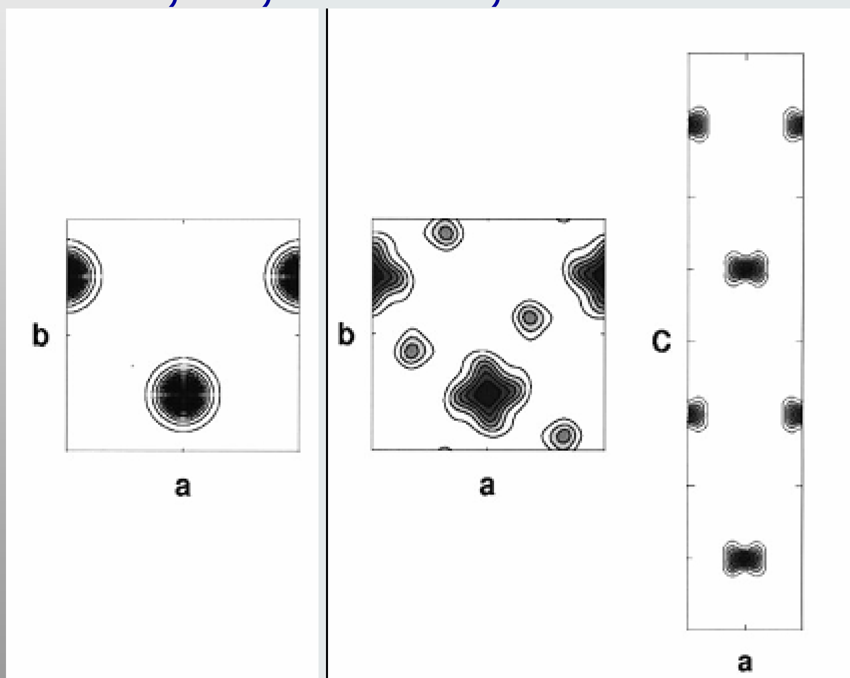

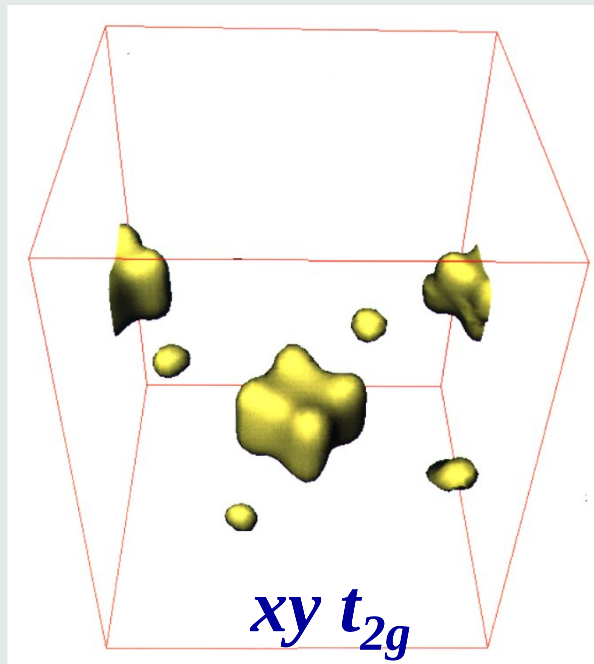

Ru^{4+} $0.36(1)\mu_B$ O^{2-} $0.070(2)\mu_B$ ≈ 19% of Ru

ON THE ORIGIN OF THE FIELD INDUCED METALIC STATE OF DOUBLE LAYERED MANGANITE $La(Pr)_{1.2}Sr_{1.8}Mn_2O_7$

F. Wang, A. Gukasov, F. Moussa, M. Hennion, M. Apostu, R. Suryanarayanan and A. Revcolevschi., PRL, 2003

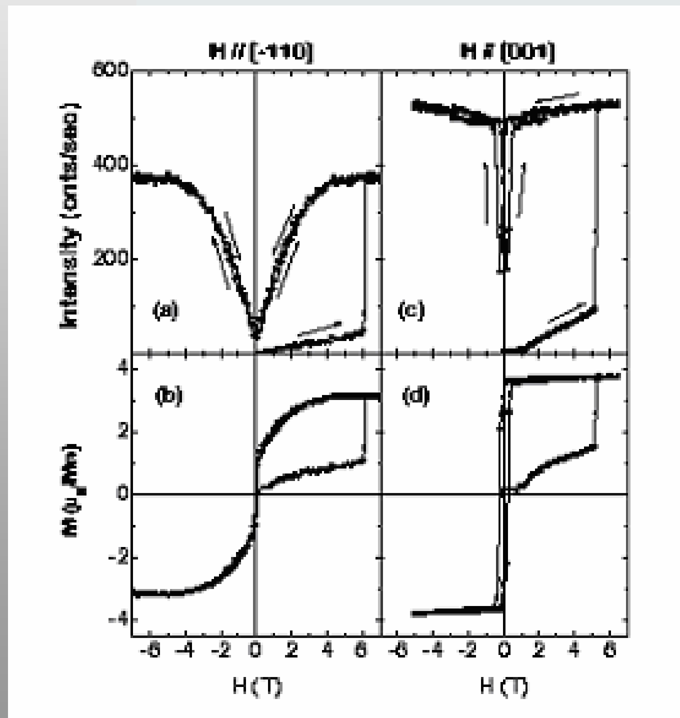

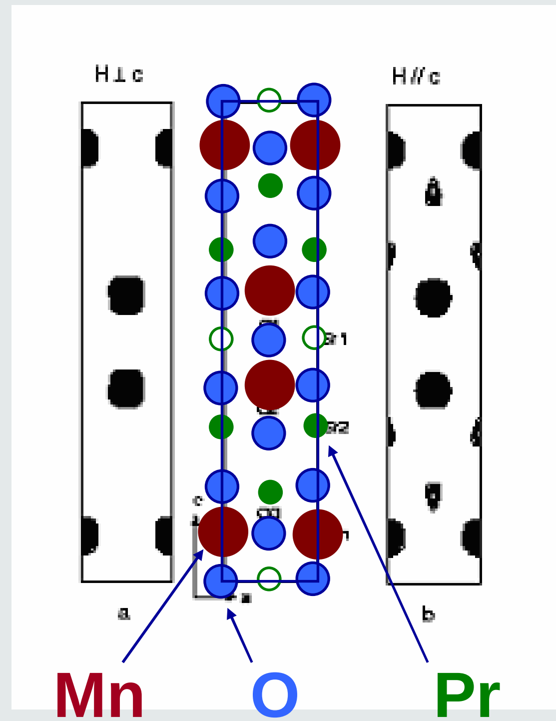

MULTIPOLE REFINEMENT FOR TWO FIELD-INDUCED STATES OF $La(Pr)_{1.2}Sr_{1.8}Mn_2O_7$

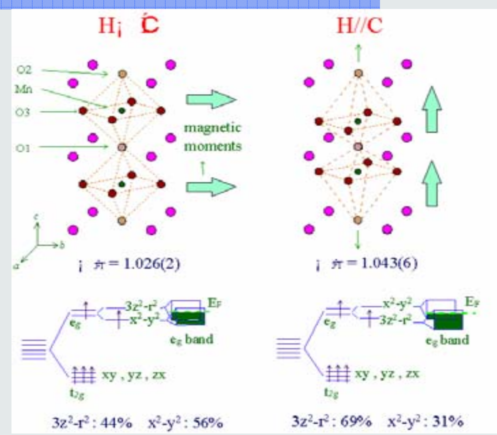

$H \perp c$	
Mn	$(\mu_S+\mu_L) = 3.36(3)\mu_B$,
Mn	$\mu_L = -0.48(4)\mu_B$
Mn	$Y_{40} = 0.50(7)$
Pr	$(\mu_s+\mu) = 0\ \mu_B$,
Pr	$\mu_L = 0\ \mu_B$

$H \parallel c$	
Mn	$(\mu_S+\mu_L) = 3.12(5)\mu_B$,
Mn	$\mu_L = -0.58\ (7)\mu_B$
Mn	$Y_{44+} = 0.35(6)$
Pr	$(\mu_s+\mu) = 0.50(3)\ \mu_B$,
Pr	$\mu_L = 0.77(4)\ \mu_B$

Spin-lattice interplay and pressure effect on the field-induced ferromagnetic metallic transition in $La(Pr)_{1.2}Sr_{1.8}Mn_2O_7$

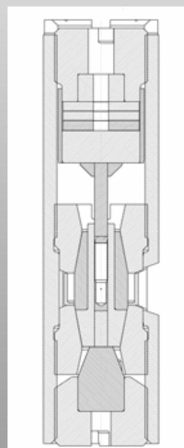

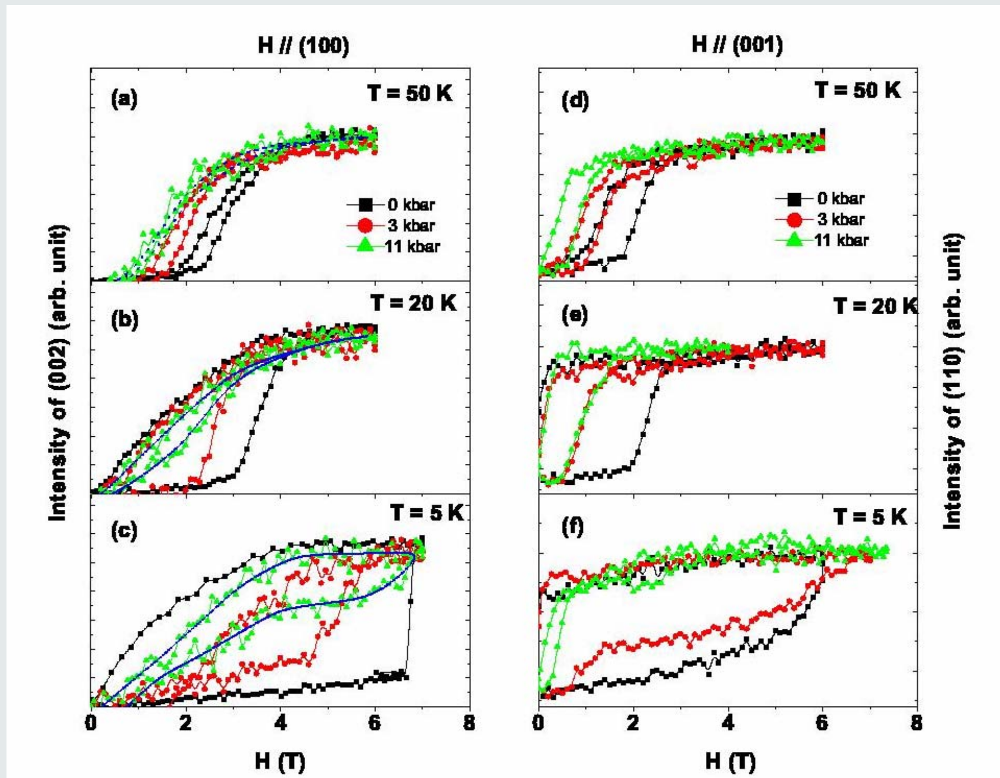

Spin-lattice interplay and pressure effect on the field-induced ferromagnetic metallic transition in $La(Pr)_{1.2}Sr_{1.8}Mn_2O_7$

A. Gukasov, B Anighoefer, F. Wang et al. (in preparation)

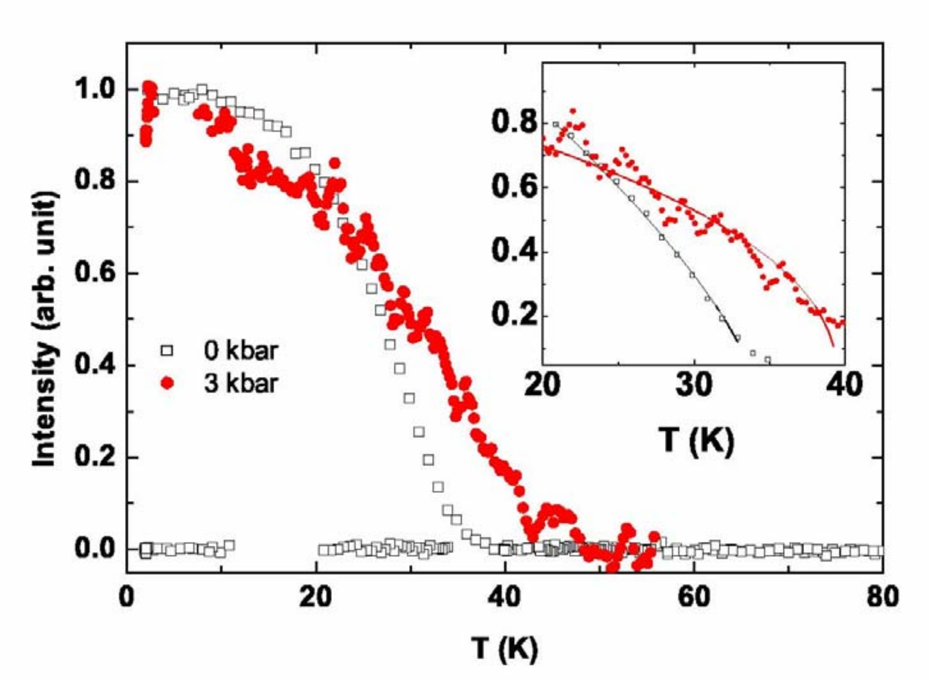

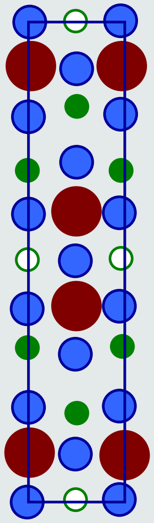

SPIN DENSITY,   WHAT IS THIS ?

DENSITY OF A PSEUDOVECTOR   ?

SPEED DENSITY

DENSITY OF A VECTOR   ?

SPEED DENSITY OF CARS IN PARIS

V_N

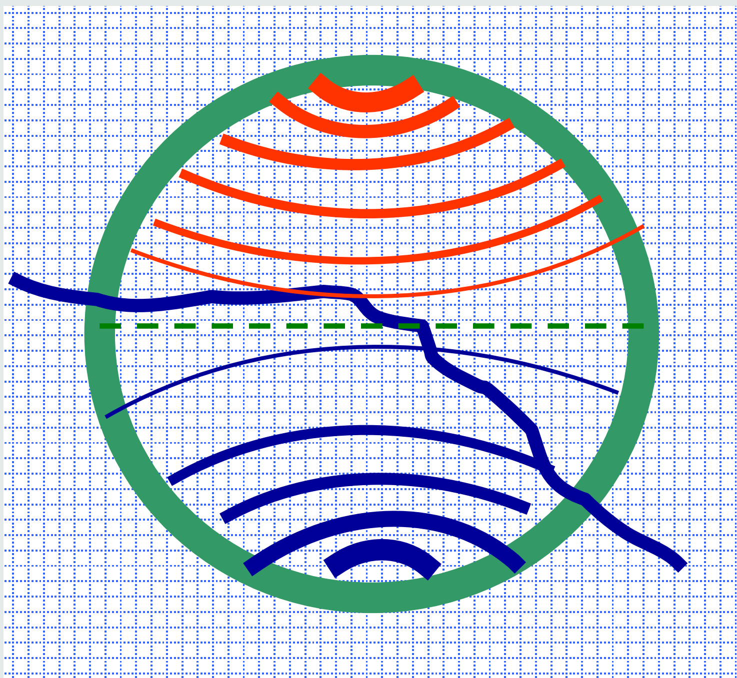

SPEED DENSITY OF CARS IN PARIS

V_E

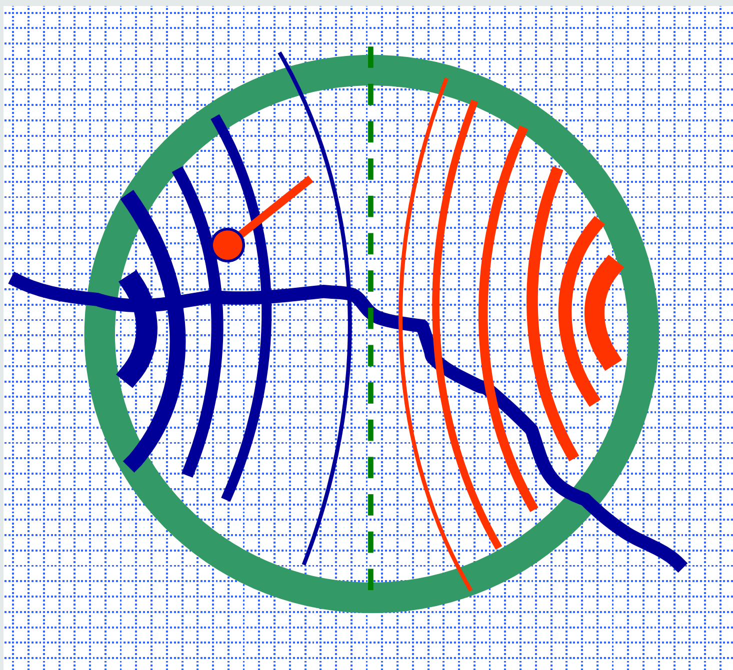

COLLINEAR AND NON-COLLINEAR SPIN DENSITIES (DISTRIBUTION)

Bulk magnetisation $M_i(r) = \chi_{ij} H_j$

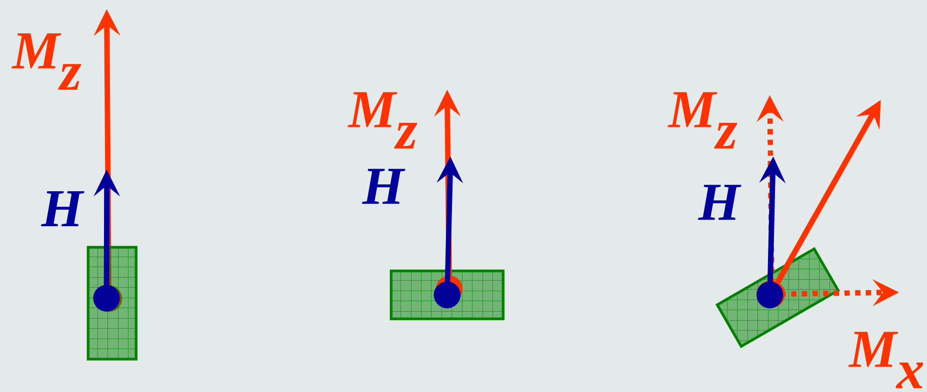

$$I^{\pm} \propto F^2_N \pm 2(\underline{P}_0 * \underline{F}_M)\, F_N + F_M^{\;2}$$

$$I^{\pm} \propto F^2_N \pm 2F_{Mz}\, F_N + F_M^{\;2}$$

NONCOLLINEAR MAGNETIZATION IN $HoCo_{10}Ti_2$

Yuri Janssen, A. Gukasov, E. Brück, K.H.J . Buschow and F.R. de Boer

$ThMn_{12}$ structure I4/mmm

a=b=8.4 A, c=4.7 A

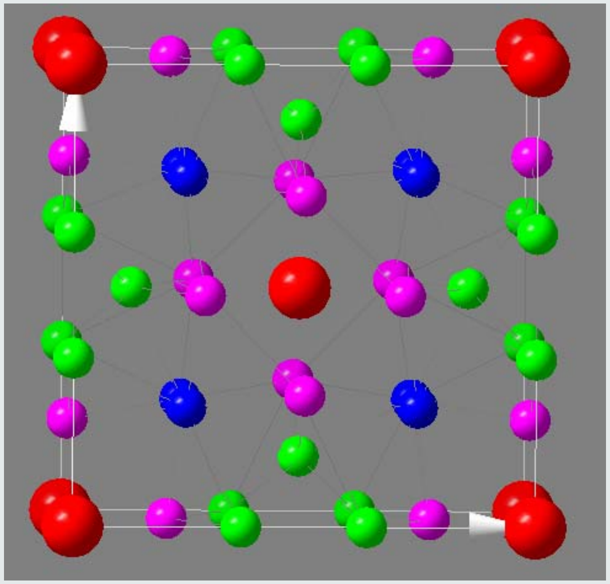

2 (a)	(0 0 0)	Ho	
8 (f)	(¼ ¼ ¼)	Co1	
8 (j)	(0.28 ½ 0)	Co2	
8 (i)	(0.36 0 0)	Co3	0.56(1)
		Ti	0.44(1)

NONCOLLINEAR MAGNETIZATION IN $HoCo_{10}Ti_2$

Yuri Janssen, A. Gukasov, E. Brück, K.H.J . Buschow and F.R. de Boer

$ThMn_{12}$ structure I4/mmm

a=b=8.4 A, c=4.7 A

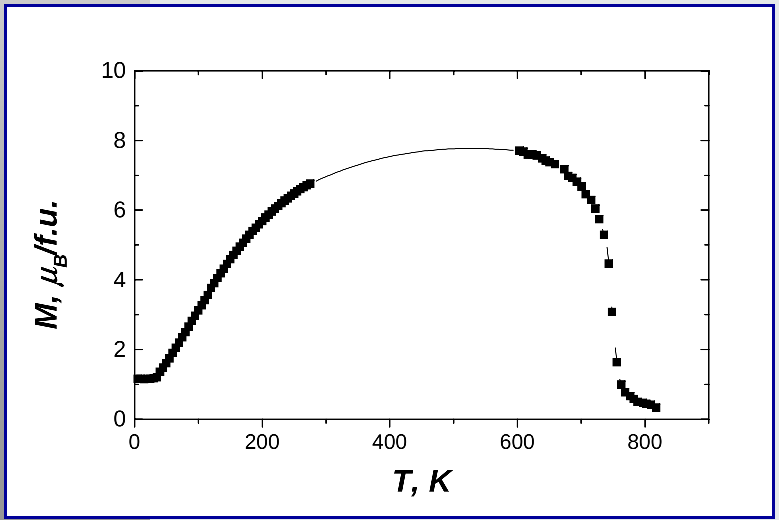

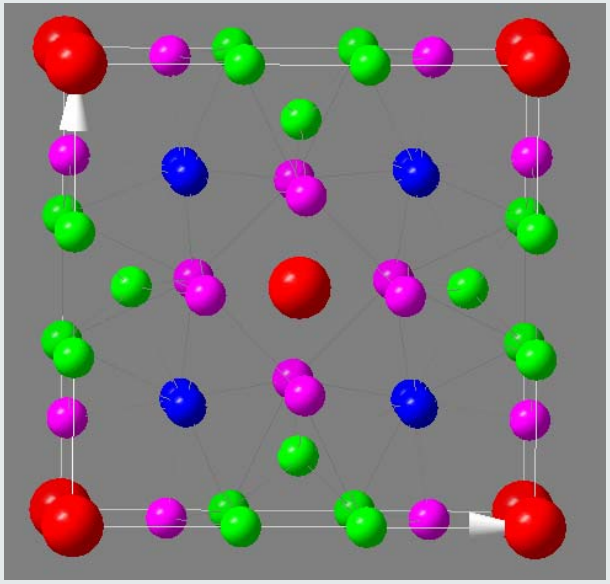

$HoCo_{10}Ti_2$, UNPOLARIZED NEUTRON DIFFRACTION

Single crystal of diameter 1.2 mm !
6T2, 4-circles LLB, 86 independent reflections per T

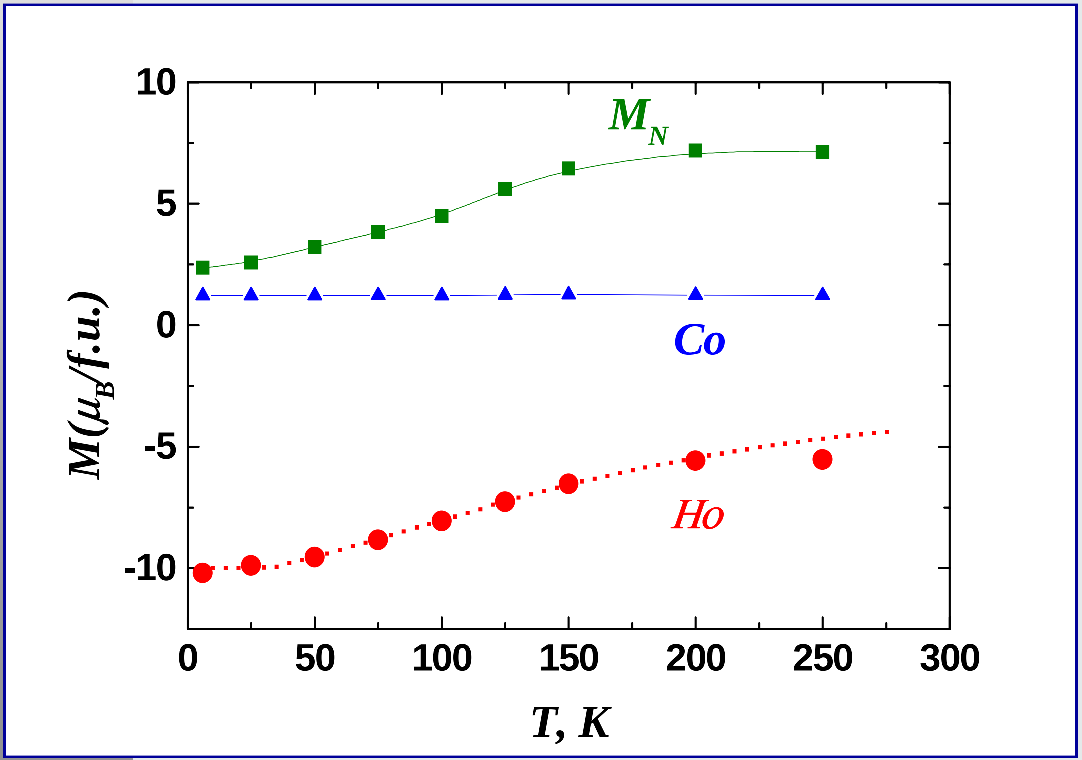

Ho 10.0(1) μ_B

Co1 1.25(3) μ_B

Co2 1.24(3) μ_B

Co3 1.27(3) μ_B

$HoCo_{10}Ti_2$, UNPOLARIZED NEUTRONS

Single crystal of diameter 1.2 mm !
6T2, 4-circles LLB, 86 independent reflections per T

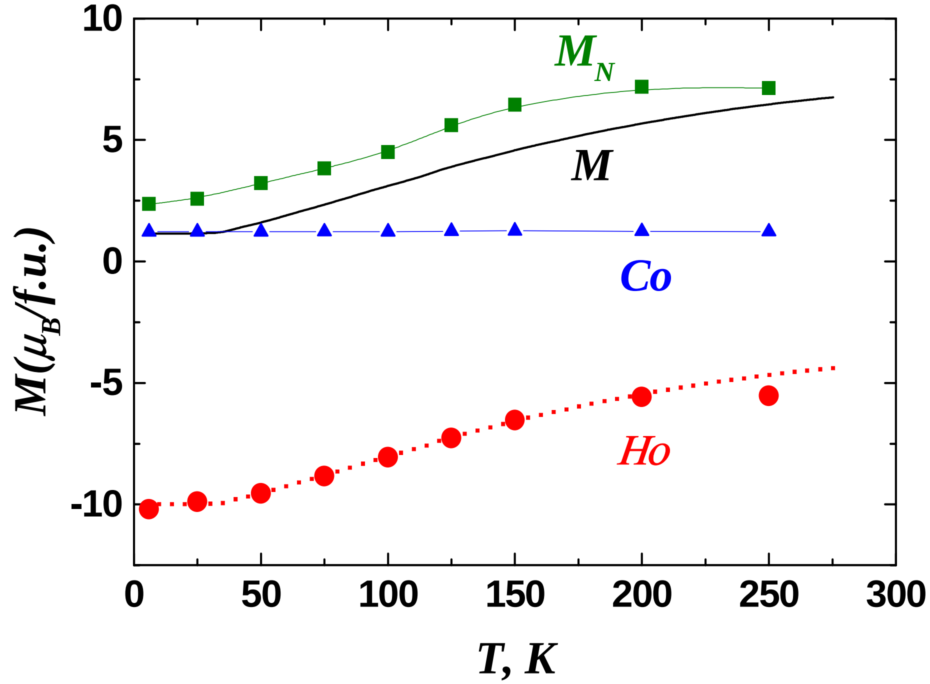

Ho 10.0(1) μ_B

Co1 1.25(3) μ_B

Co2 1.24(3) μ_B

Co3 1.27(3) μ_B

M_N 2.5 μ_B

M 1.2 μ_B

$HoCo_{10}Ti_2$, UNPOLARIZED NEUTRONS

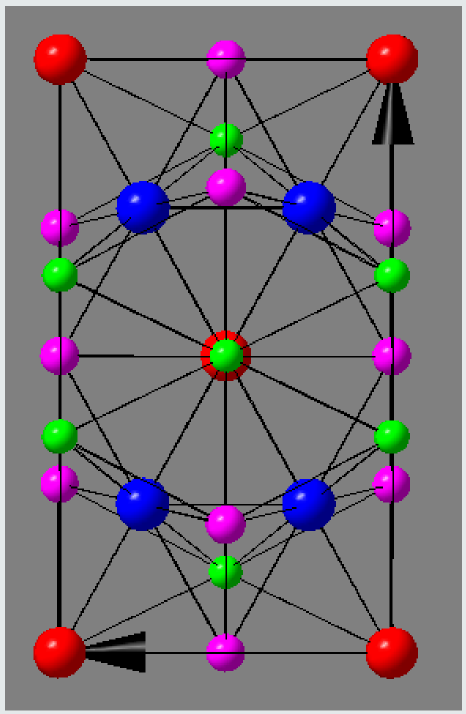

5 K

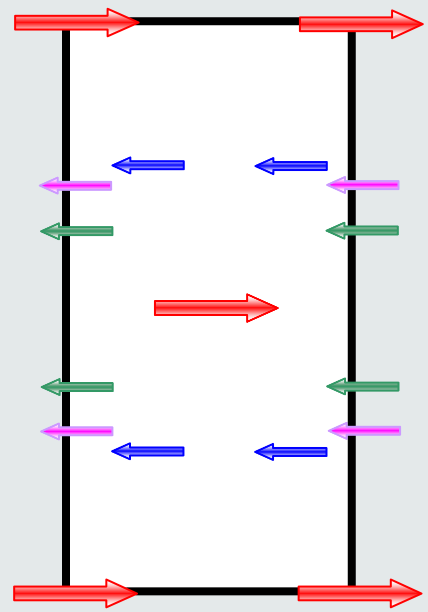

M_N=2.5 μ_B M=1.2 μ_B

$M_{cond=}$ 0.13 μ_B / Co

MAGNETIC ANISOTROPY IN $HoCo_{10}Ti_2$

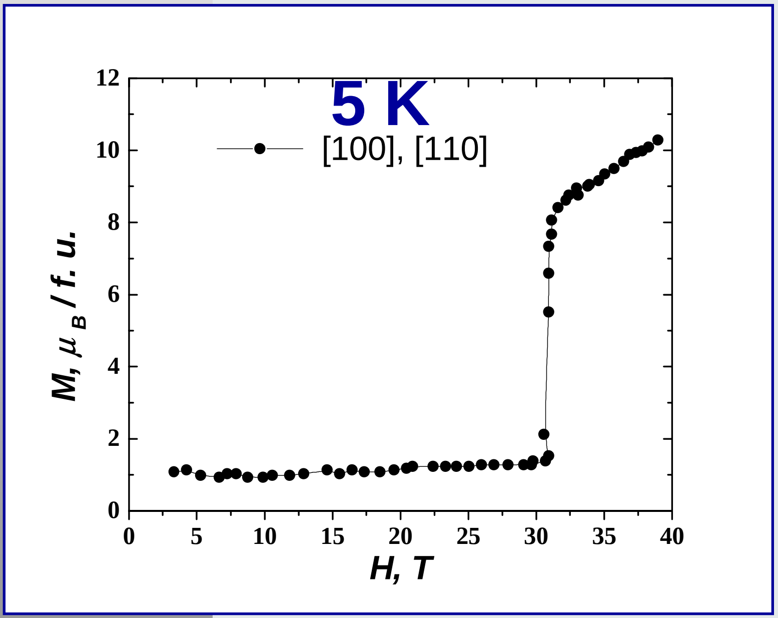

5 K

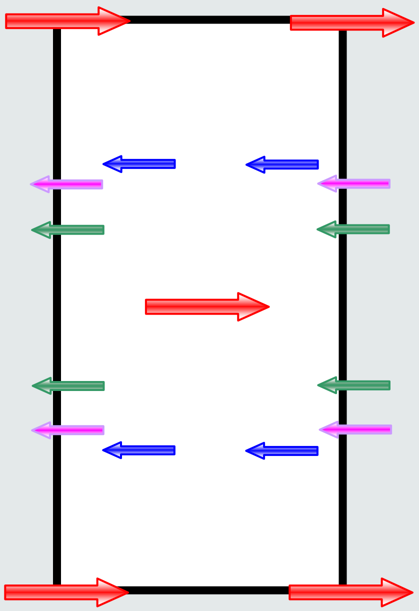

M_{TOT}=10x1.25+10 =22.5 μ_B

MAGNETIC ANISOTROPY IN $HoCo_{10}Ti_2$

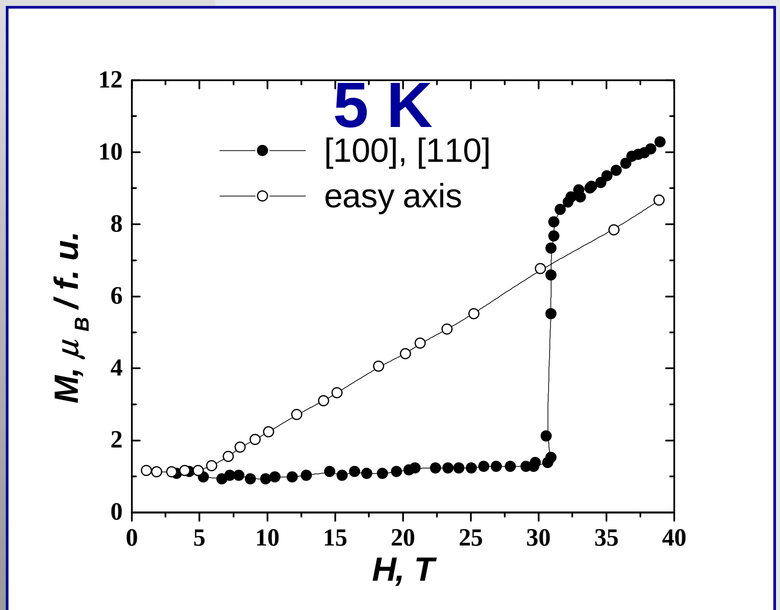

5 K

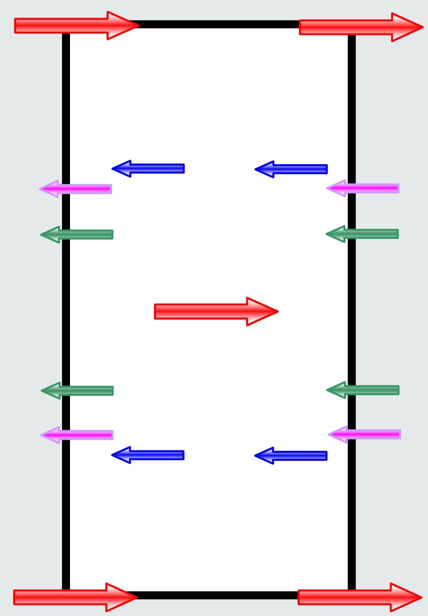

M_{TOT}=10x1.25+10 =22.5 μ_B

LONGITUDINAL MAGNETIZATION IN $HoCo_{10}Ti_2$

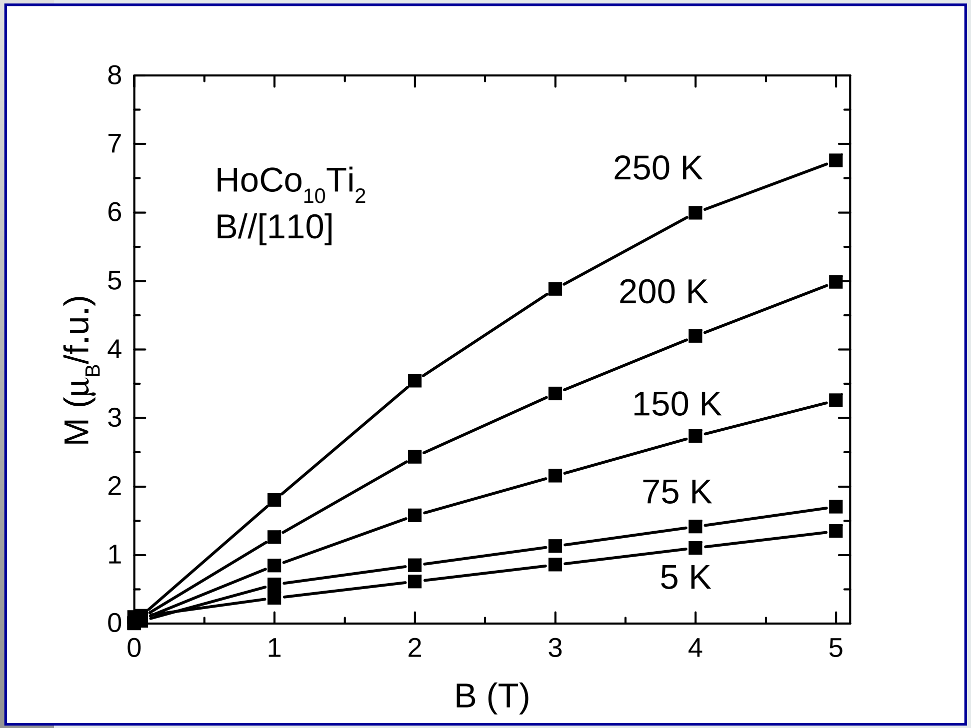

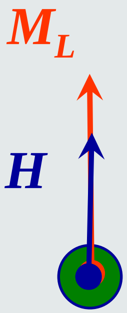

POLAR MAGNETIZATION MEASUREMENT IN $HoCo_{10}Ti_2$

Yuri Janssen. Ph. D Thesis

250 K

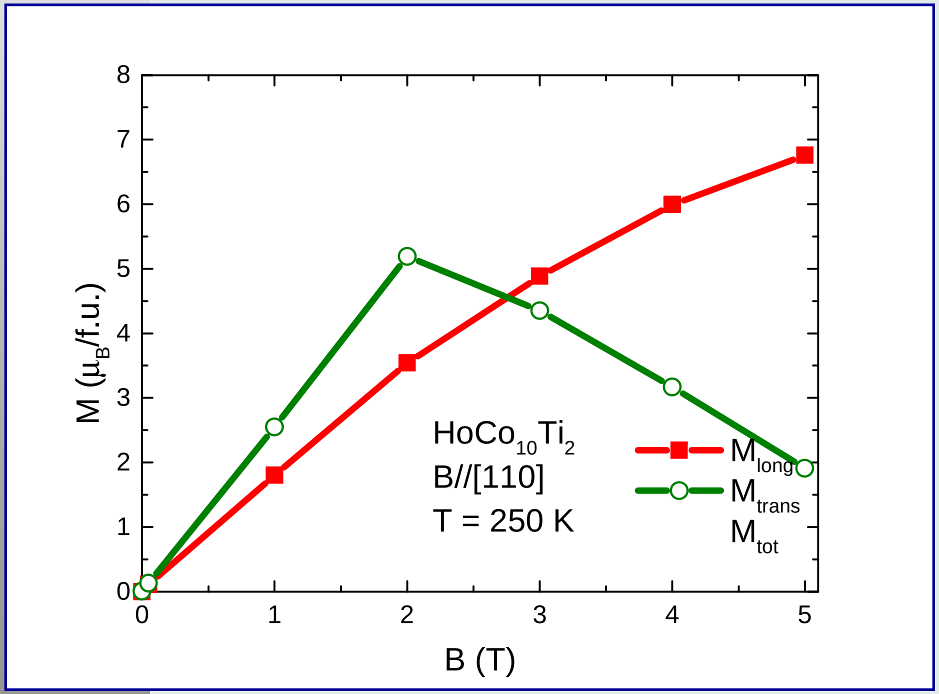

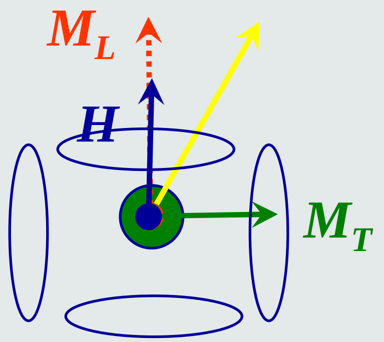

MAGNETIC ANISOTROPY IN $HoCo_{10}Ti_2$

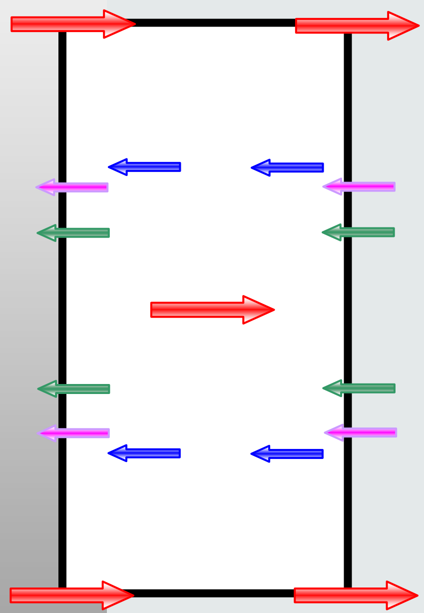

5 K

H 7.5 T 5 K

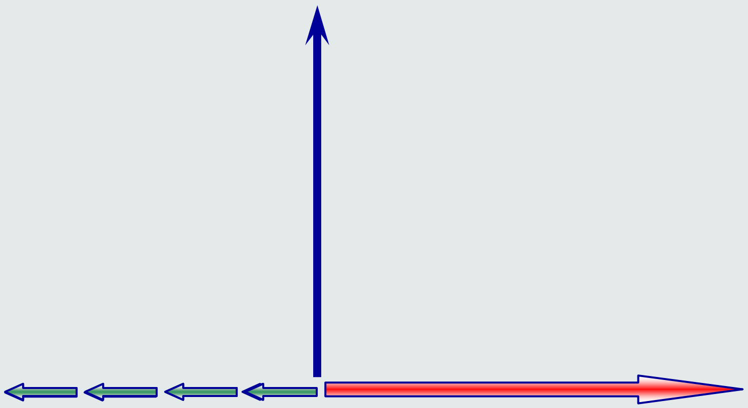

MAGNETIC ANISOTROPY IN $HoCo_{10}Ti_2$

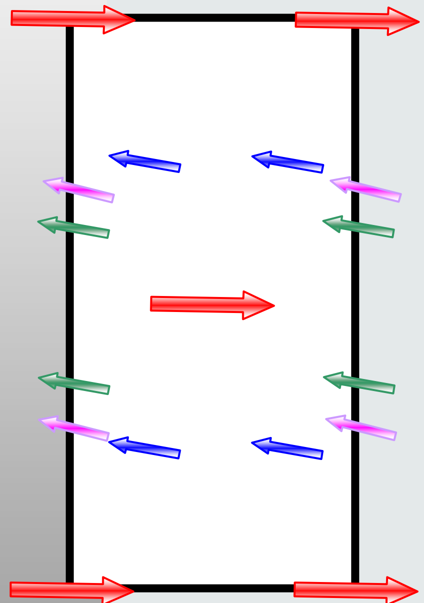

50 K

H 7.5 T 50 K

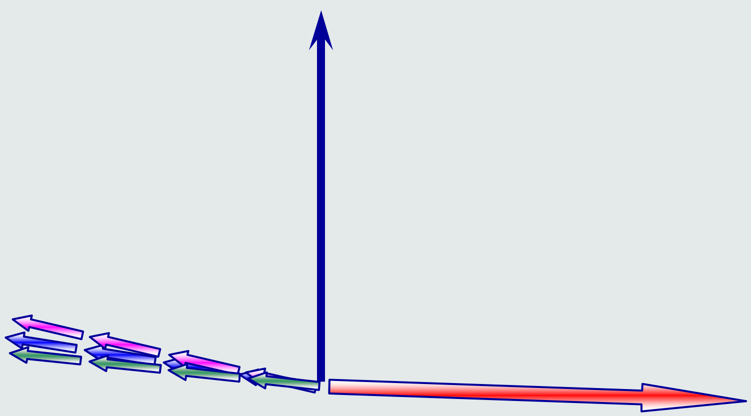

MAGNETIC ANISOTROPY IN $HoCo_{10}Ti_2$

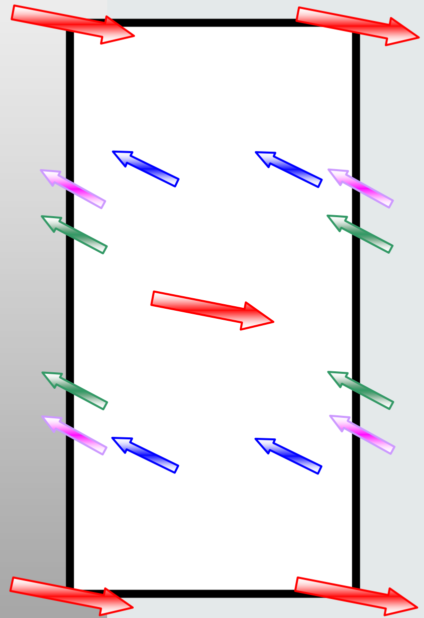

100 K

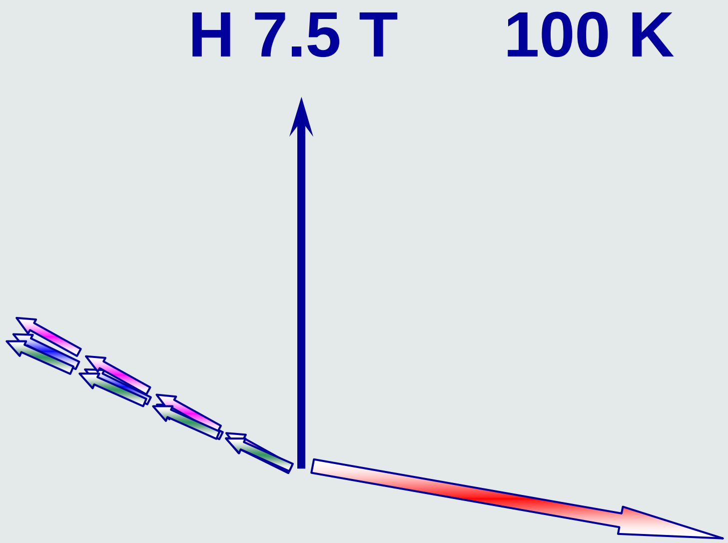

MAGNETIC ANISOTROPY IN $HoCo_{10}Ti_2$

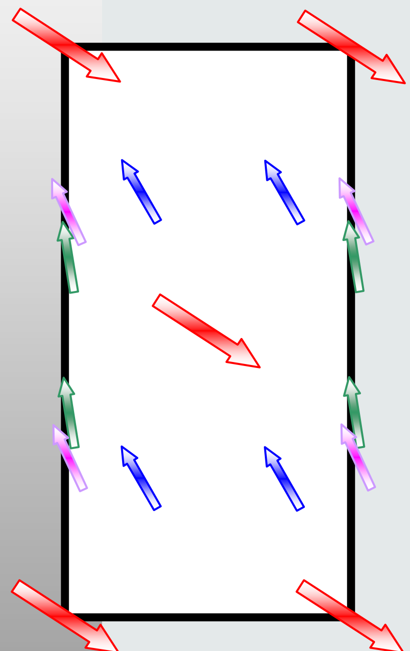

150 K

H 7.5 T   150 K

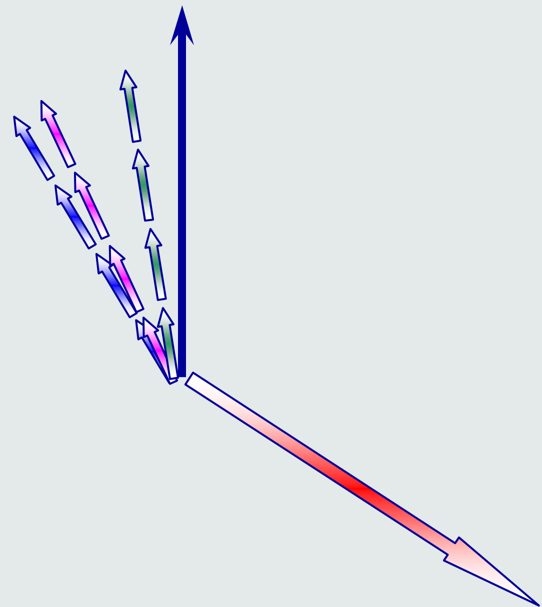

MAGNETIC ANISOTROPY IN $HoCo_{10}Ti_2$

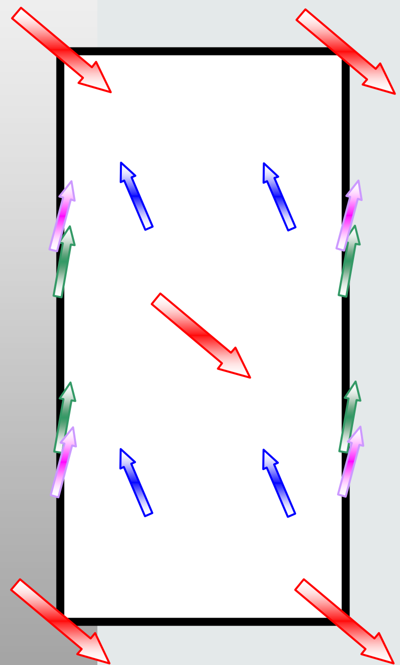

200 K

H 7.5 T 200 K

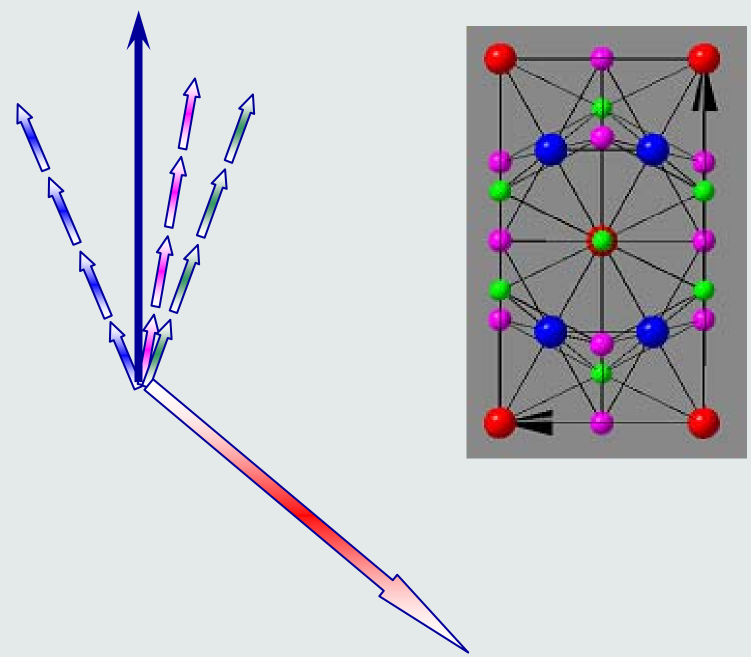

CONCLUSION

- **PND gives POLAR SITE MAGNETISATION**

250 K H=7.5 T

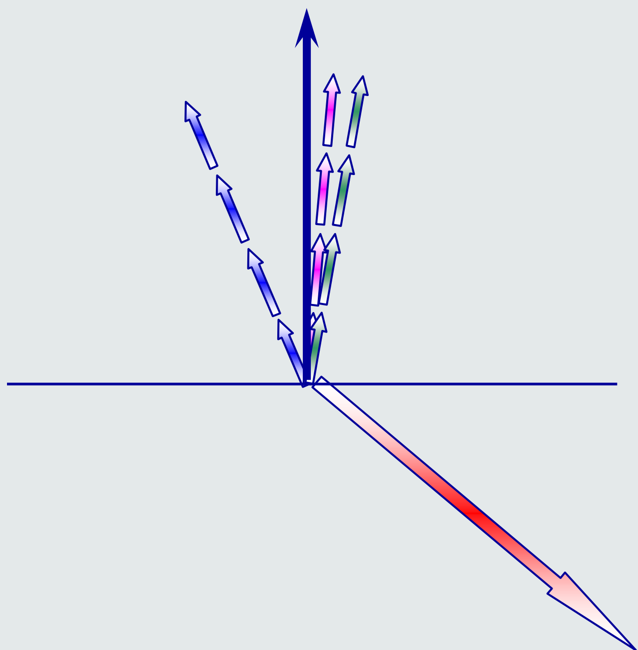

Yu. Janssen, A. Gukasov, E. Brück, K.H.J . Buschow and F.R. de Boer.

MAGNETIC STRUCTURE OF $U_3Al_2Si_3$: POLARIZED NEUTRONS DIFFRACTION REFINEMENT

Ternary compounds $U_3M_2M'_3$ with M=Al,Ga M' =Si, Ge
SG I4/mcm derivative of the antitype-Cr_5B_3

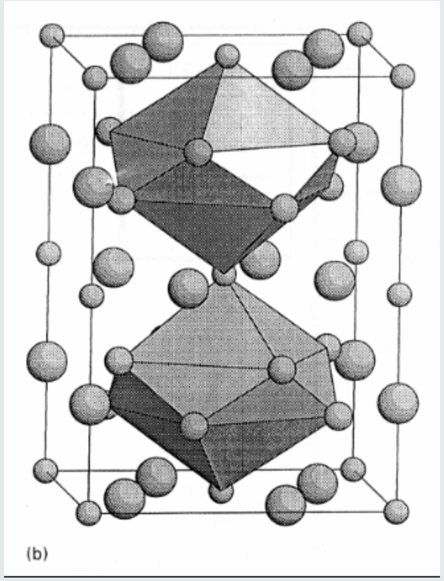

U1,U2

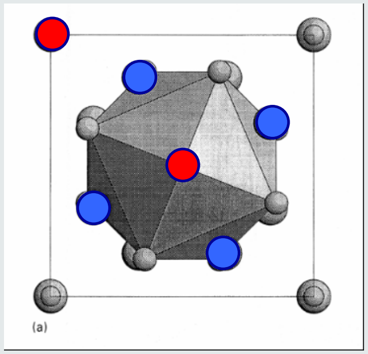

4_z x U3

F. Weitzer, M Potel, H Noel, P Rogl, J Sol. St. Chem, 111, 267, 1994

NEUTRON POWDER DIFFRACTION FROM $U_3Al_2Si_3$

G4.1 ORPHEE, CEA-Saclay

no extra peaks
***k*=0**

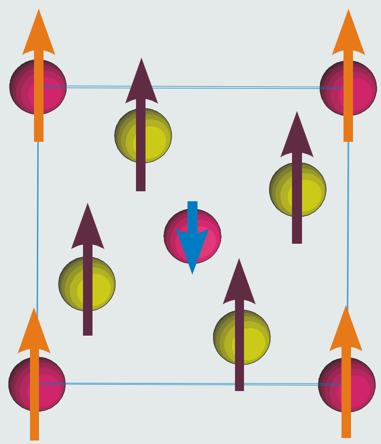

U1 = 1.13 μ_B
U2 = -0.46 μ_B
4 x U3 = 1.26 μ_B

Spin direction in the ab plane

P Rogl , G Andre, F Bouree and H Noel, JMMM, 191, 291, 1999

SINGLE CRYSTAL . UNPOLARIZED NEUTRONS

4-circle 6T2 LLB, Saclay 0.9 Å; 227 reflections (122 independent) measured at 70K
R_{F2} =5.05%

Magnetic structure

-compatible with powder results but -
there is another (noncollinear) solutions with about the same *R_{F2} =6.8-7.1%*

POLARIZED NEUTRONS

5C1 LLB, Saclay 0.84 Å H=2T || 110 and H ||100

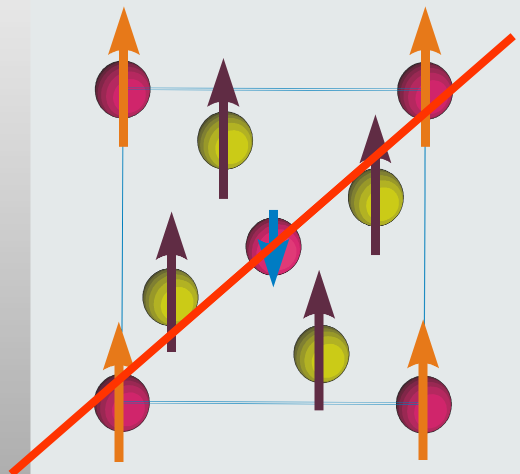

χ^2=62.5

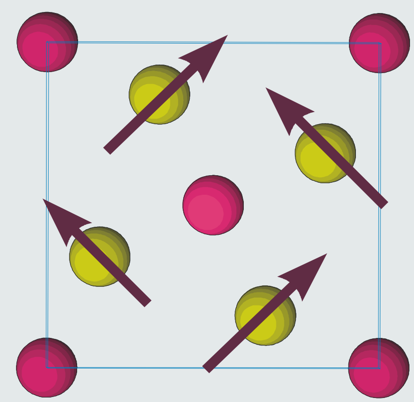

χ^2=5.3

BEST MODEL : χ^2=3.2

θ=38°(3) θ=-42°(3) U1 = U2 = 0.16 μ_B

4 x U3 = 1.29 μ_B

SITE SUSCEPTIBILITY IN PARAMAGNETIC REGION ($U_3Al_2Si_3$)

T=100 K T_c =37 K

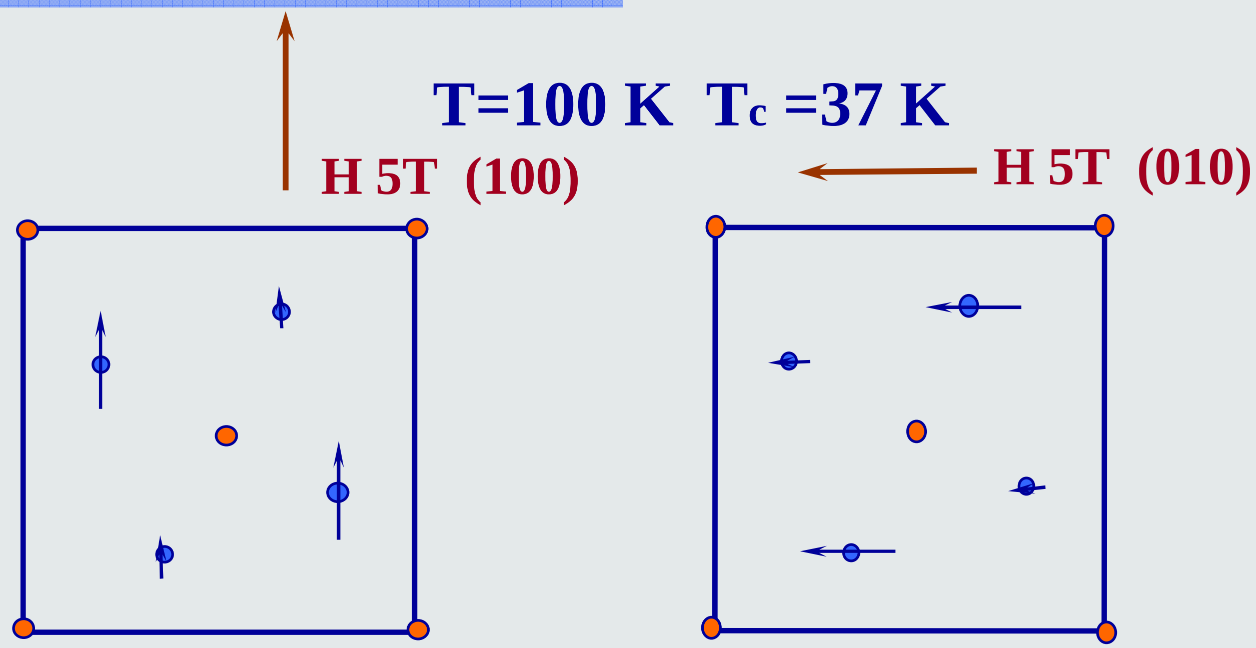

SITE SUSCEPTIBILITY IN PARAMAGNETIC REGION ($U_3Al_2Si_3$)

100 K H 5T (100)

100 K H 5T (110)

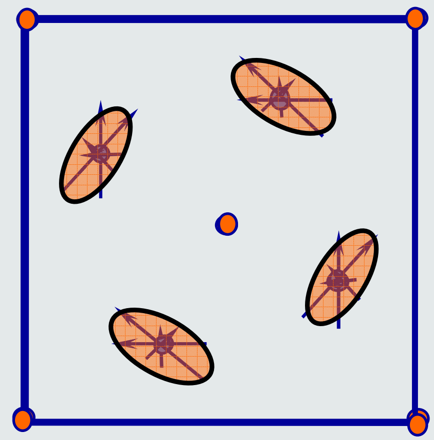

$$M^{\alpha}(\mathbf{r})=\chi^{\alpha\beta}(\mathbf{r})\,H^{\beta}$$

$U_3Al_2Si_3$ IN PARAMAGNETIC REGION

A Gukasov, P Rogl, P J Brown, M Mihalik and A Menovsky.
J. Phys. C, 14, 8984 2002

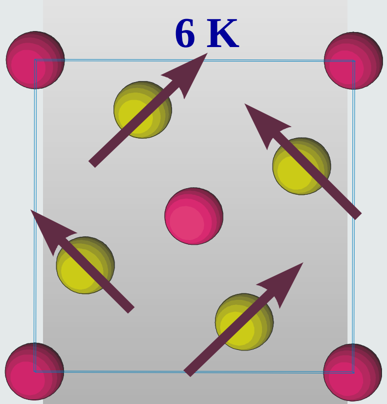

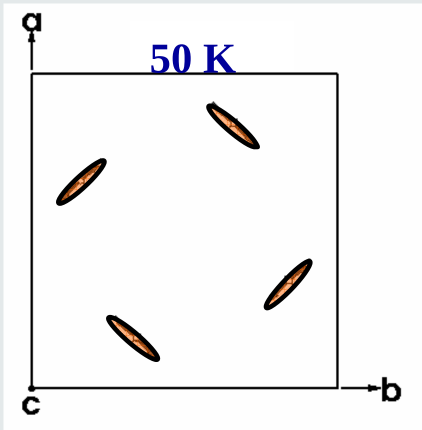

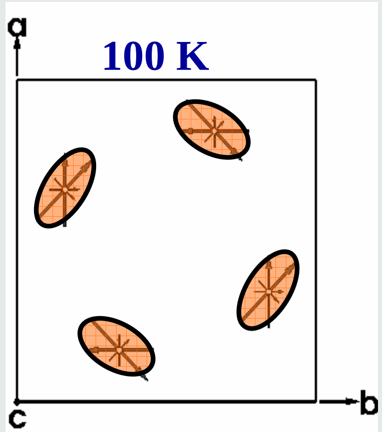

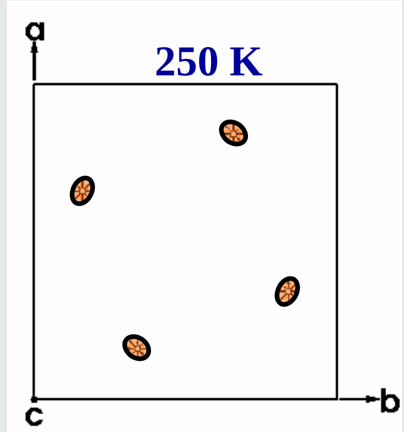

ANISOTROPIC SUSCEPTIBILITY

CUBIC, $\chi_{11} = \chi_{22} = \chi_{33}$

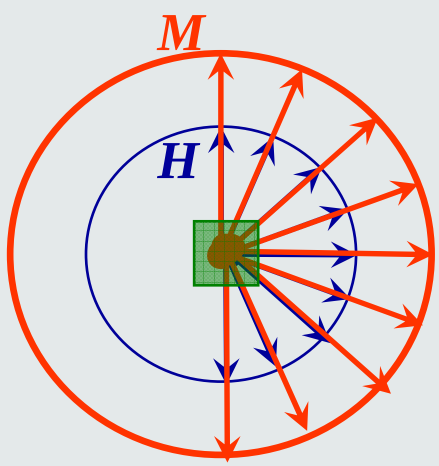

$$\chi_{ij} = \begin{pmatrix} \chi_{11} & 0 & 0 \\ 0 & \chi_{11} & 0 \\ 0 & 0 & \chi_{11} \end{pmatrix}$$

UNIAXIAL $\chi_{11} = \chi_{22} < \chi_{3}$

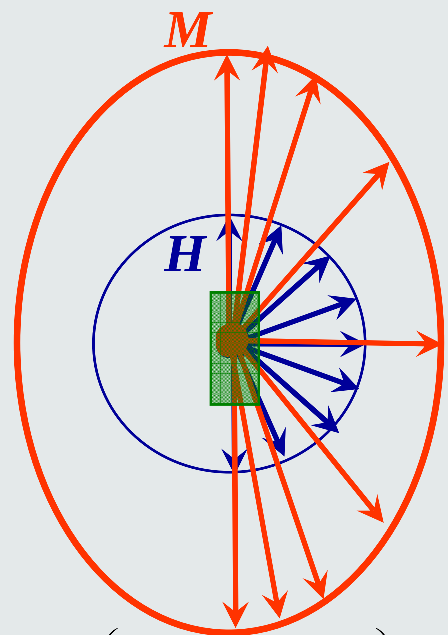

$$\chi_{ij} = \begin{pmatrix} \chi_{11} & 0 & 0 \\ 0 & \chi_{11} & 0 \\ 0 & 0 & \chi_{33} \end{pmatrix}$$

ANISOTROPIC SUSCEPTIBILITIES

$$\chi_{ij} = \begin{pmatrix} \chi_{11} & \chi_{12} & \chi_{13} \\ & \chi_{22} & \chi_{23} \\ & & \chi_{33} \end{pmatrix}$$

Bulk magnetisation $M_i(r) = \chi_{ij} H_j$

The number of independent components of χ_{ij} is determined by the crystal symmetry class:

cubic groups	**1**	**parameter**
all uniaxial groups	**2**	**parameters**
Orthorhombic	**3**	**...**
Monoclinic	**4**	**...**
Triclinic	**6**	

ANISOTROPIC SUSCEPTIBILITIES

Bulk magnetisation

$$M_i = \Sigma_a M^a{}_i = \Sigma_a \chi^a{}_{ij} H_j$$

$$M^b{}_i = R(t)\, \chi^a{}_{ij}\, R(t)^{-1} H_j$$

$R(t)$ is the symmetry operator $\quad r_b = R(t)\, r_a$

$$M_i = \Sigma_a R(t)\, \chi^a{}_{ij}\, R(t)^{-1} H_j$$

REFINEMENT OF ANISOTROPIC SUSCEPTIBILITIES

$$I^{\pm} \propto N^2 \pm 2 P_0 N M_z + M^2$$

$$M_i = \chi^a_{ij} H_j$$

$$\chi_{ij} = \begin{pmatrix} \chi_{11} & \chi_{12} & \chi_{13} \\ & \chi_{22} & \chi_{23} \\ & & \chi_{33} \end{pmatrix}$$

$$I^{\pm} \propto N^2 \pm 2F_N(P_0 * \chi^a_{ij} H_j) + |\chi^a_{ij} H_j|^2$$

$$R = I^+ / I^-$$

TEMPERATURE DEPENDENCE OF *MAGNETIC ELLIPSOIDS* IN $U_3Al_2Si_3$

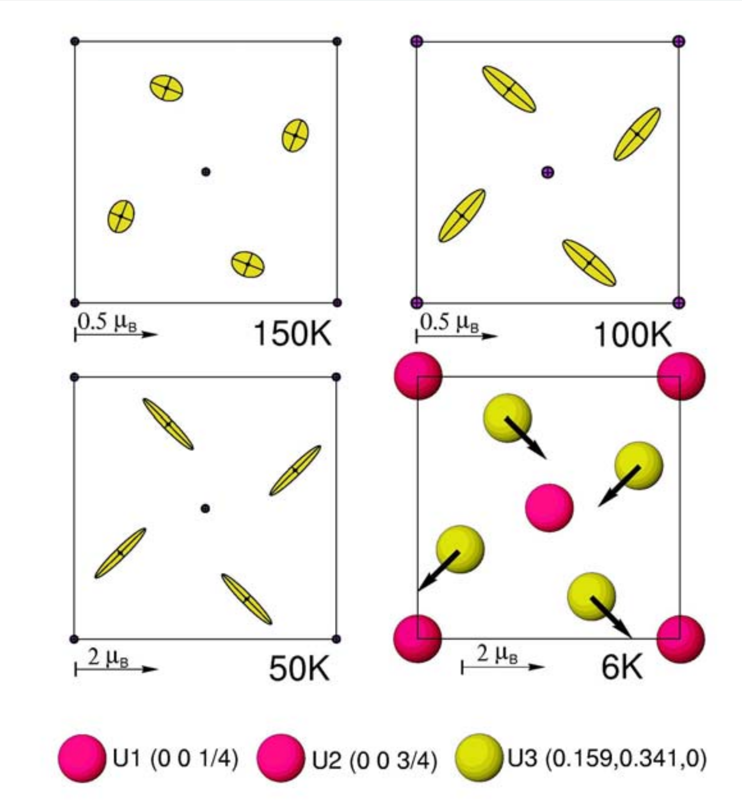

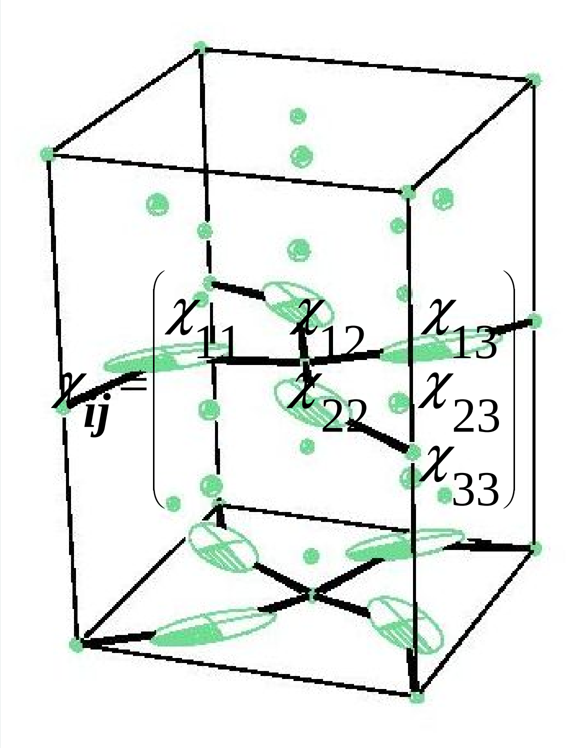

TEMPERATURE DEPENDENCE OF *MAGNETIC ELLIPSOIDS* IN $U_3Al_2Si_3$

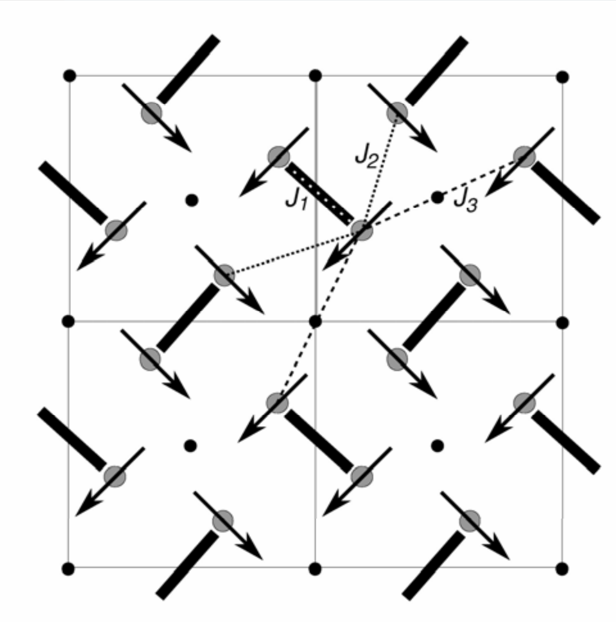

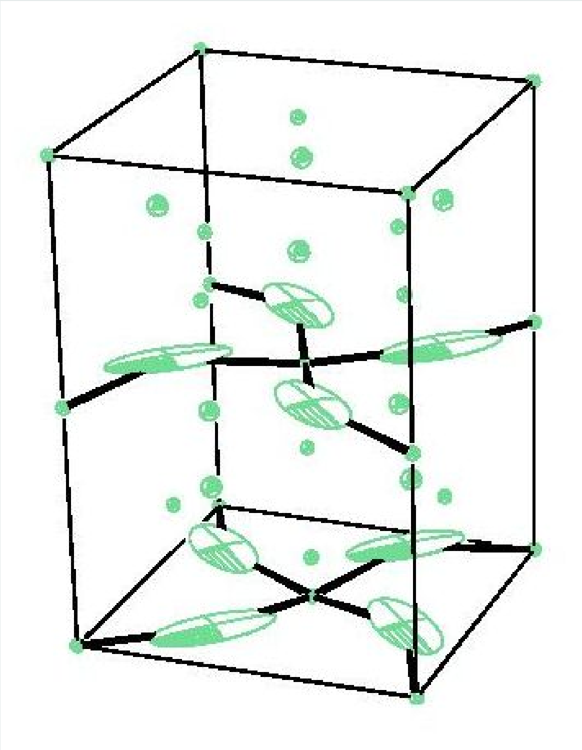

PROLATE AND OBLATE MAGNETIC ELLIPSOIDS

Prolate **$Sm_3 Te_4$**

$\chi_{11} < \chi_{33}$

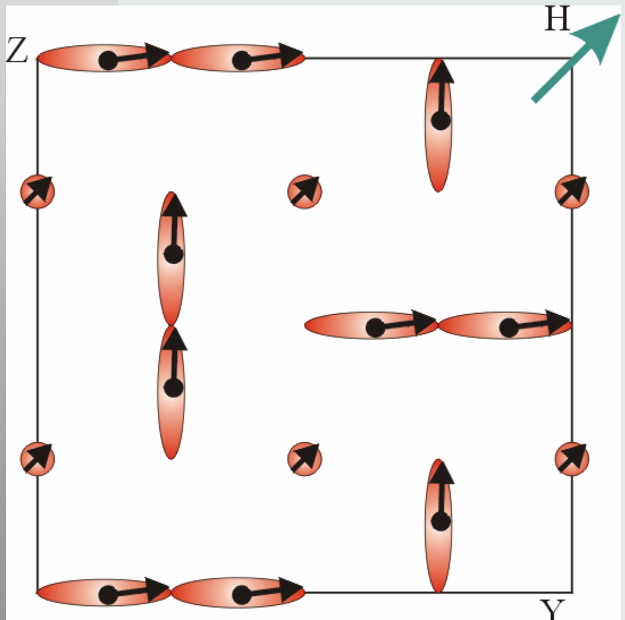

Oblate **$Nd_{3-x} S_4$**

$\chi_{11} > \chi_{33}$

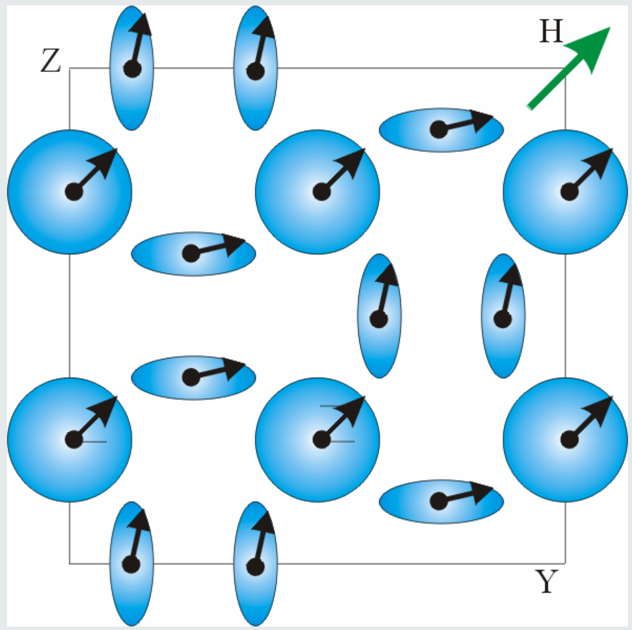

OBLATE MAGNETIC ELLIPSOIDS IN $Nd_{3-x}S_4$

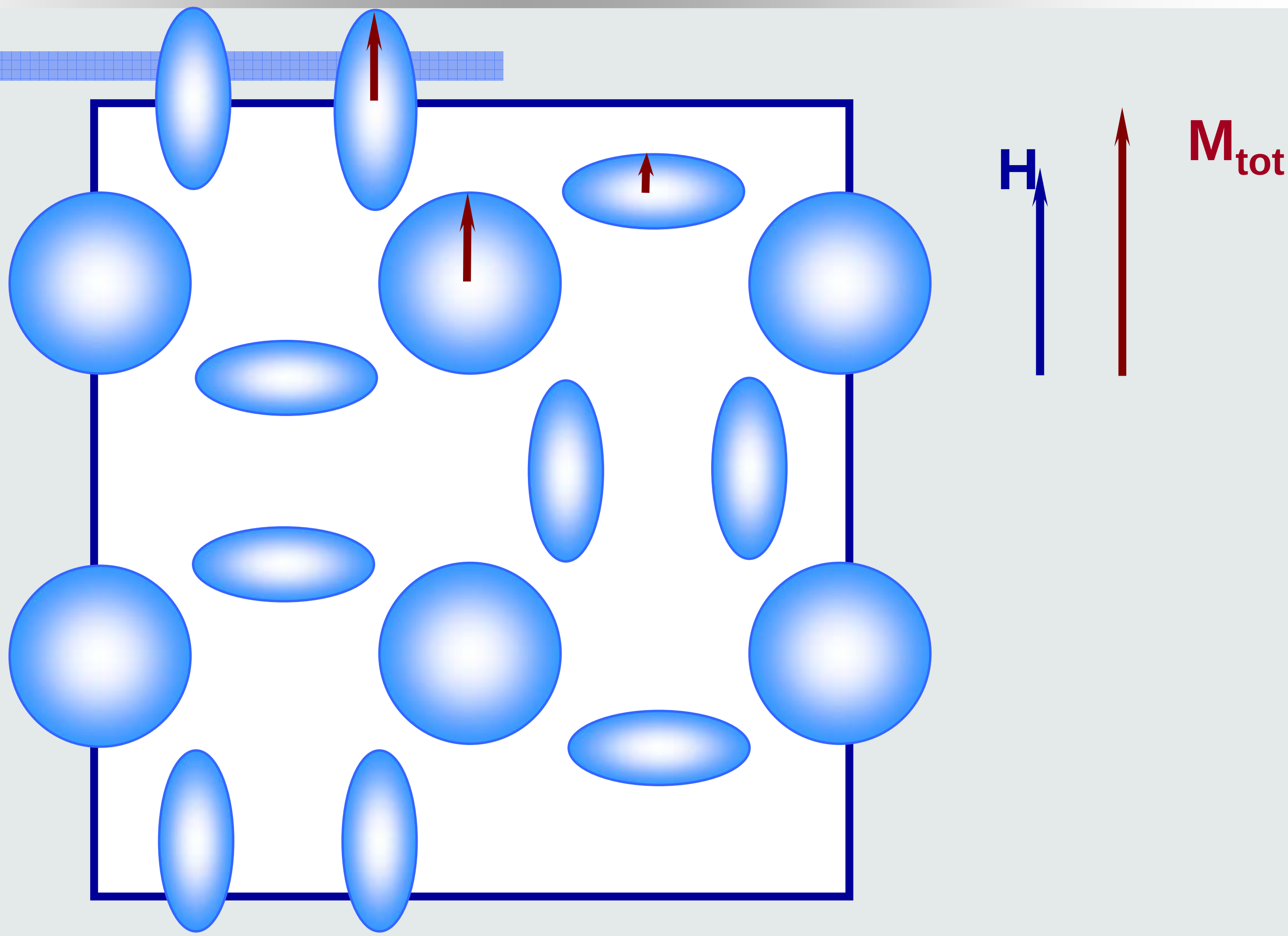

A Gukasov and P J Brown, J Phys C, 14, 8831, 2002

OBLATE MAGNETIC ELLIPSOIDS IN $Nd_{3-x} S_4$

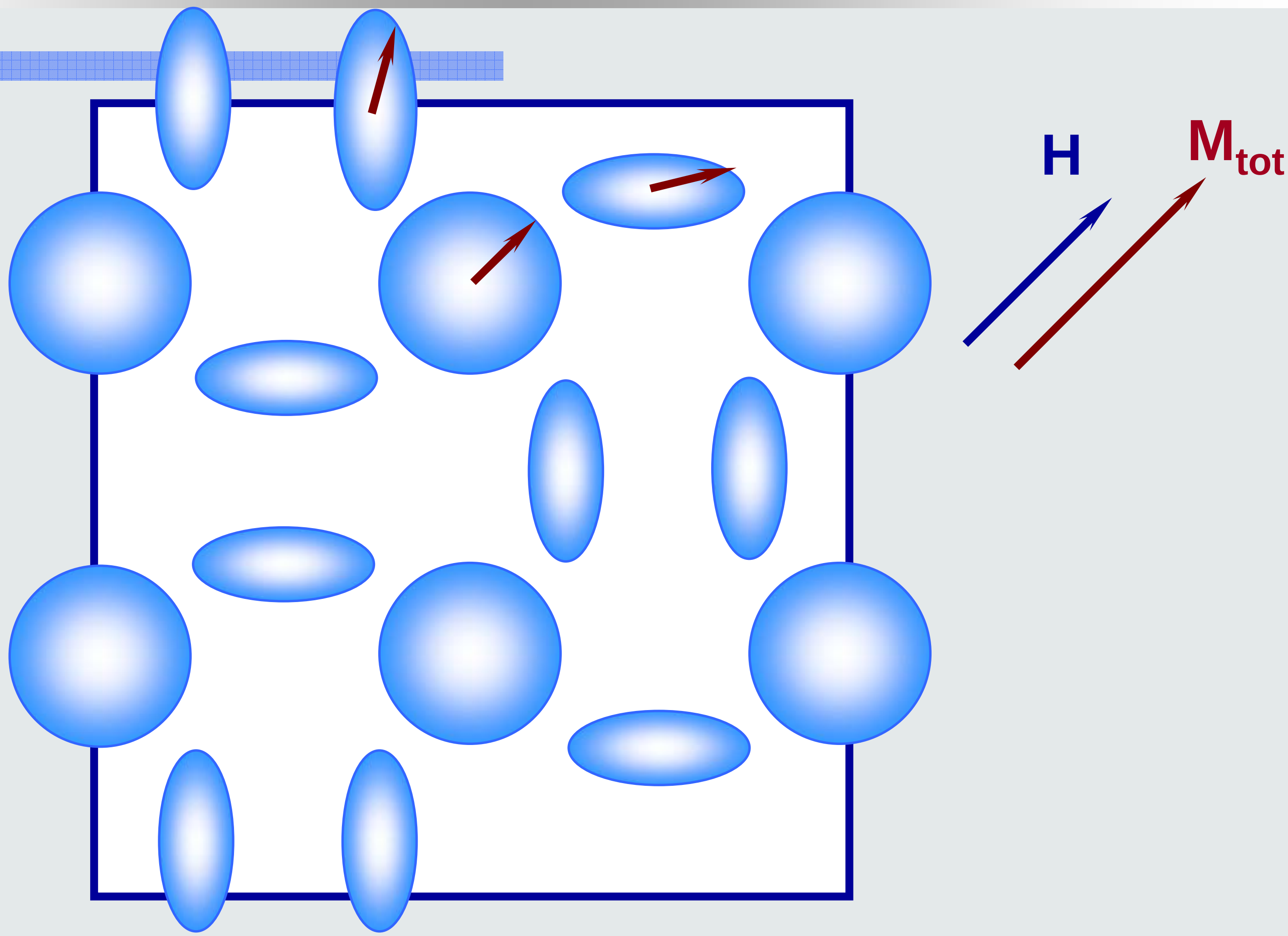

A Gukasov and P J Brown, J Phys C, 14, 8831, 2002

OBLATE MAGNETIC ELLIPSOIDS IN $Nd_{3-x}S_4$

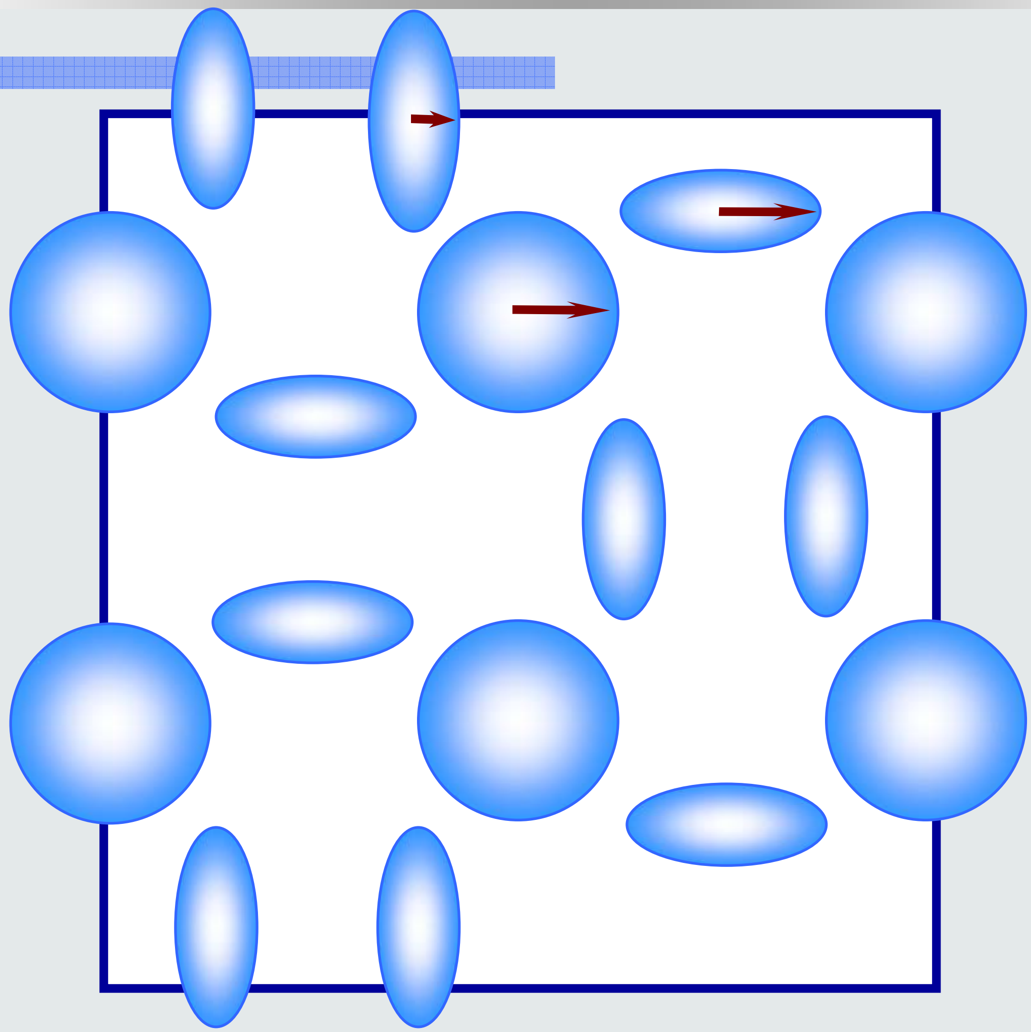

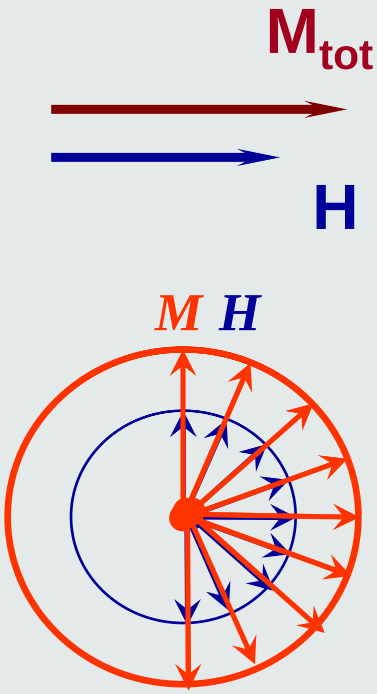

A Gukasov and P J Brown, J Phys C, 14, 8831, 2002

ATOMIC DISPLACEMENT PARAMETERS (ADPs) AND ATOMIC SUSCEPTIBILITY PARAMETES (ASPs)

- ADPs are a probe of the shape of elastic potential well
- ADPs give informaton about atomic vibration, dynamics, disorder ...

- ASPs :are a probe of magnetic interaction
- symmetry constraints of ASPs the same as for ADPs
- Anomalous ASPs indicate strong local anisotropy and a possible channel of ordering

CONCLUSIONS

- PN give access :
  - to small magnetic densities (10^{-3} μB)
  - wave vector susceptibility χ (q)
  - local susceptibility tensor $\chi^{\alpha\beta}$ (r)
- Very large covalency in Rutenates and rather ordinary one in garnets
- Very high magnetisation ‘ prolate ’ anisotropy for Sm3Te4 and medium ‘ oblate ’ for Nd3S4

MOST IMPORTANT CONCLUSION

- **In a paramagnetic state the moments of equivalent atoms are equal, but...**
- **under magnetic field some of them will be more equal than the others !**

Light Induced Excited Spin State Trapping (LIESST) in $Fe(ptz)_6](BF_4)_2$

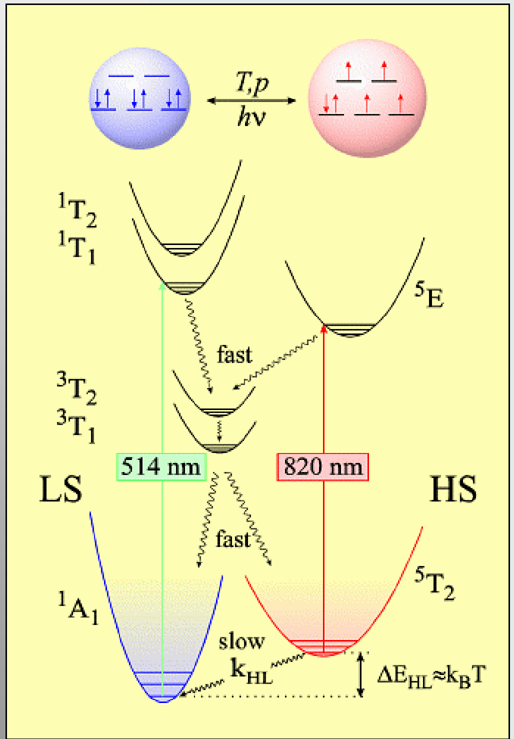

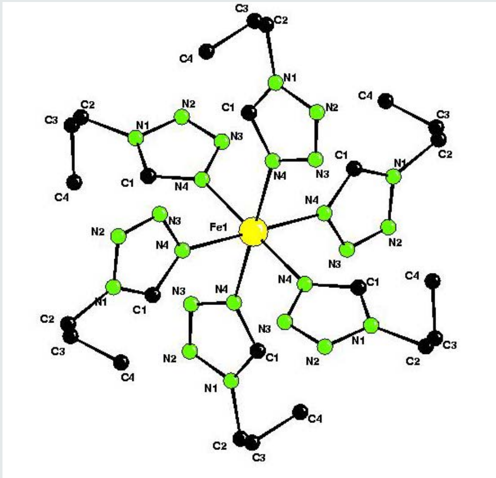

λ ~ 514 nm direct

λ = 820 nm reverse

S. Decurtins et al. Inorg. Chem. 24 (1985) 2174

Photo-excitation setup at 5C1 diffractometer

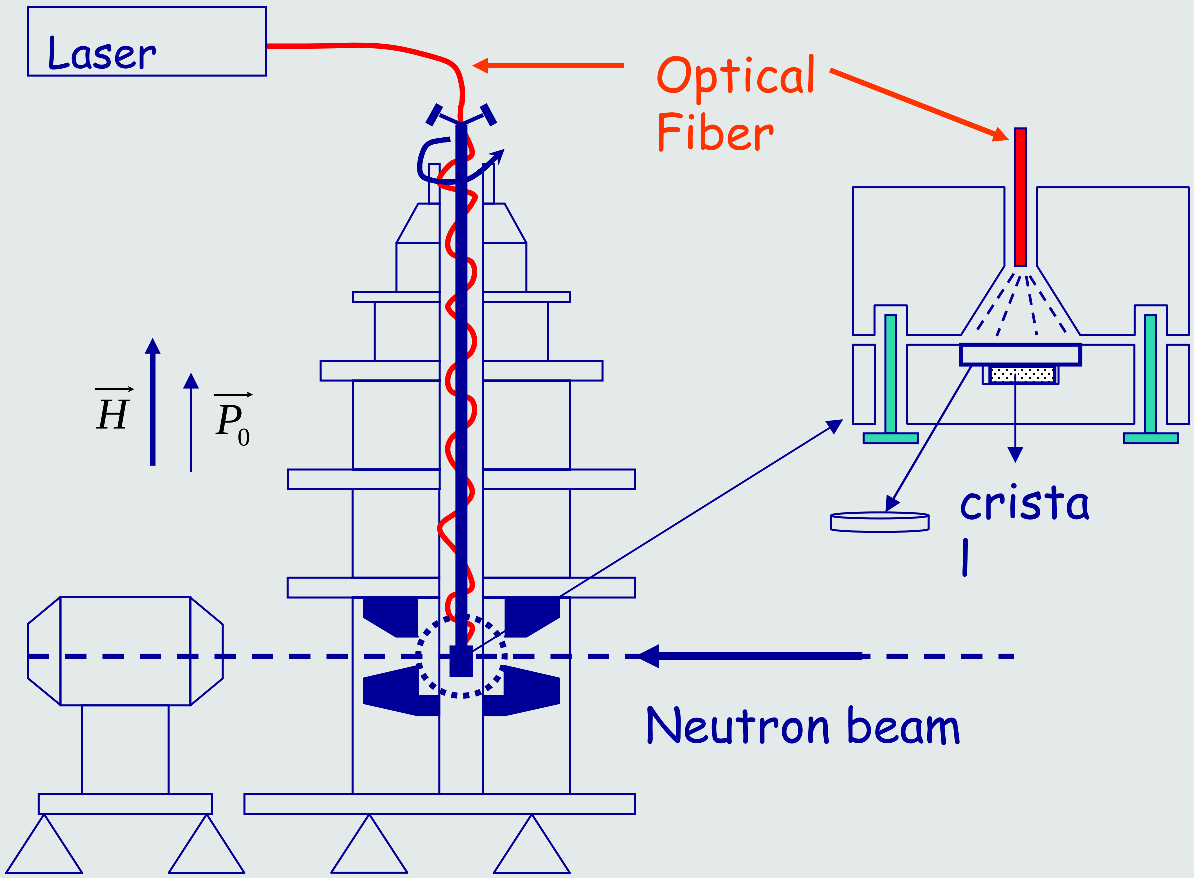

Photo-excited state in $[Fe(ptz)_6](BF_4)_2$

A. Goujon, B. Gillon A Gukasov, J Jeftic, and F Varret Phys. Rev. B 67, 2003

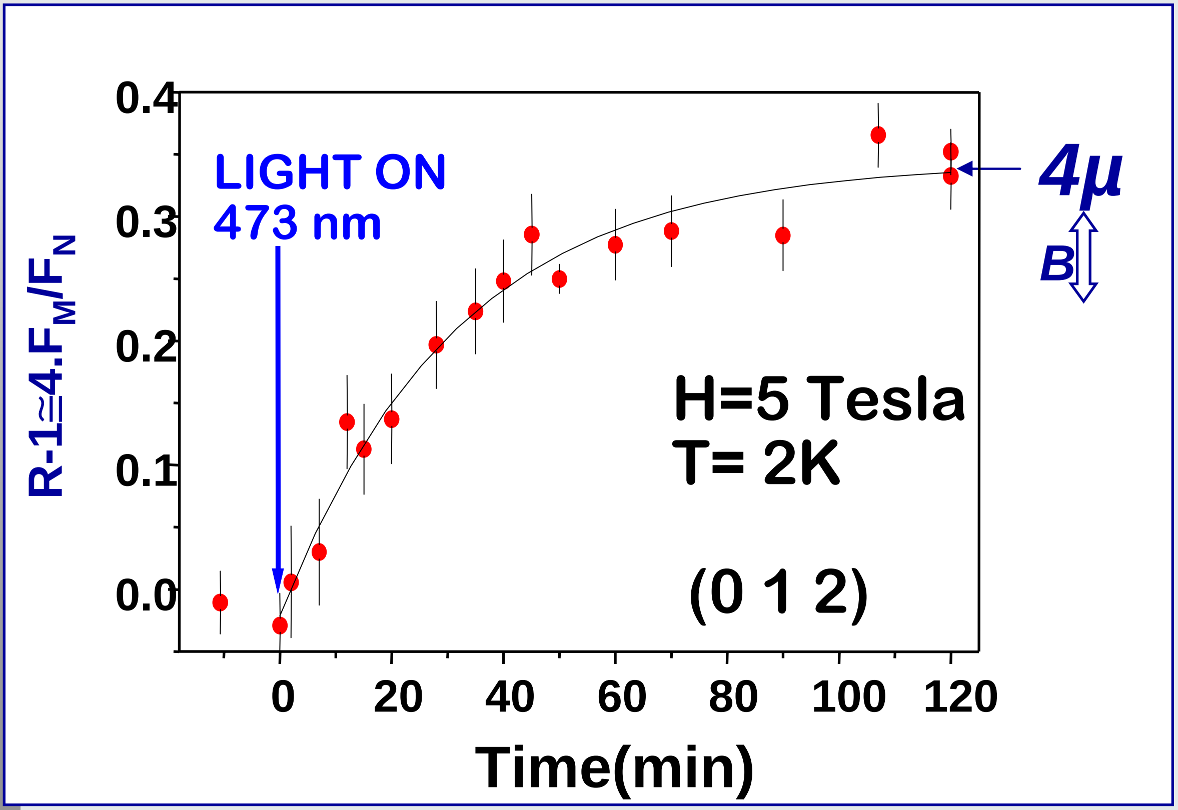

Magnetization

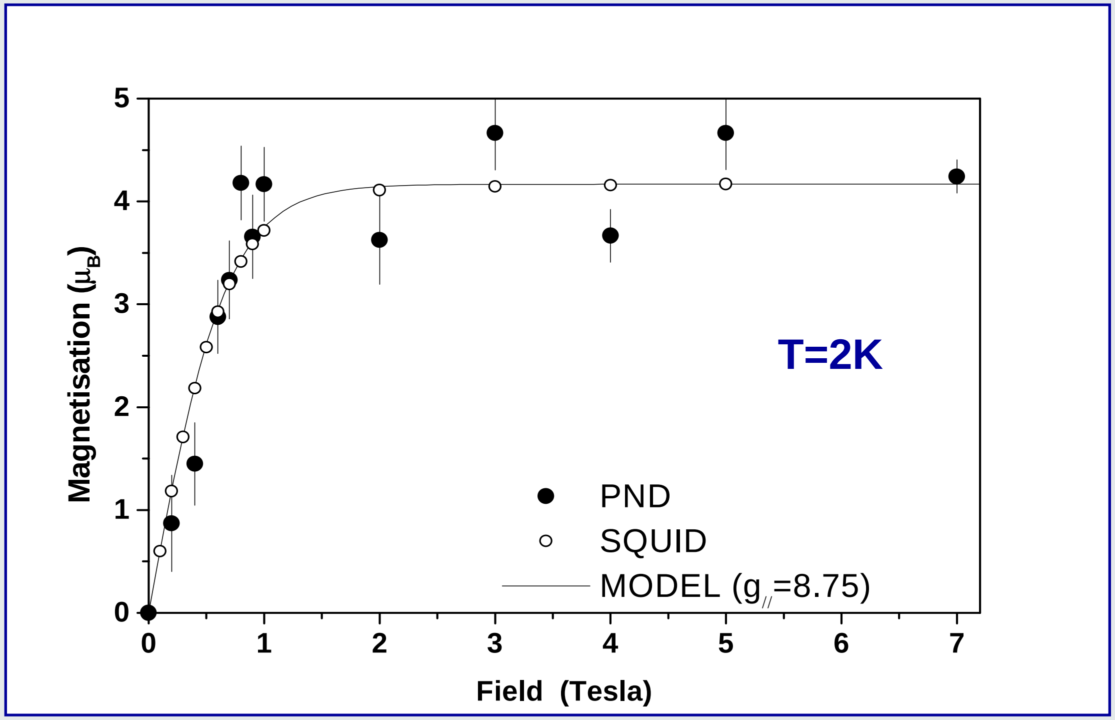

TEMPERATURE BEHAVIOUR

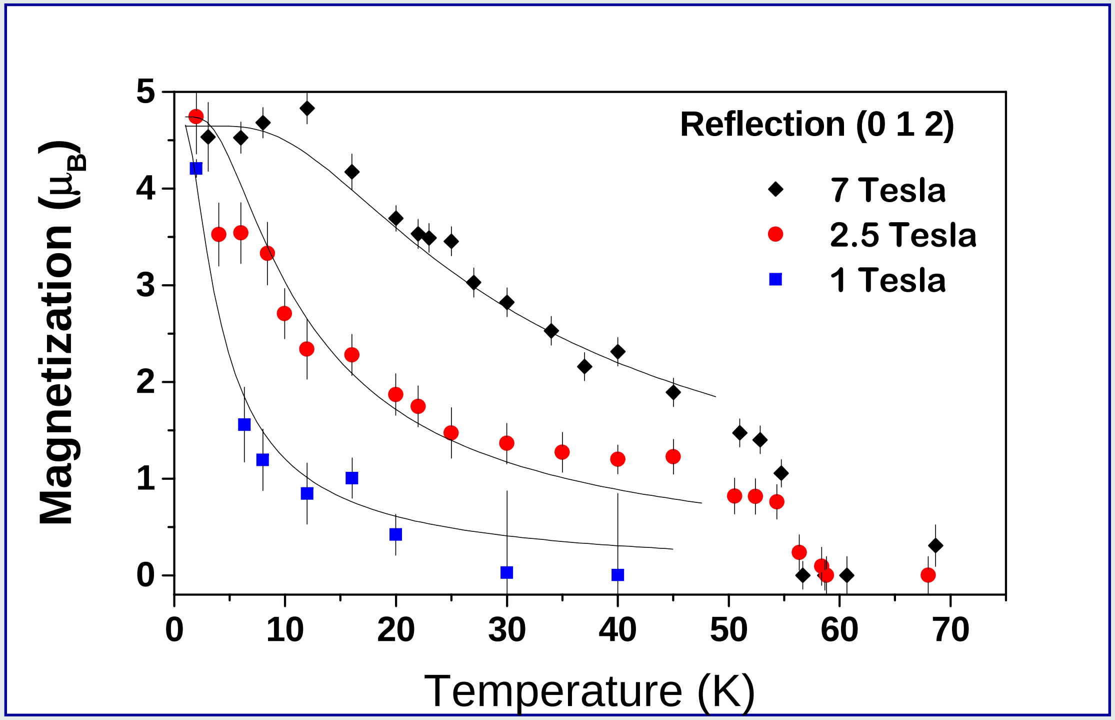

Spin Density of in Photo-induced State

projection on **c**

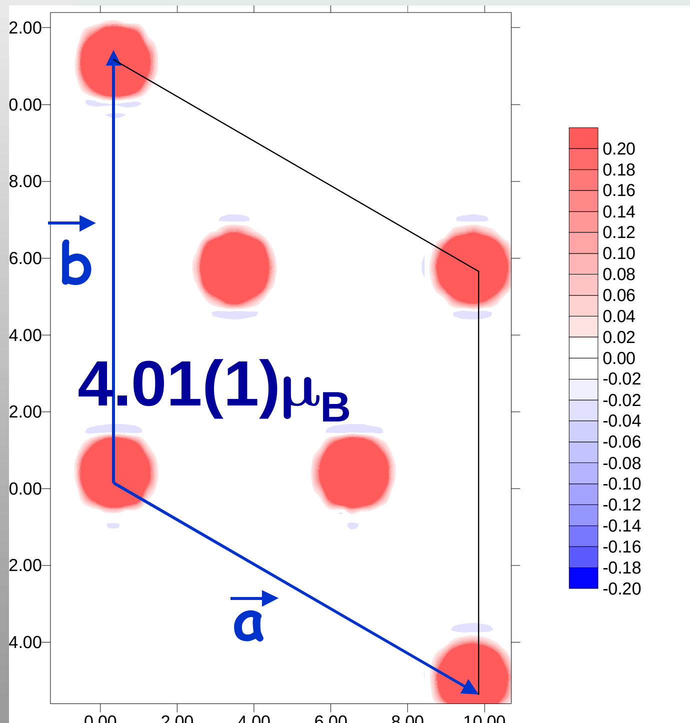

0.06(3) μ_B

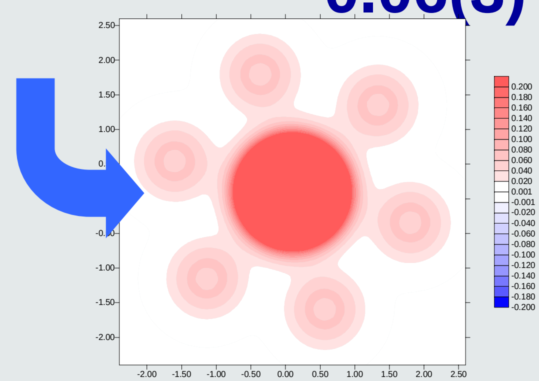

SOME EXPERIMENTAL ASPECTS OF POLARIZED NEUTRON DIFFRACTION

A. GUKASOV

Laboratoire Léon Brillouin, CEA-CNRS, Saclay, France

CONVENTIONAL METHOD

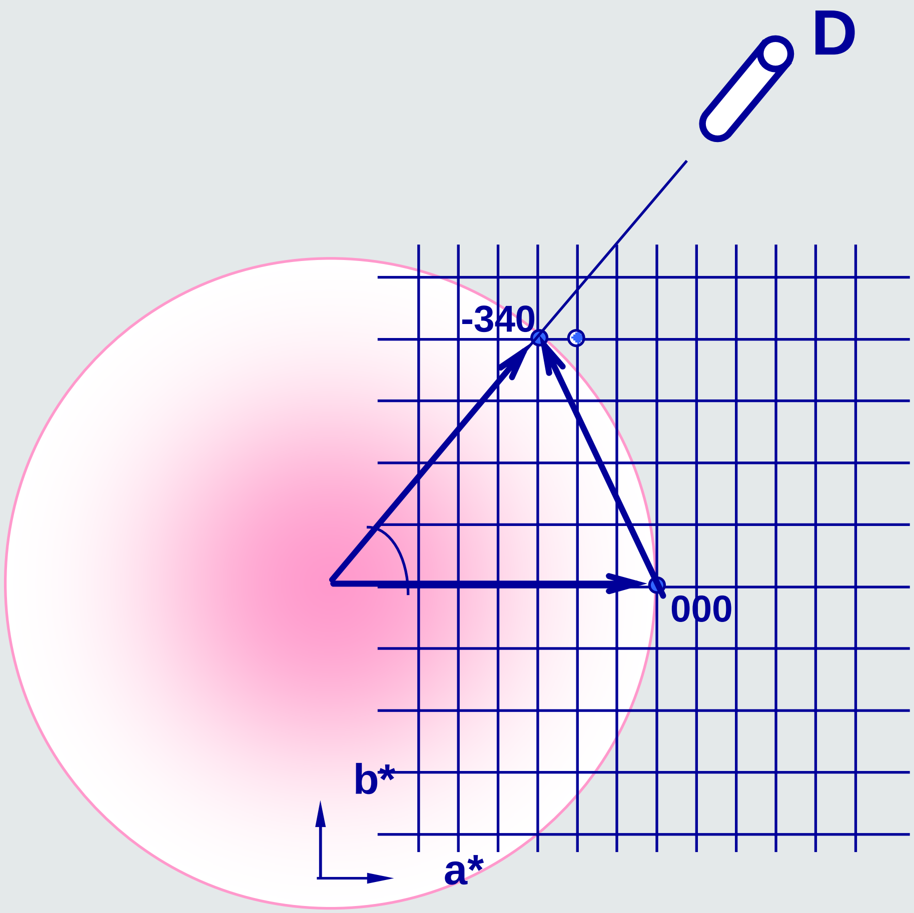

Unpolarized Neutron Diffraction

- 6T2,   4-circles mode
- Cu (220) 0.90 A
- PG   1.55, 2.35 A
- 5-300 K

- 6T2,   Lifting counter mode
- 7.5 T + 40 mK
- 7.5 T +10 Gpa+40 mK

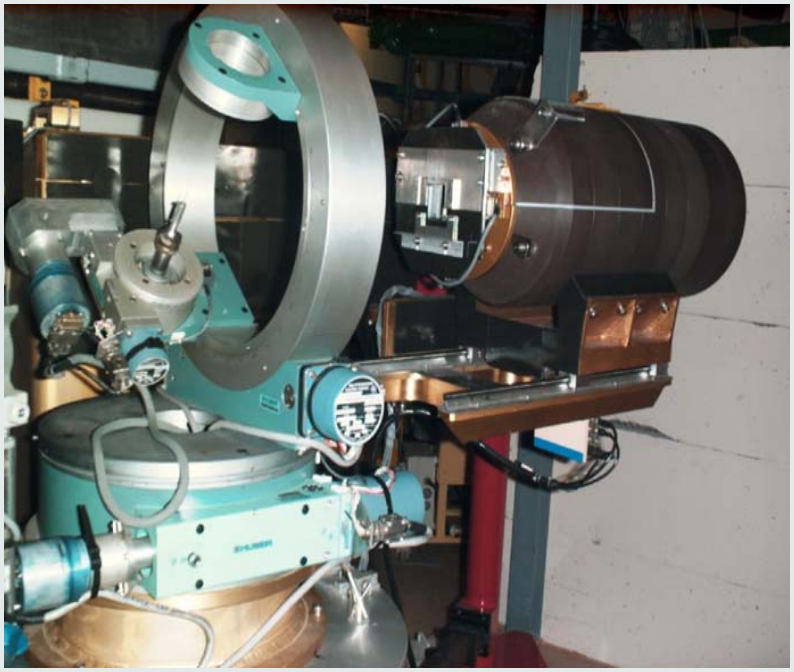

PRINCIPLES OF NEUTRON POLARIZATION IN DIFFRACTION

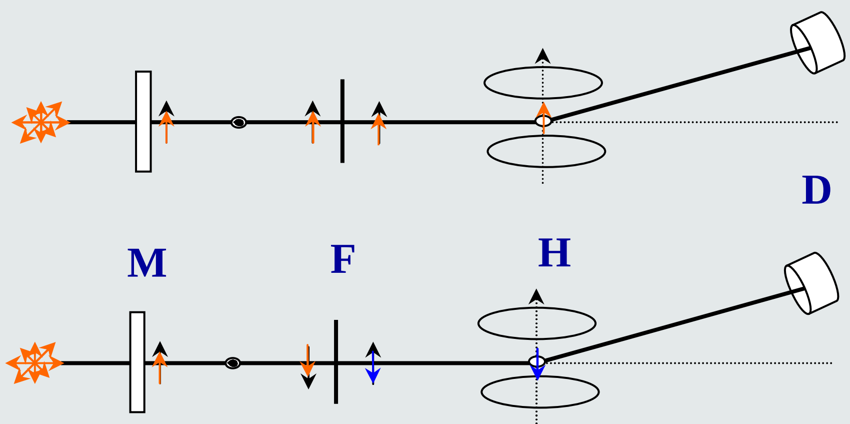

I^{+} P_0 parallel to H

I^{-} P_0 antiparallel to H

$$I^{\pm} \propto =(F_N \pm F_M)^2$$

$$I^{\pm} \propto F^{2}_N \pm 2F_N(P_0 * F_M) + F_M^{2} \qquad (P_0=1)$$

If $F_N = F_M$ $\quad I^{+} = 4F_N^{2}$ $\quad I^{-} = 0$

if $P_0=0$ $\quad I \propto F_N^{2} + F_M^{2} = 2F_N^{2}$

PRINCIPLES OF NEUTRON POLARIZATION BY TOTAL REFLECTION

N9. Double Refraction and Polarization of Neutron Beams. OTTO HALPERN, *University of Southern California.*—The magnetic double-refraction[1] of neutrons can be utilized to obtain completely polarized neutron beams with an intensity loss of only 50 percent of the primary beam. For this purpose a well defined neutron beam of moderate spread in wave-length is allowed to fall on a sheet of iron which can be magnetized. To obtain a maximum effect the direction of magnetization should be chosen parallel to the projection of the beam on the iron sheet. Total reflection will then occur for the two spin states at different critical glancing angles which will be smaller and larger than the critical angle for unmagnetized iron. Theory leads in the case of iron to values of 12.5 minutes and 6 minutes, respectively. Variation of the direction of magnetization should permit a test of the assumed expression for the interaction energy of the magnetic moments of neutron and ion.

[1] Halpern, Hamermesh, and Johnson, Phys. Rev. **59**, 981 (1941). The formula preceding (5.1) suffers from misprints; the denominator obviously is k^2 and not k; furthermore $+1$ must be added to the right side.

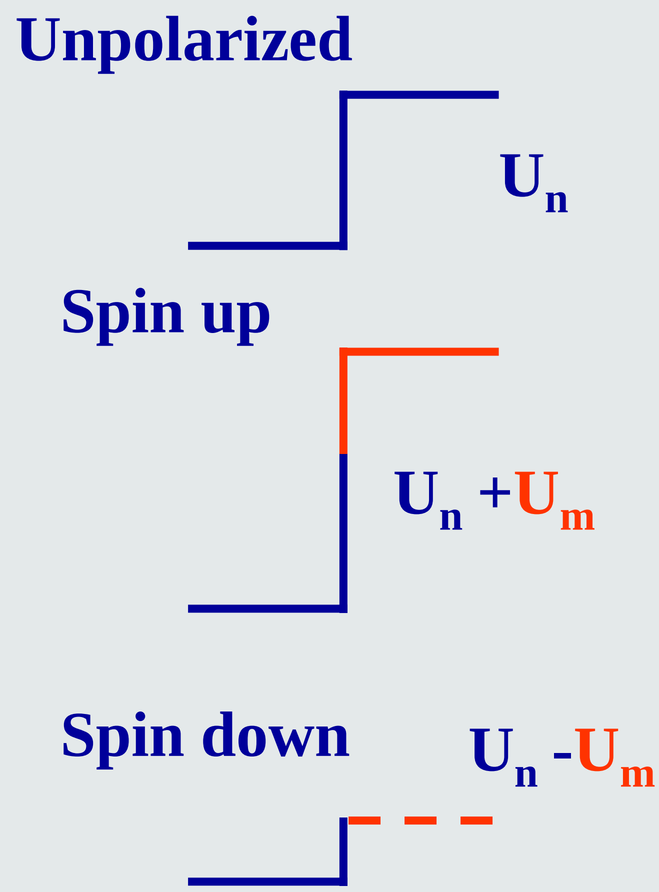

TOTAL REFLECTION FROM IRON

$U_n \sim 9.4$ Fm

$U_m \sim 6.0$ Fm

Unpolarized

Spin up

Spin down

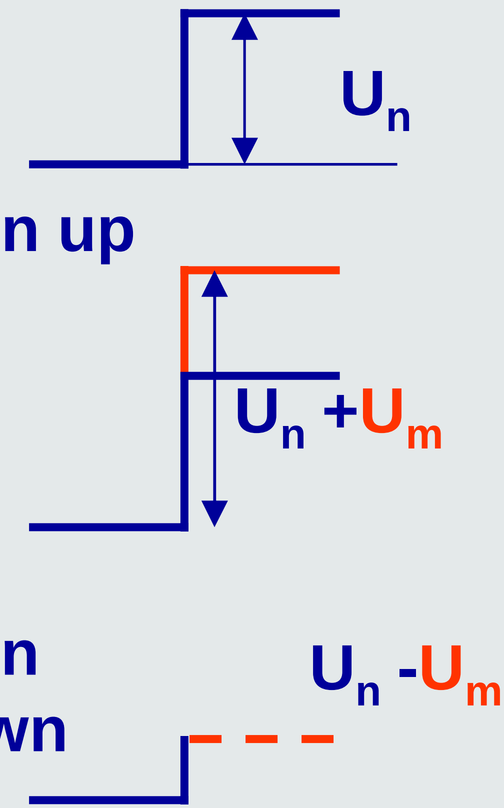

PRINCIPLES OF NEUTRON POLARIZATION BY TOTAL REFLECTION

Total Reflection of Neutrons on Cobalt

MORTON HAMERMESH
Argonne National Laboratory, Chicago, Illinois

April 13, 1949

barns for Fe. At the same time, the magnetic amplitude for Co is $\sim 4.6 \times 10^{-13}$ cm, which is only slightly below the value 6.0×10^{-13} for Fe, so that for Co the magnetic amplitude *exceeds* the nuclear amplitude. Consequently, the refractive indices for the two spin states lie on opposite sides of unity for *all* wave-lengths, and only one of the spin components is capable of undergoing total reflection. With an arbitrarily broad spectrum of incident neutrons, the mirror will reflect a completely polarized beam.

D. J. Hughes and his associates are now conducting reflection experiments with Fe and Co.

[1] O. Halpern, Phys. Rev. **75**, 343 (1949).
[2] C. G. Shull and E. O. Wollan, unpublished.

Total Reflection of Neutrons on Cobalt

MORTON HAMERMESH
Argonne National Laboratory, Chicago, Illinois
April 13, 1949

barns for Fe. At the same time, the magnetic amplitude for Co is $\sim 4.6 \times 10^{-13}$ cm, which is only slightly below the value 6.0×10^{-13} for Fe, so that for Co the magnetic amplitude *exceeds* the nuclear amplitude. Consequently, the refractive indices for the two spin states lie on opposite sides of unity for *all* wave-lengths, and only one of the spin components is capable of undergoing total reflection. With an arbitrarily broad spectrum of incident neutrons, the mirror will reflect a completely polarized beam.

D. J. Hughes and his associates are now conducting reflection experiments with Fe and Co.

[1] O. Halpern, Phys. Rev. **75**, 343 (1949).
[2] C. G. Shull and E. O. Wollan, unpublished.

Heusler polarising monochromator of IN20, ILL

5C1 polarised neutron diffractometer (LLB)

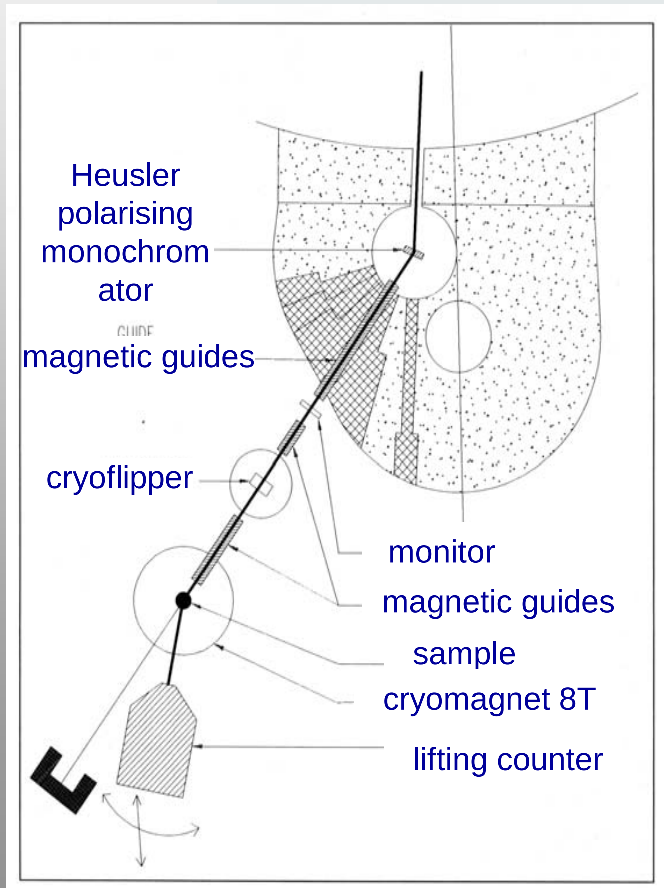

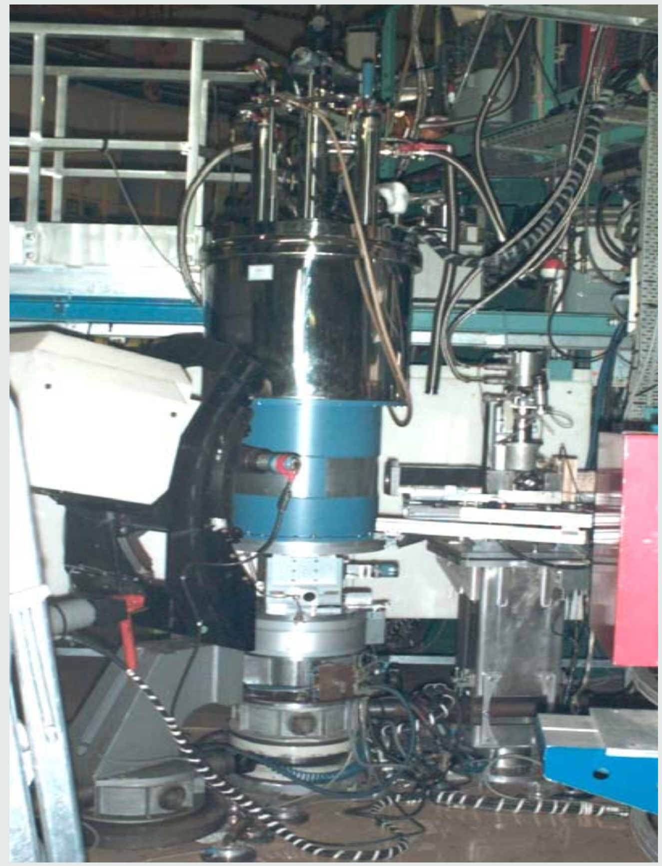

CONVENTIONAL METHOD

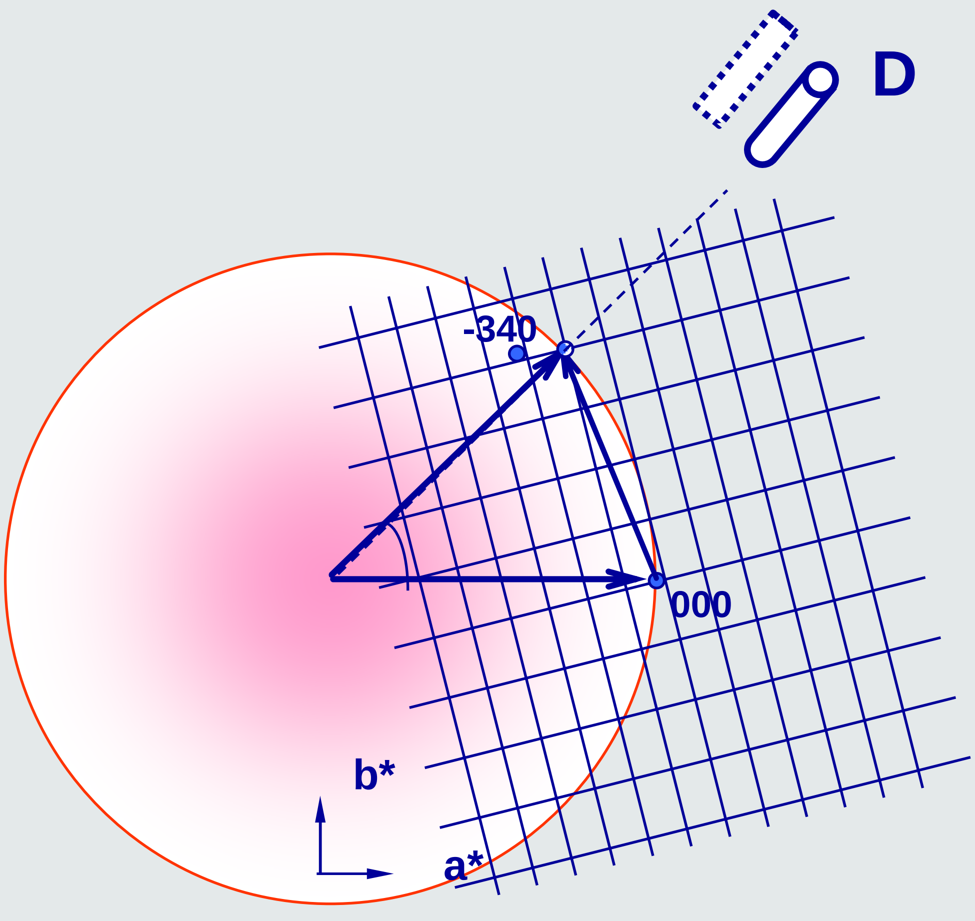

ROTATION (OSCILLATION) METHOD

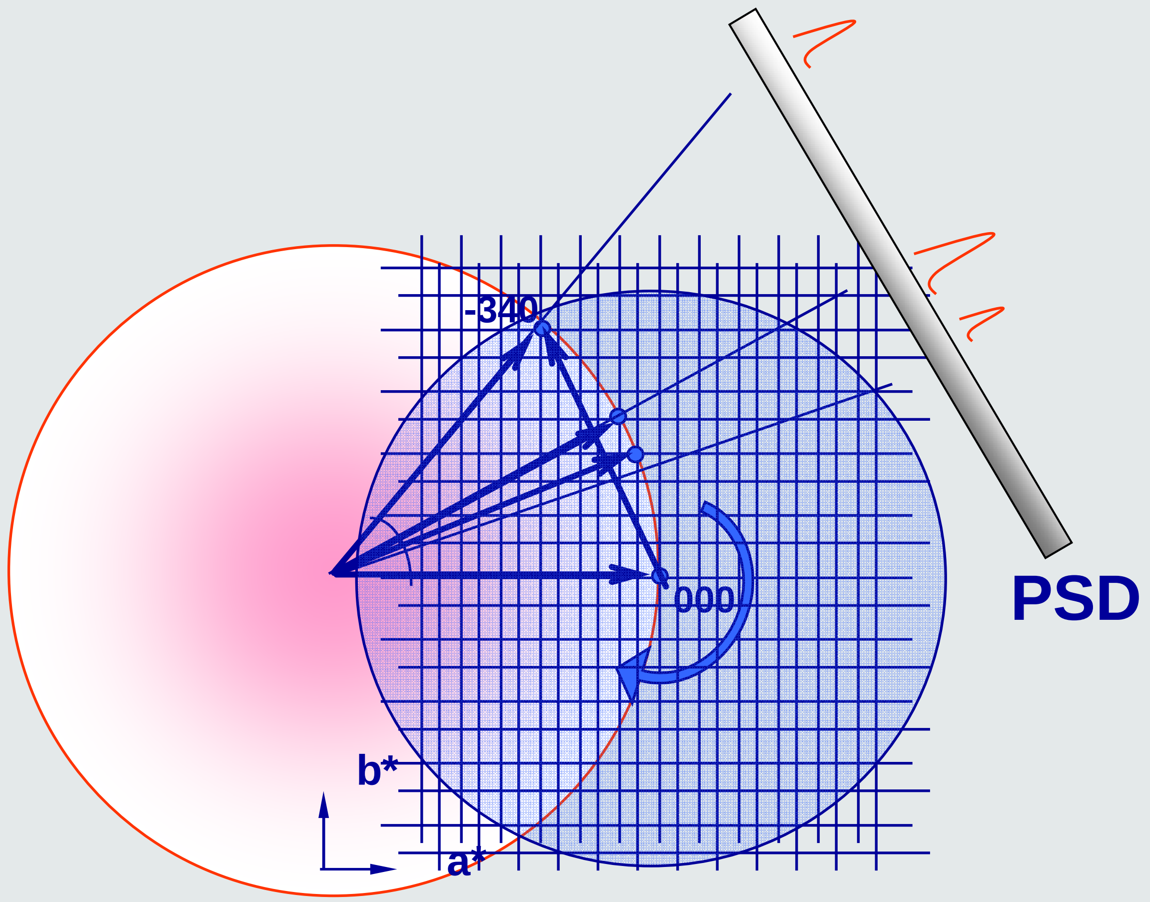

Cap 2010

Very Intense Polarized Neutron Diffractometer

5C1, juin 2005

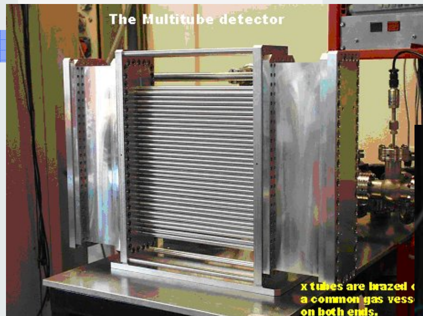

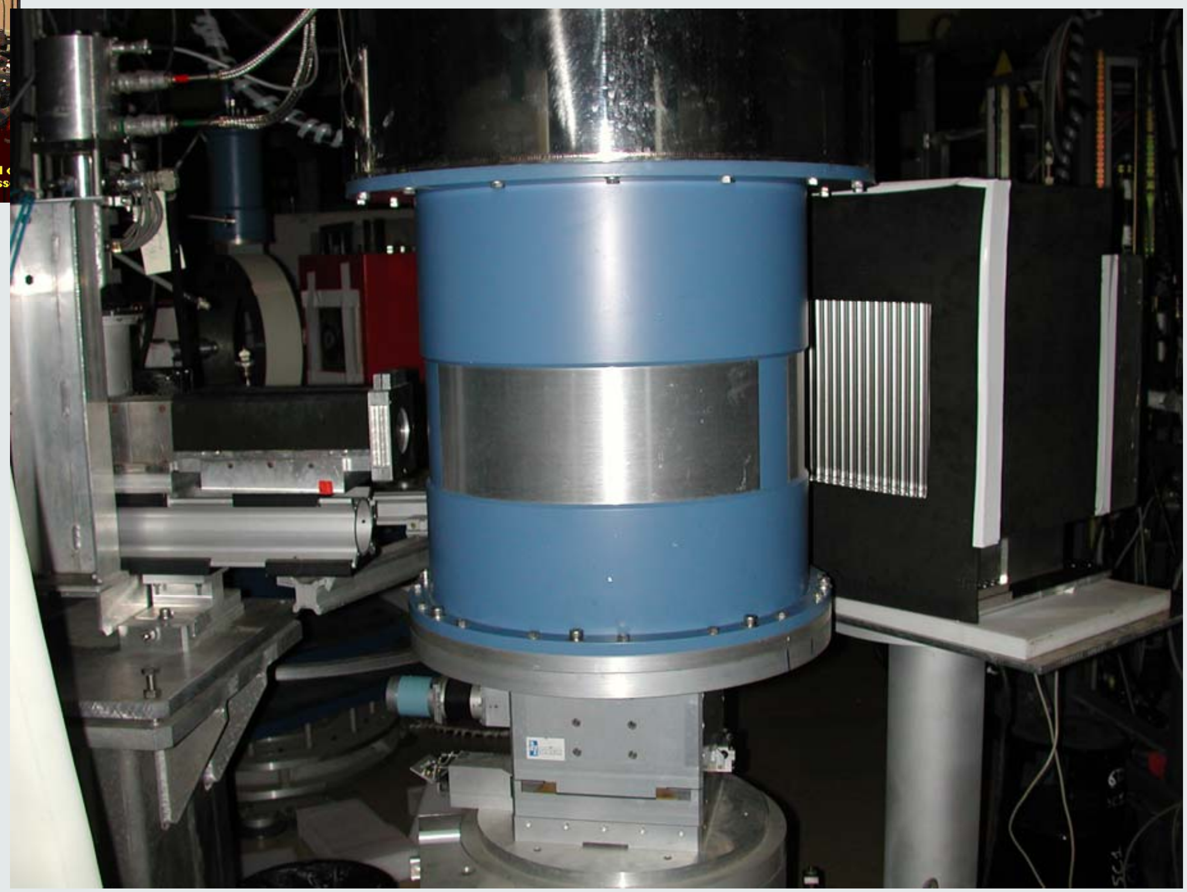

SINGLE SECTION OF ROTATION IMAGE (correspond to 1 tube rebinned in 64 pixels)

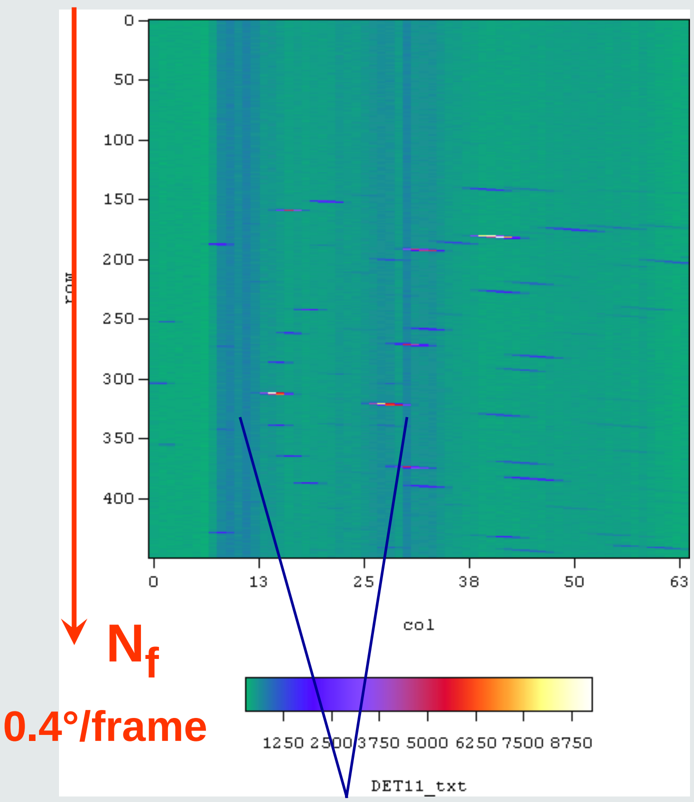

Aluminium lines

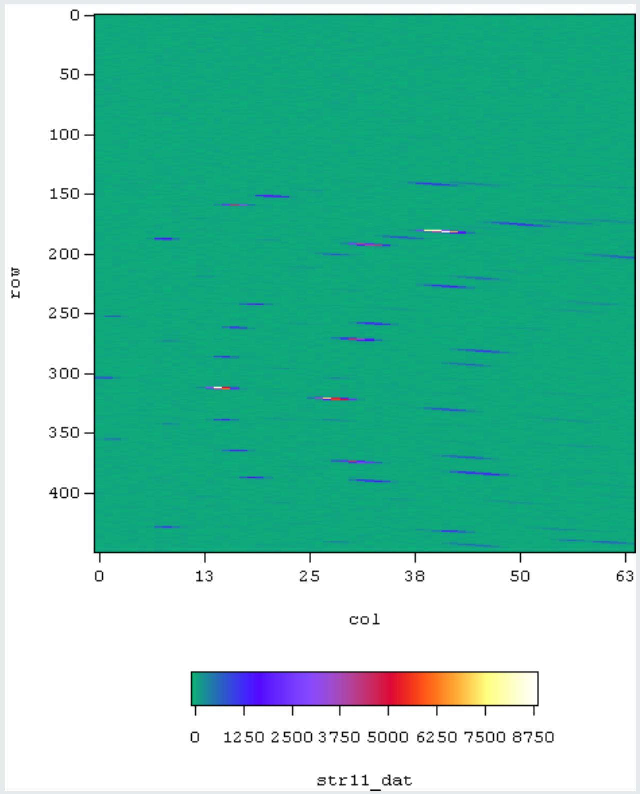

Background substructed

ROTATION IMAGES OF 2 NEIGHBOUR TUBES (rebinned in 64 pixels)

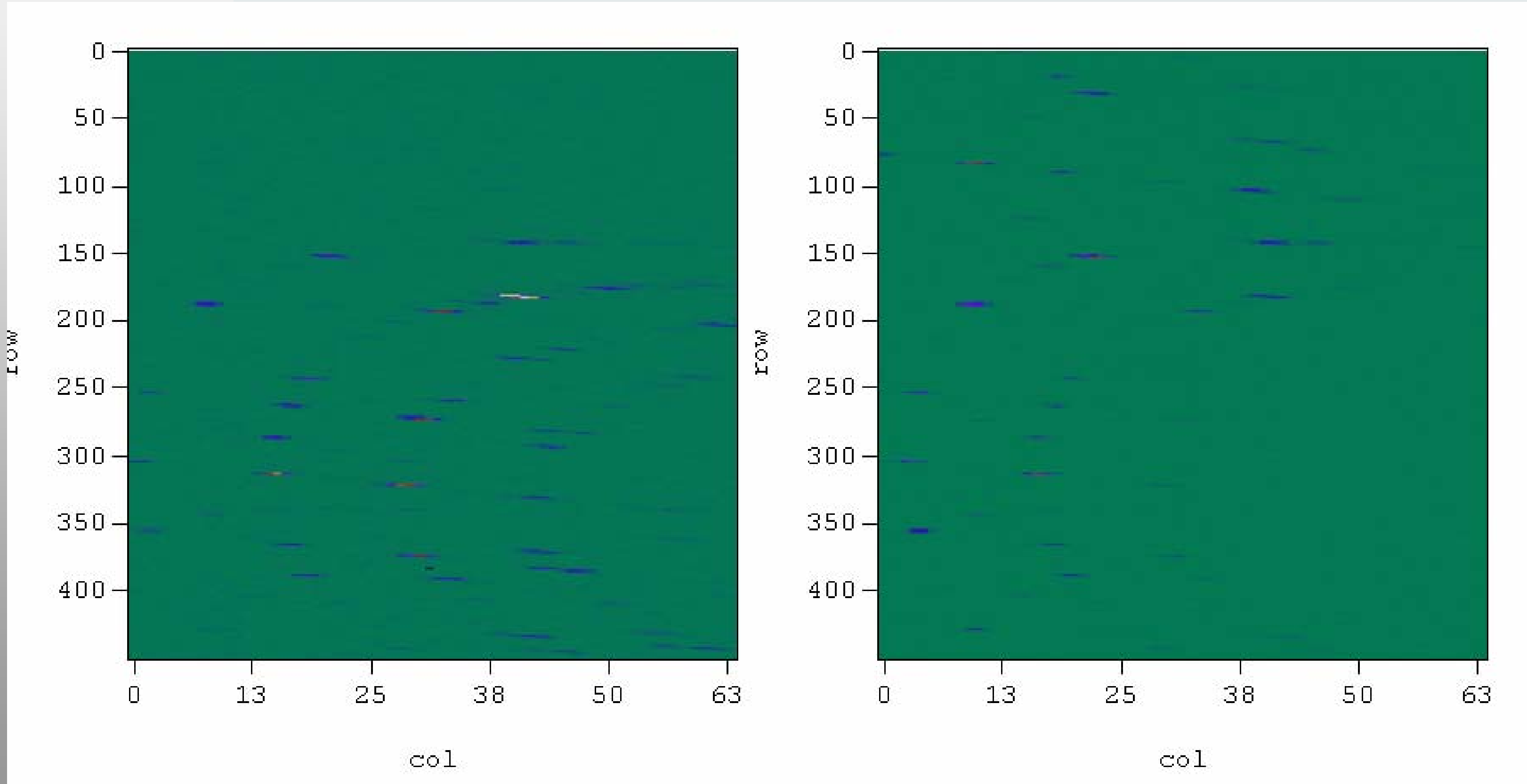

Very Intense Polarized Neutron Diffractometer
Étape 2005

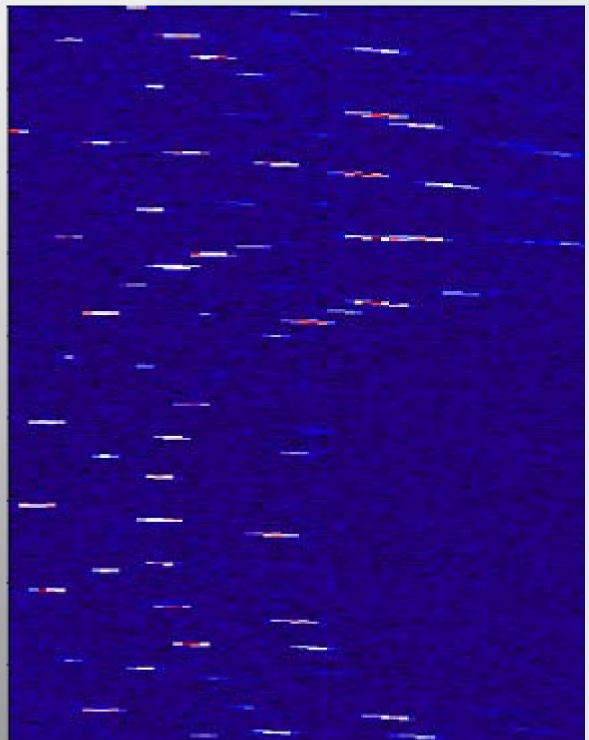

Section d'image de precéssion de $Mn(dca)(N_2C_4H_4)(H_2O)$ a 1.5 K

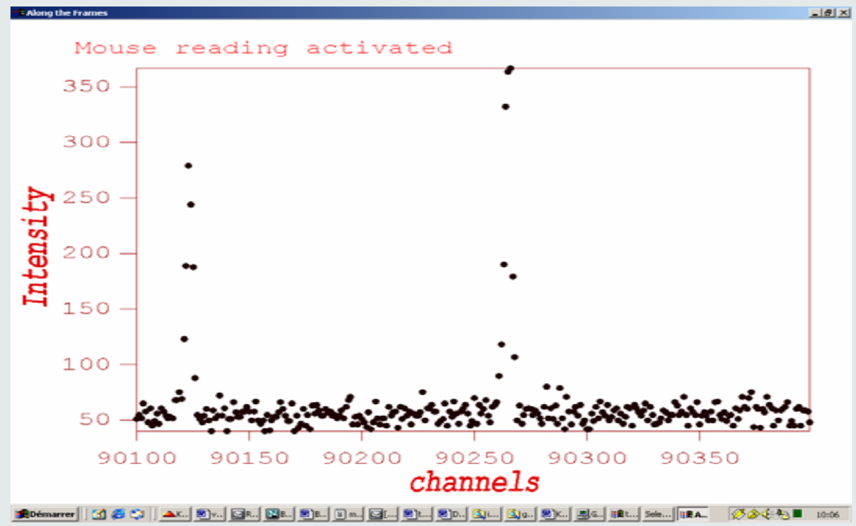

Intensity of one *pixel* as a function of *rotation angle,* step 0.1 °

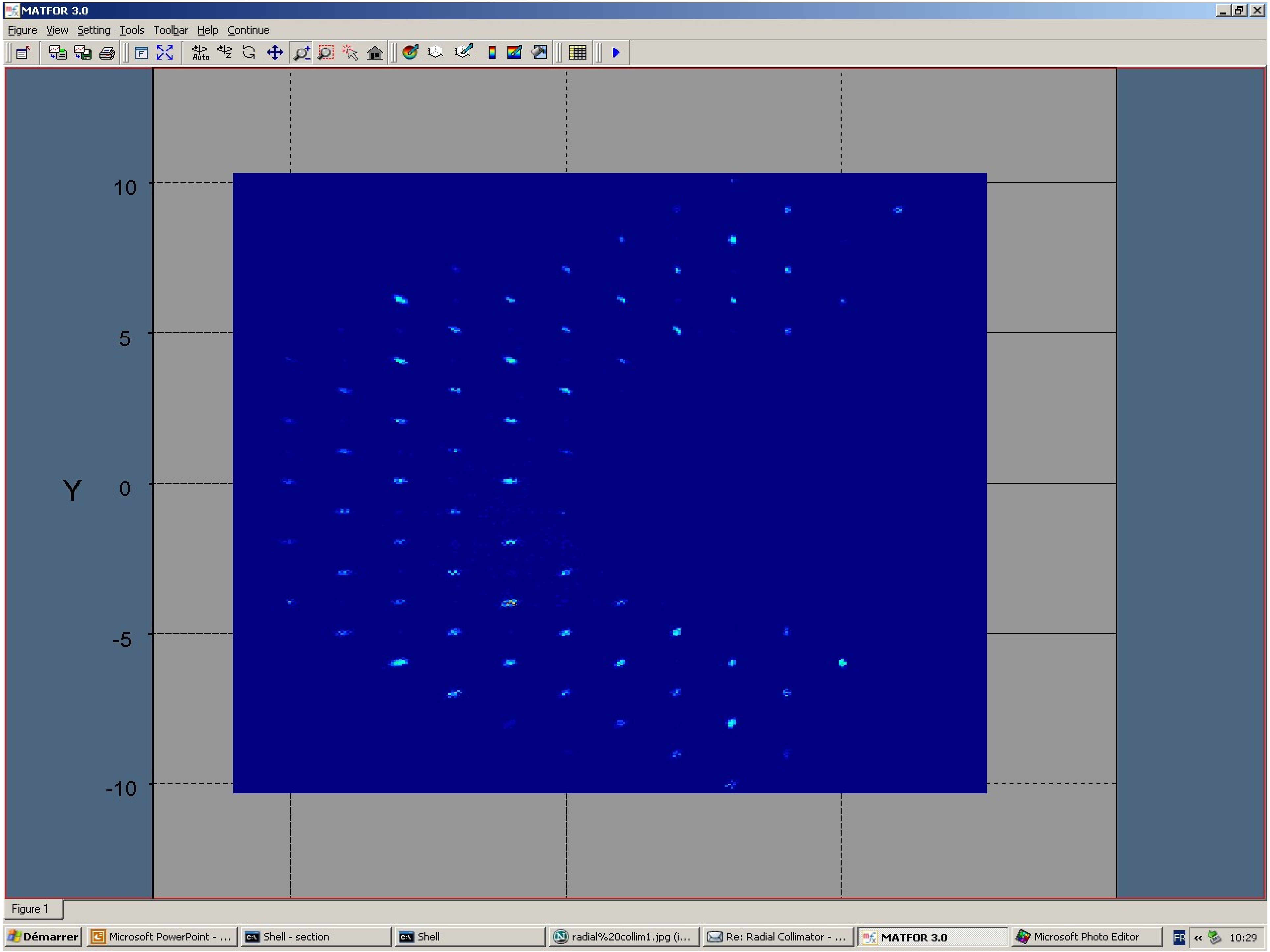
MATFOR 3.0
Figure View Setting Tools Toolbar Help Continue
10
5
Y
0
-5
-10
Figure 1
Démarrer
Microsoft PowerPoint - ...
Shell - section
Shell
radial%20collim1.jpg (i...
Re: Radial Collimator - ...
MATFOR 3.0
Microsoft Photo Editor
FR
10:29

CRYOFLIPPER

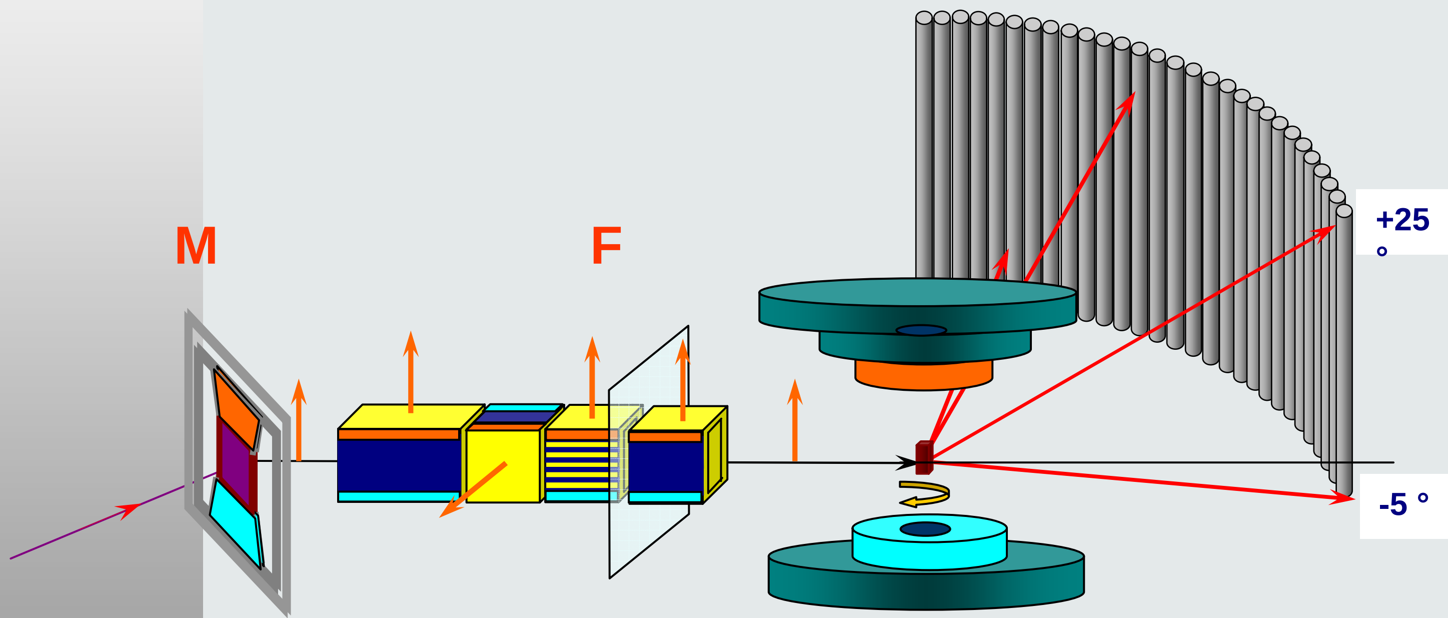

CRYOFLIPPER

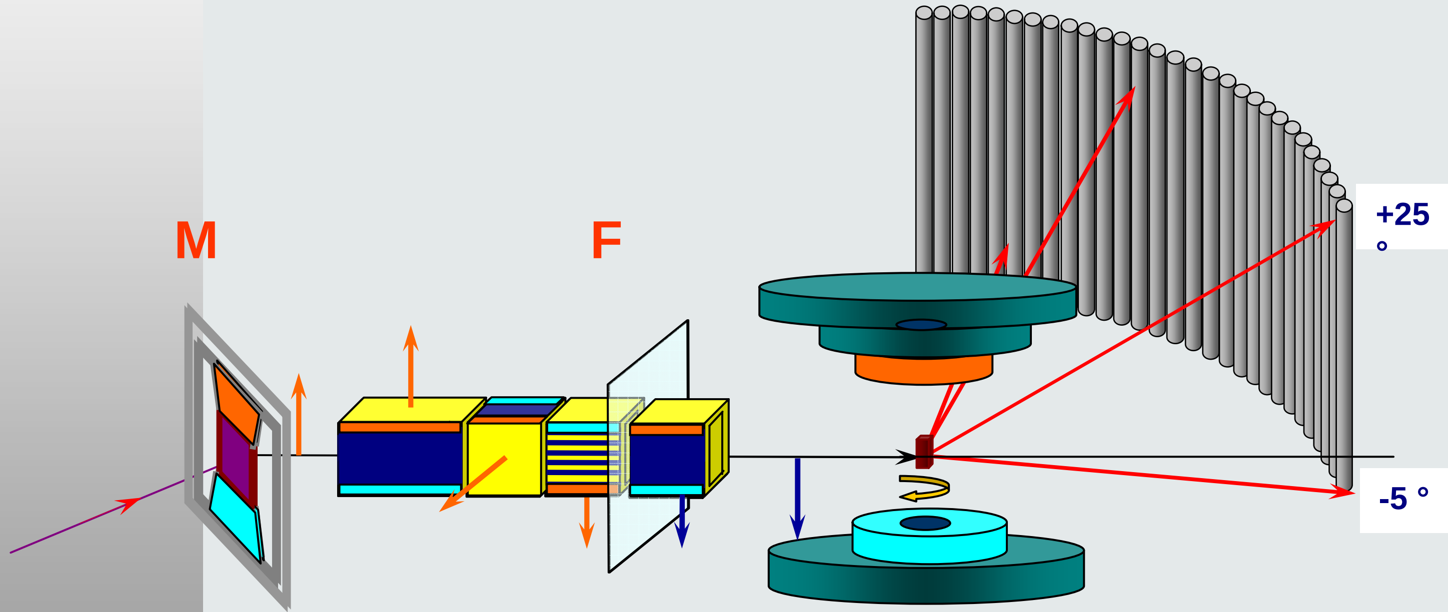

SUPERMIRROR BENDER, made in PNPI (Gatchina)

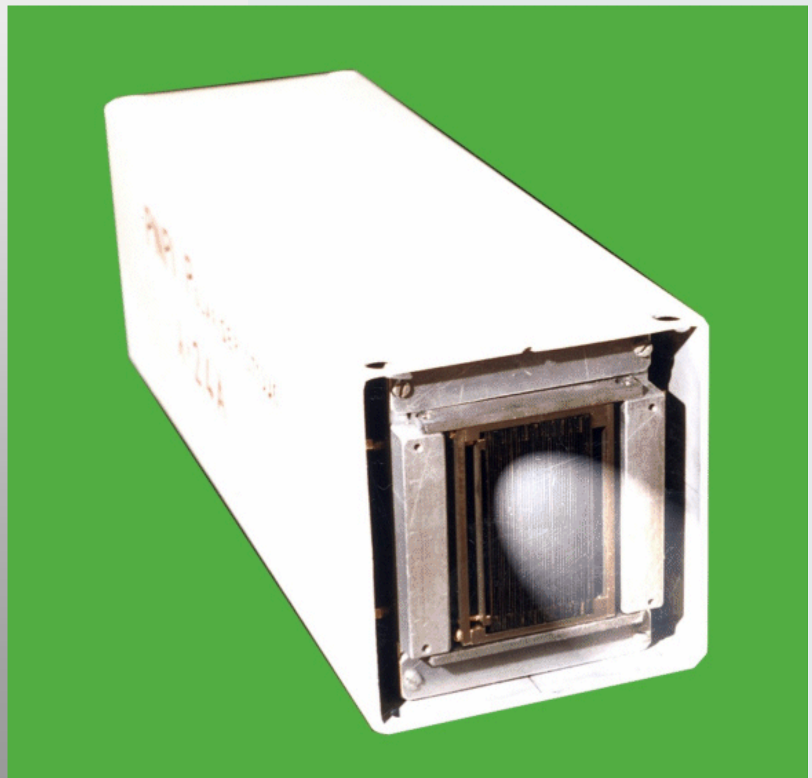

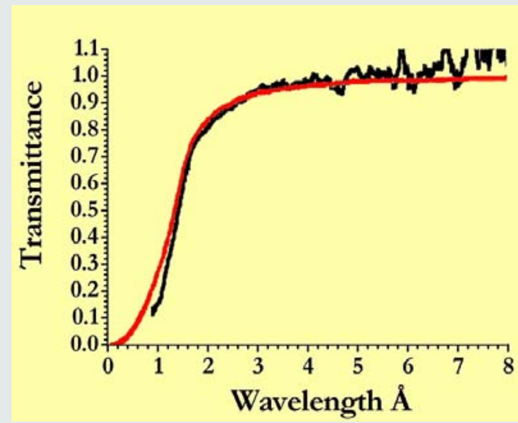

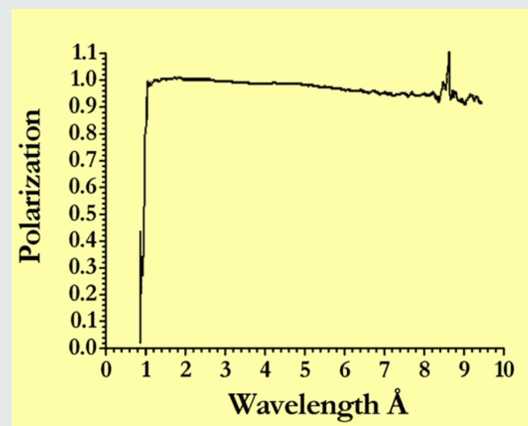

Very Intense Polarized Neutron Diffractometer

6T2 february 2006

- **1.4 A, PSD mode**
- **25x25° acceptance angle**
- **7.5 T + 40 mK**
- **7.5 T +10 Gpa+40 mK**
- **Laser, UV source**

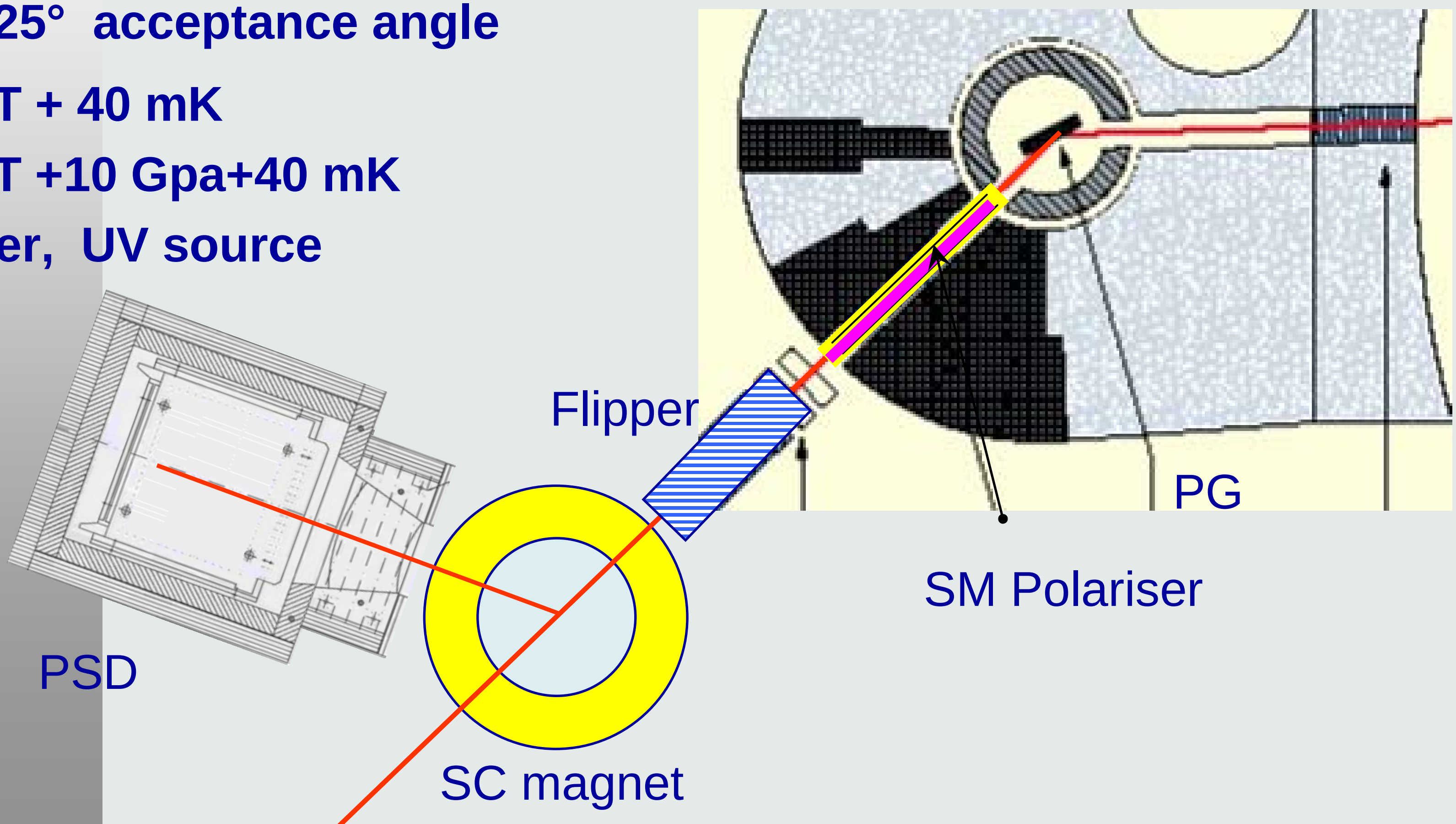

Very Intense Polarized Neutron Diffractometer

6T2 february 2006

- 1.4 A, PSD mode
- 25x25° acceptance angle
- 7.5 T + 40 mK
- 7.5 T +10 Gpa+40 mK
- Laser, UV source

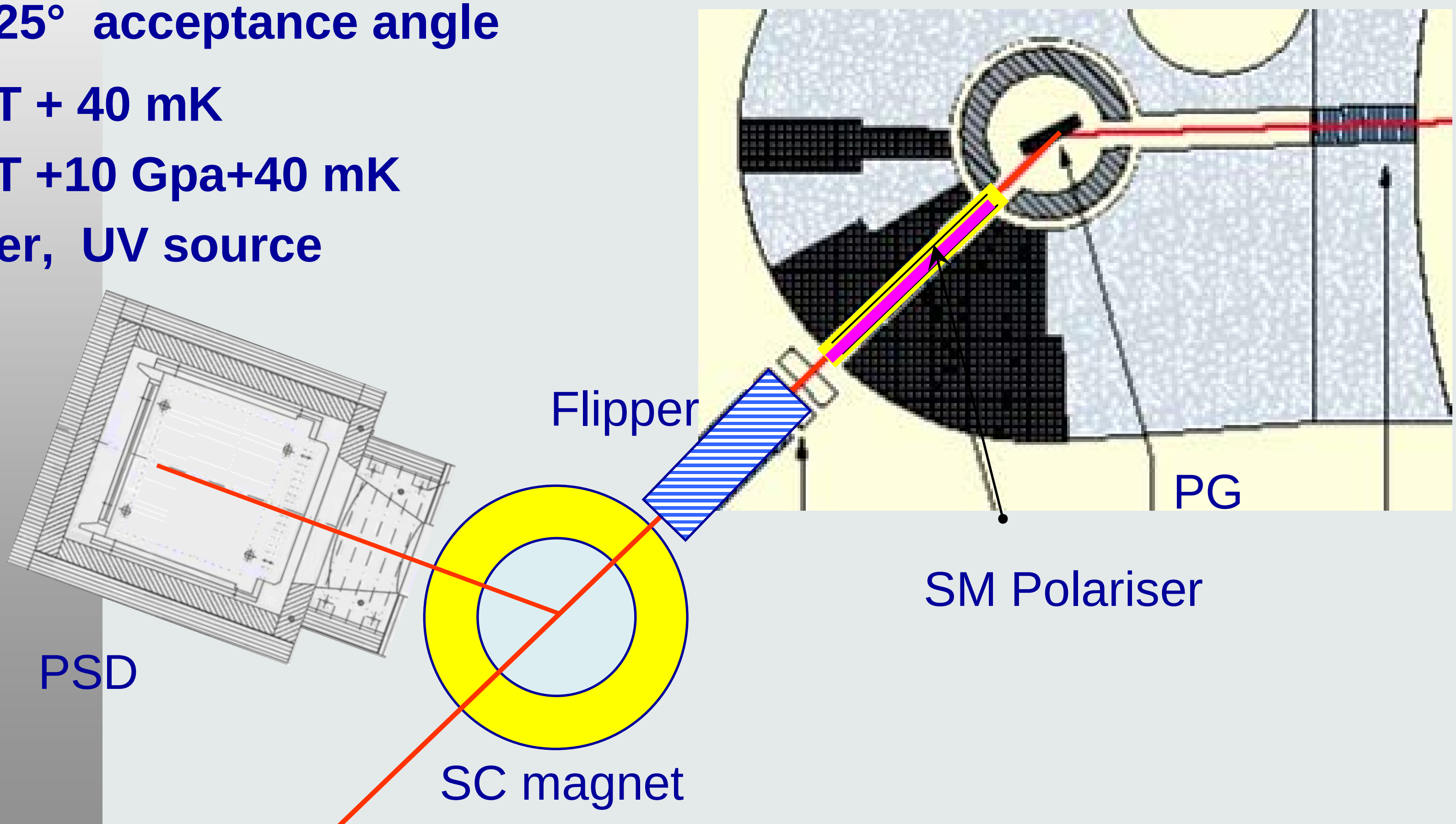

Very Intense Polarized Neutron Diffractometer

6T2 february 2006

- **1.4 A, PSD**
- **25x25° acceptance an**

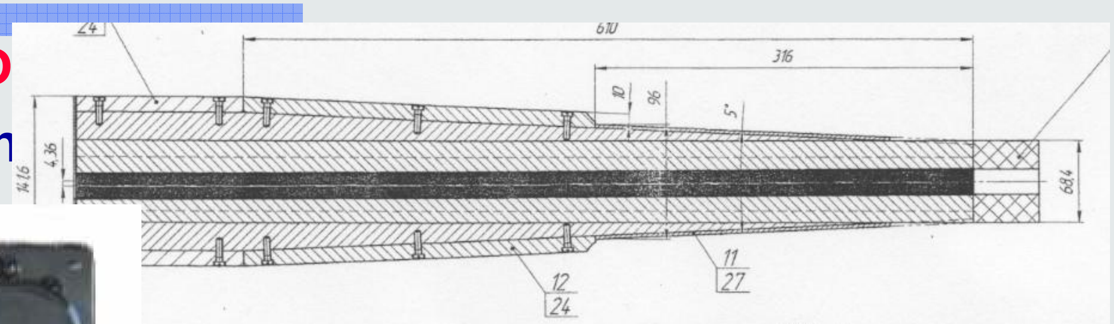

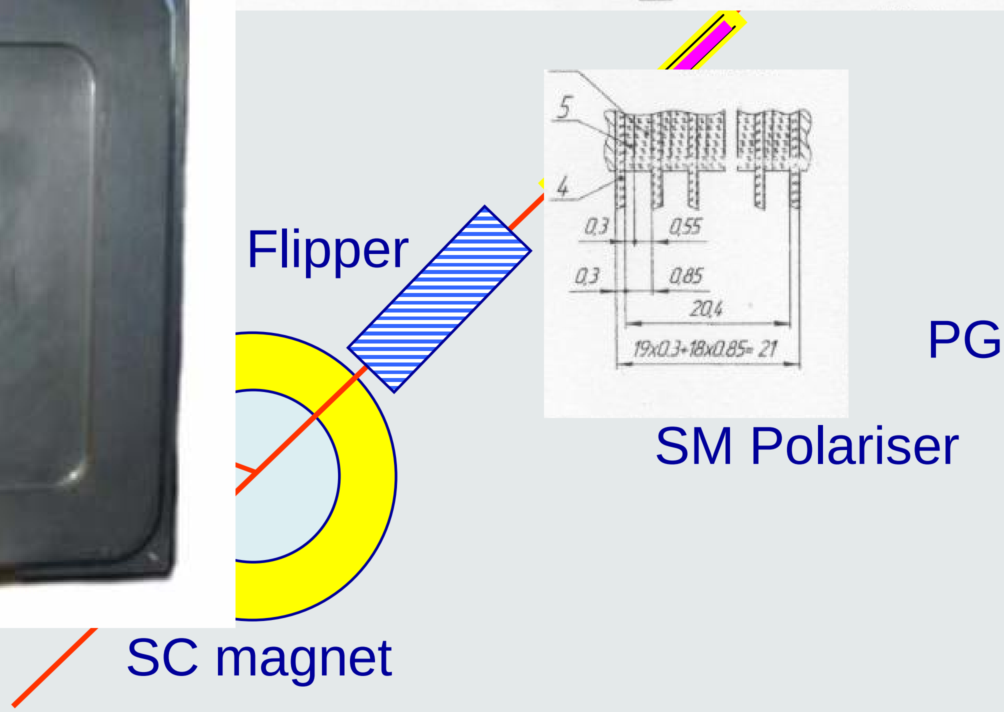

Very Intense Polarized Neutron Diffractometer

- 1.4 A, PSD mode
- 25x25° acceptance angle

Very Intense Polarized Neutron Diffractometer

- **Radial Collimator**
- **25x25° acceptance angle**

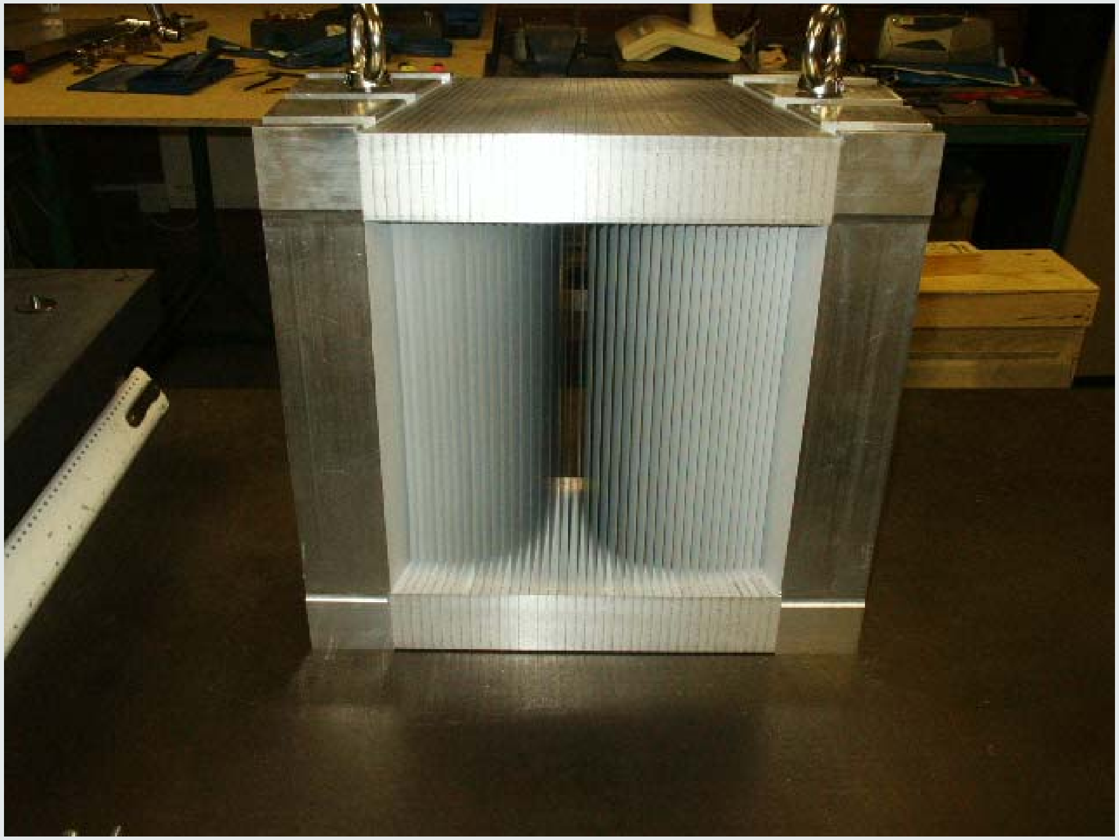

LENGTH OF RADIAL COLLIMATOR AND ITS DIVERGENCE

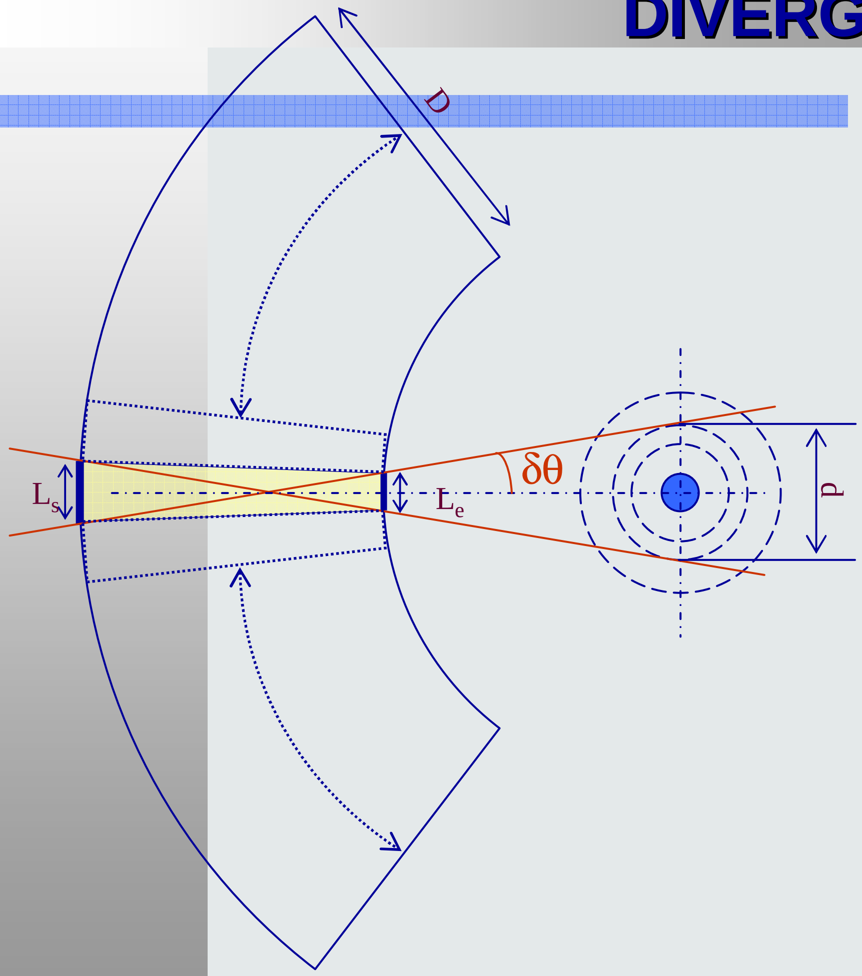

$$\tan(\delta\theta) = \frac{L_e + L_s}{2.D}$$

$$\delta\theta = \frac{d - L_e}{2.D_{ec}}$$

$$D = \frac{L_e/2 + \tan(\beta/2).D_{ec}}{\tan(\delta\theta) - \tan(\beta/2)}$$

$$L_s = 2.\tan(\beta/2).(D + D_{ec})$$

L_e (mm)	L_s (mm)	β (°)	$\delta\theta$ (°)	D (mm)
7,05	15,23	1,15	1,71	355,48